

DETERMINATION OF MUSCLE, LIGAMENT
AND ARTICULAR FORCES AT THE KNEE
DURING A SIMULATED SKATING THRUST

by

ALBERT A. HALLIWELL

B.Eng., Clarkson College of Technology, 1963

M.Eng., McGill University, 1967

B.P.E., University of British Columbia, 1974

A THESIS SUBMITTED IN PARTIAL FULFILLMENT OF
THE REQUIREMENTS FOR THE DEGREE OF
MASTER OF PHYSICAL EDUCATION

in

THE FACULTY OF GRADUATE STUDIES
(School of Physical Education and Recreation)

We accept this thesis as conforming
to the required standard

THE UNIVERSITY OF BRITISH COLUMBIA

September, 1977

© Albert Alexander Halliwell, 1977

In presenting this thesis in partial fulfilment of the requirements for an advanced degree at the University of British Columbia, I agree that the Library shall make it freely available for reference and study.

I further agree that permission for extensive copying of this thesis for scholarly purposes may be granted by the Head of my Department or by his representatives. It is understood that copying or publication of this thesis for financial gain shall not be allowed without my written permission.

Department of Physical Education and Recreation

The University of British Columbia
2075 Wesbrook Place
Vancouver, Canada
V6T 1W5

Date September 22nd, 1977

ABSTRACT

A number of investigators have determined the joint forces acting at the hip and knee for normal human locomotion as related to the design of prosthetic devices. This research has been extended to allow the calculation or estimation of the muscular and ligamentous forces operating at the knee joint for normal walking. The current study expanded upon the past research to evaluate the magnitude and temporal sequence of the muscle, ligament and articular forces acting at the knee joint for a simulated skating thrust.

A skilled ice hockey player was filmed in two reference planes while making a skating thrust from a laboratory force platform. The cine film data was synchronized with the force plate output to allow calculation of the orthogonal forces and moments imposed on the knee joint. The orthogonal force system was determined from a knowledge of the inertial, gravitational and reaction forces acting on the lower limb during the skating thrust. The muscle, ligament and joint forces were determined from equations derived from the conditions of joint equilibrium. The equations of equilibrium were indeterminate and had to be reduced by making assumptions from electromyographic records

to allow solution. Forces were calculated for a simplified muscle and ligament system which included the hamstrings, quadriceps and gastrocnemius muscle groups, the collateral ligaments and the cruciate ligaments of the knee joint. In addition, the articular joint force, joint torque and centre of pressure of the joint force were determined.

Results of the investigation revealed that the magnitude of the muscle, ligament and joint forces developed in a skating thrust were considerably greater than respective forces exerted during level walking while the temporal sequence of the skating forces was comparable to walking upstairs. The quadriceps muscle group exerted the greatest contractile force while the gastrocnemius and hamstrings groups developed much smaller forces. The largest ligament forces were developed in the collateral ligaments and the posterior cruciate ligament to maintain stability of the joint. The knee joint is subject to the combined effects of a joint force six times body weight and a large joint torque superimposed upon each other during the skating thrust and this fact is considered important when discussing the cause of menisci knee injuries.

TABLE OF CONTENTS

CHAPTER	Page
I. INTRODUCTION.....	1
II. REVIEW OF LITERATURE.....	7
III. METHODS AND PROCEDURES.....	19
Anatomy of the Knee Joint.....	19
Concepts of Analysis.....	27
Anthropometry.....	35
Testing Procedures.....	39
Analysis.....	49
IV. RESULTS AND DISCUSSION.....	73
Results.....	73
Discussion.....	89
V. SUMMARY AND CONCLUSIONS.....	106
REFERENCES.....	110
APPENDICES.....	117

LIST OF TABLES

TABLE	Page
1. Anthropometric Data.....	37
2. Anthropometric Data.....	74
3. Maximum Muscle, Ligament and Joint Forces for the Simulated Skating Thrust.....	90
4. The Maximum Muscle and Ligament Forces of Various Activities.....	102
5. Maximum Joint Forces and Torques of Various Activities.....	104

LIST OF FIGURES

FIGURE		Page
3.01	Right Knee Joint - Bone Structure.....	20
3.02	Superior Surface - Tibia.....	22
3.03	Ligaments of Knee Joint.....	22
3.04	Ligaments of Knee Joint.....	24
3.05	Patellar Ligament.....	24
3.06	Muscles Controlling Knee Joint.....	26
3.07	Tibial Reference Axes.....	28
3.08	Tibial Condyles.....	28
3.09	Reference Axes - Femur, Tibia.....	30
3.10	Error in Assumed Centre of Rotation of Femur in 90° Flexion.....	31
3.11	Pelvic Reference Axes.....	32
3.12	Simplified Muscle and Ligament System Acting at Knee Joint.....	35
3.13	Angle of Patellar Ligament Relative to Angle of Knee Flexion.....	38
3.14	Location of Reference Markers.....	41
3.15	Experimental Set-Up.....	43
3.16	Force Record of Force Plate Expressed as Six Measured Variables.....	44
3.17	Experimental Set-Up Showing Test Subject on Force Platform.....	47
3.18	Analysis of Data.....	50
3.19	External Force System at Knee Expressed in Terms of Tibial Reference Axes of Right Knee.....	52
3.20	Forces Acting on Lower Limb Including Reaction Forces, Gravity Forces and Acceleration Forces.....	53
3.21	Muscle Force in Quadriceps to Balance Moment + Mxk.....	58
3.22	Muscle Force in Hamstrings to Balance Moment - Mxk.....	58
3.23	Muscle Force in Gastrocnemius to Balance Moment - Mxk.....	62
3.24	Force in Posterior Cruciate and Anterior Cruciate Ligaments.....	64
3.25	Collateral Ligament Forces.....	67
3.26	Compressive Joint Force, Rz.....	69
4.01	Force Plate Output in Form of Oscilloscope Trace - Trial No. 4.....	76

4.02	Electromyogram - Skating Thrust on Ice.....	77
4.03	Illustrated Sequence of Skating Thrust.....	78
4.04	Limb Linear Accelerations.....	80
4.05	Limb Angular Accelerations.....	81
4.06	Resolved Force Components at Knee Trial No. 4.....	83
4.07	Muscle and Ligament Forces for Trial No. 4.....	85
4.08	Muscle and Ligament Forces.....	86
4.09	Joint Forces Acting at Knee.....	88
4.10	Centre of Pressure on Condyles of Knee.....	99

NOTATIONS

Reference Axes

- Xg, Yg, Zg Grid reference axes, origin at centre of force plate, point p.
- Xs, Ys, Zs Reference axes of tibia, origin at centre of tibial condyles, point k.
- Xf, Yf, Zf Reference axes of femur, origin at centre of femoral condyles, point fc.
- Xp, Yp, Zp Reference axes of pelvis, origin at centre of femoral head, point fh.

Co-ordinates

The co-ordinates of a point, p, relative to a set of reference axes, for example, the grid reference axes, are expressed as Xgp, Ygp, and Zgp.

Points

- a Ankle joint centre.
- k Knee joint centre at centre of superior surface of tibia.
- fc Centre of femoral condyles.
- fh Centre of femoral head of hip joint.

Muscle and Ligament Attachments

- h Insertion of hamstrings.
- g Insertion of gastrocnemius.

q	Insertion of patellar ligament (quadriceps femoris).
l	Lateral collateral attachment to fibula.
m	Medial collateral attachment to tibia.
a	Anterior cruciate attachment to tibia.
p	Posterior cruciate attachment to tibia.
ph	Origin of hamstrings.
fg	Origin of gastrocnemius.
fl	Lateral collateral attachment to femur.
fm	Medial collateral attachment to femur.
fa	Anterior cruciate attachment to femur.
fp	Posterior cruciate attachment to femur.

Force Actions

Fxi, Fyi, Fzi	Components of force acting in directions of X, Y, and Z reference axes respectively.
Mxi, Myi, Mzi	Components of moment acting in X, Y and Z reference axes respectively.
Rx, Ry, Rz	Components of joint force acting at the knee joint.
Pa, Pp, Pm and Pl	Force actions in anterior cruciate, posterior cruciate, medial collateral and lateral collateral ligaments respectively.
Pq, Ph and Pg	Force actions in quadriceps femoris, hamstrings and gastrocnemius muscle groups respectively.

F_{xm}, F_{ym}, F_{zm}	Components of force acting in muscle groups in the X_s, Y_s and Z_s directions respectively.
F_{xcr}, F_{ycr} and F_{zcr}	Components of force acting in the cruciate ligaments in the X_s, Y_s and Z_s directions respectively.
F_{xcol}, F_{ycol} and F_{zcol}	Components of force acting in the collateral ligaments in the X_s, Y_s and Z_s directions respectively.

Symbols

g	Acceleration of gravity.
bw	Body weight of subject.
w_i	Weight of body segment i .
I_i	Moment of inertia of segment i about axis perpendicular to the long axis of the segment and passing through the centre of mass of the segment.
t	Thigh segment.
s	Shank segment.
f	Foot segment.
R_i	Radius of segment or joint i .
L_i	Length of body segment i .
r_i	Radius of gyration of segment i about the axis perpendicular to the long axis of the segment and passing through the centre of mass of the segment.
LFO	Left foot off during skating thrust.
PO	Push off of right foot in skating thrust.

ACKNOWLEDGEMENTS

The author is indebted to several people for their guidance and assistance in completing this investigation. To these individuals I would like to express my sincere appreciation.

Dr. Ted Rhodes, my committee chairman, provided both inspirational and monetary assistance towards the research study and made himself available for many hours of helpful consultation. To the other members of my thesis committee, Dr. Merv Olson, Dr. Bob Hindmarch and Dr. Doris Miller, I extend a special thanks. In particular, to Dr. Miller who supervised the testing at the University of Washington and gave invaluable advice regarding cinematography techniques.

A further thanks is expressed to the test subject, Grant Cumberbirch, for his participation in the study, to Terry Schultz and Bruce Goldsmid for their help in the data collection and to Mr. Hsu for his technical advice and development of testing equipment.

The investigator is also indebted to the assistance of Mr. Frank Maurer of the Institute of Animal Resource Ecology at U.B.C. in making available film reduction equipment. Finally, the author gratefully appreciates the aid of Dr. James Morrison who provided a copy of his doctoral thesis.

The author is further indebted to Elizabeth Orne for the typing of this manuscript.

CHAPTER I

INTRODUCTION

The study of human locomotion over the past several decades has been approached from two separate directions. Dillman (1970) and others who were interested in understanding accomplished athletic performance studied the time-displacement of the lower limbs utilizing cinematographic techniques. Dillman was specifically concerned with the action of the lower limb during the recovery phase of running and determined limb velocity and acceleration data which allowed an in depth analysis of the temporal sequence of running. A second group of researchers were more interested in examining human locomotion from a biomechanical and bio-engineering point of view. Bresler (1950), Morrison (1968) and Paul (1964) determined the forces developed at the joints of the lower limbs during walking. These force-time analyses were initiated to study the biomedical problems of persons fitted with prosthetic devices such as artificial limbs and replacement hip joints. With the aid of sophisticated force measuring devices that accurately record reaction forces, these researchers calculated the joint forces acting at the ankle, knee and hip joints during the walking cycle from heel strike to toe off. These studies indicated that

the joint forces imposed at the knee and hip during normal level walking were equal to three to four times the body weight. Morrison (1970) extended the study of human locomotion to include the calculation of muscle and ligament forces developed at the knee joint for level walking, inclined walking and stair climbing. In a recent study, Chao (1973) measured the vertical reaction force, the lateral and posterior reaction forces and the twisting moment of the pushing foot of a hockey player wearing skates. These reaction forces were recorded for a simulated energetic push off action with a force plate.

The present study was designed to extend the work of Chao utilizing the methodology of Morrison (1968) to examine the magnitude of the joint, muscle and ligament forces imposed at the knee during a simulated skating thrust. Because of the powerful nature of the skating thrust it is considered that the joint and ligament forces developed at the knee are quite significant compared to the respective forces of normal locomotion. The investigation is therefore a fact finding and descriptive study of a specific athletic movement, the skating thrust. A knowledge of the forces acting during this manoeuvre are important in terms of the functional anatomy of the knee joint and could assist the practitioner or therapist in judgements concerning the specific forces affecting the stability of the knee during the game of ice hockey.

Significance of the Study

To date, no data has been published regarding the magnitude of lower limb joint forces including muscle, ligament and articular forces developed during an exerted athletic movement. Also, the methodology of determining the above forces from a knowledge of force plate reaction forces (Morrison, 1968) was developed for locomotion in a single plane, i.e., the anterior-posterior plane. The current study has extended the methodology so that it is more general and can be applied to athletic skills such as skating which have more than one plane of movement.

Statement of the Problem

The purpose of the investigation is to determine the articular and ligamentous forces imposed at the knee joint during a simulated skating thrust by an ice hockey player.

Definition of Terms

The following list of definition of terms is essential to allow interpretation of the somewhat technical text of the report.

Articular forces - the compressive and shear forces acting at the articular surfaces of a joint. For the knee, they represent the forces imposed on the condyles of the tibia and the femur of the joint.

Ligamentous forces - the tensile forces acting in the liga-

ments that support a joint. For the knee, these forces act in the collateral and cruciate ligaments.

Time-space co-ordinates - the location of a body segment or a point of that segment with time as defined by the x, y and z co-ordinates. For the lower limb these co-ordinates represent displacement of the centre of mass of the foot and shank and the displacement of the joint centres of the hip, knee and ankle.

Reaction forces - the equal and opposite forces exerted on a body by a resisting body or surface at the point of contact with that body or surface. In this study the reaction forces are exerted on the skate blade by the force plate surface and recorded by the force platform.

Inertial forces - the planar forces developed by the linear acceleration of a body segment as determined by Newtonian principles of mass times acceleration. The inertial forces of the study represent the product of the linear acceleration of the centre of mass of the foot or shank and the respective mass of the segment.

Inertial torques - the moment determined from the product of the angular acceleration of the foot and shank and the respective moment of inertia of the segment about the x, y and z axes.

Skating thrust - skating has three components: the thrust, the weight shift to the glide leg and the glide on that leg. A skating thrust represents the extension of the thrust leg to drive the skater forward.

Limitations

The knee joint forces calculated in the study were for a simulated skating thrust. The skate blade to force plate contact does not exhibit the same frictional characteristics of the actual skate blade to ice contact of the normal skating environment. Therefore, the calculated joint forces represent those forces corresponding to the reaction forces as recorded in the laboratory by the force platform measurement technique. To develop the required frictional resistance force at the surface of the force platform the skater was required to wear specially prepared rubber skate blade coverings. This procedure introduced further error into the laboratory estimate of the actual reaction forces of a skating thrust executed on ice.

The results of the study are limited to the particular skating thrust of one skilled hockey player.

The nature of the experimental set-up required that the skating thrust be executed from a starting stationary position.

Delimitations and Assumptions

The following assumptions were made for the purpose

of force analysis of the knee joint forces (Morrison, 1968):

- (i) Rotation at the knee is controlled by the forces in three major muscle groups, the quadriceps femoris, hamstrings and gastrocnemius groups. The muscles of each group are considered to have confluent lines of action and the direction of the resultant force in each group is assumed to be constant with increasing force.
- (ii) The line of action of a muscle group or ligament is assumed to be coincident with the line joining its origin and insertion.
- (iii) The axis of rotation of the femur is assumed to be constant relative to the co-ordinate axes of the tibia.
- (iv) The effects of friction at the articular surface of the knee joint is neglected for the anterior-posterior movement of the joint.

To allow analysis of the external forces imposed on the knee joint the simplified muscle and ligament system shown in Figure 3.12 was adopted.

CHAPTER II

REVIEW OF LITERATURE

Introduction

The joints of the lower limbs provide the structural means for human locomotion in all activities. With the aid of muscular actions the human body can perform a multitude of co-ordinated locomotive movements through the articulating joints. However these movements and activities necessarily subject the joints and the supporting ligamentous structures to forces that must be equilibrated. The nature of athletics increases the effect of these forces on the joints of the lower limb and specifically the knee joint as pointed out by Hughston, Whatley and Dodelin (1961) and Klein (1963). The prevalence of knee injuries has been documented by several investigators such as Bender (1964) and Smillie (1970) while the function of the knee joint in various activities of locomotion has been studied and detailed by Morrison (1969).

Locomotion Studies

Walking is the most common of human locomotive activities and was initially investigated by Elftman (1938, 1939) who examined the external forces exerted, the energy changes in the leg and the function of the muscles in

walking. Elftman employed an experimental technique that determined ground reaction forces from the calibrated deflections of a force plate supported by stiff springs. Bresler and Frankel (1950) measured the orthogonal reaction forces and moments of walking using a force plate based on the force-time measuring properties of strain gauges and designed by Cunningham and Brown (1952). The reaction forces and moments together with cine film records of the position of the leg in space allowed Bresler and Frankel to evaluate the joint forces transmitted at the ankle, knee and hip during level walking. Cinematography has played an important role in the study of locomotion. Murray, Drought and Kory (1964) investigated the displacement of the lower limbs in the walking patterns of normal men while Winter (1974) has studied the kinematics of normal locomotion from TV data.

The development of electromyography as a research tool by researchers such as Basmajian (1962) has allowed investigators to study the function of muscles and muscle groups in locomotion. Joseph and Nightingale (1952) and Houtz and Walsh (1959) analyzed the function of the muscles of the lower extremity during weight bearing and normal posture using electromyographic techniques. The phasic activity of the muscles of the leg was studied by Close and Todd (1959) while Linge (1961) examined the specific behaviour of the quadriceps muscle group during walking from electromyograms. Although electromyography has been

accepted as a means of measuring muscle activity the relation between the action potentials of an electromyogram and muscle tension as studied by Lippold (1952) and others is not well established.

Biomechanical Analyses of Joint Forces

The original studies of joint forces were confined to the hip joint as related to the design of endo-prostheses for the hip. Direct determination of hip joint force was conducted by Rydell (1965, 1966) who fitted two of his patients with hip-joint prostheses instrumented with strain gauges. The largest force acting on the femoral head was 4.33 times the body weight during running while level walking forces reached values of 3.3 times the body weight. Radcliffe (1962) and Cunningham and Brown (1952) have both investigated the biomechanics of below knee prostheses using instrumented prosthetic devices. Other researchers such as Williams and Evenson (1968), Denham (1959) and Inman (1947) determined joint forces directly from tests on dissected limbs with muscles and ligaments removed. Dynamometers were used to estimate the value of hip joint force for the standing position. McLeish and Charnley (1970) determined hip joint forces in the one-legged stance.

The most definitive analysis of reaction forces at the hip joint during walking has been the recent work of Paul (1964, 1966, 1967, 1971). Paul determined the variation

with time of the magnitude of the hip joint force during walking from cine film records of leg segments and the ground reaction forces on the foot measured with a force plate. Paul found maximum hip joint forces ranging from 3.39 to 4.46 times body weight. Morrison (1968, 1970) extended Paul's studies to an engineering analysis of the forces transmitted between the femoral and tibial condyles of the knee joint during various walking activities. Maximum knee joint forces measured varied between 2.06 and 4.0 times body weight with an average value of 3.03. Morrison also integrated force plate, cinematographic and electromyographic records to estimate the tensions developed in muscle groups acting across the knee joint including the phasic relation of these forces during walking. By adopting a simplified model of the knee joint Morrison expressed the mechanics of the joint in mathematical terms and was able to evaluate the ligamentous forces from the experimental data. The greatest muscle force calculated was 405 lb acting in the quadriceps femoris group and the maximum ligament force determined was 148 lb in the lateral collateral ligament. Morrison's studies provided the first data published with respect to the magnitude of the tensile forces acting in the ligamentous structures of a joint during activity.

Recent Biomechanical Analyses

The advent of computer technology led to new methods of

evaluating locomotion data from film. Beckett and Chang (1968) determined the kinematics of gait while Dillman (1970) made a specific kinematic analysis of the recovery leg during sprint running. These studies made use of computer analysis to reduce cine film data to calculate the translational and angular accelerations of the lower limb segments. Thornton-Trump and Daher (1975) used anthropometric data including limb segment weight and mass moments of inertia to predict the moments acting at the hip and knee and the floor reaction forces from gait data. The reaction forces and knee moment data were then applied to the problem of the design of an external prosthetic polycentric knee joint.

A number of mathematical models have been developed for analysis of human body dynamics. Chaffin (1969) represented the body as a series of seven solid links articulating at the ankles, knees, hips, shoulders, elbows and wrists to develop a computerized model for several body movements. The model was designed to study body movements of lifting and carrying but the assumptions made limited the models practical applications. Seireg and Arvikar (1973, 1975) developed a mathematical model to simulate the muscular actions of the lower extremities for different static postures. They used anatomical data for the points of origin and insertion of muscles to approximate the lines of action of the muscular tensile forces. Since the mathematical formulation is statically indeterminate a linear programming method based on

a selected minimizing criteria was used to determine the muscle load sharing and corresponding hip, knee and ankle joint reactions. In a subsequent study Seireg and Arvikar extended their previous work to the analysis of muscular load sharing and joint reactions for quasi-static walking patterns. Dynamic limb data including inertia forces and moments were not included in the analysis and the ground to foot reaction force was assumed to vary linearly from zero to the body weight. Seireg and Arvikar's calculated muscle forces agreed closely with Morrison's (1969) results but their joint forces were considerably larger. Maximum joint reaction forces during the considered quasi-static walking cycle were 5.4, 7.1 and 5.2 times the body weight for hip, knee and ankle joint respectively.

Other researchers such as Chao and Kwam (1973) have employed optimization principles to evaluate the applied moments in the leg during walking while Penrod, Dary and Singh (1974) used a similar method to estimate tendon force.

Mechanics of the Knee Joint

The most comprehensive study of the movements of the knee joint and the function of the ligaments controlling these movements was made by Brantigan and Voshell (1941). Tests of function and motion were made on approximately 100 fresh and preserved knee joints stripped of all parts except the ligaments. Individual ligaments and combinations of

ligaments were cut and the function of the intact ligaments and motion of the joint was observed. A simple vice apparatus was used to measure the degree of lateral motion and rotation of the tibia on the femur. The results indicated that there is a close interrelationship of the ligaments in maintaining joint stability which can be summarized as follows:

- (1) Lateral motion in extension is controlled by the capsule, collateral ligaments and cruciate ligaments; in flexion by the same structures minus the lateral collateral.
- (2) Rotary motion in extension is controlled by the capsule, collateral ligaments and cruciate ligaments; in flexion by the same structures minus the lateral collateral.
- (3) Forward gliding of the tibia on the femur is controlled by the anterior cruciate ligament.
- (4) Backward gliding of the tibia on the femur is controlled by the posterior cruciate ligament.
- (5) Lateral gliding of the tibia on the femur is controlled by the tibial inter-condyloid eminence and the femoral condyles with aid of all the ligaments.
- (6) Hyperextension is controlled by both the collateral ligaments, both cruciate ligaments, both menisci, the posterior aspect of the articular capsule, the oblique popliteal ligament and the architecture

of the femoral condyles.

- (7) Hyperflexion is controlled by both cruciate ligaments, both menisci, the femoral attachment of the posterior aspect of the capsule, the femoral attachment of both heads of the gastrocnemius and the condyles of the femur and tibia.

Recent studies have examined the length of the ligaments for different knee positions. Edwards, Lafferty and Lange (1970) attached gauges to the ligaments of a dissected joint to measure the tensions at different angles of flexion and thereby estimate ligament length. Wang, Walker and Wolf (1973) determined the ligament length patterns for 12 specimens for various angles of flexion and degrees of rotation. The joint capsule, the four major ligaments and the quadriceps muscle together with patella attachment were retained in the testing. The length of the ligaments was determined from radiographic measurement of long metal pins inserted through drill holes in the femur and tibia so that the ends of the pins located the respective ligament attachments. Results showed that the collaterals shortened about 20 percent in length in flexion while the cruciates action was reciprocal with the anterior cruciate lengthening and the posterior cruciate shortening during flexion.

The biomechanics of normal and abnormal knee joints was examined by Engin and Korde (1974). The investigation was concerned with an experimental and theoretical study of

the changes in knee joint mechanics in degenerative joint disease. Experimental tests were conducted to determine the strain at the straingauged cross-sections of a femur and tibia specimen for normal and abnormal configuration. Soft tissues were dissected away leaving only the remaining ligaments of the joint to maintain the joint integrity. For normal joint configuration the lateral condyle contact force was greater than the medial condyle contact force with a varus deformity increasing the medial contact force and a valgus deformity increasing the lateral contact force. The tensions in the collateral ligaments were found to be dependent on the degree of knee abnormality and not on magnitude of axial load. Kettlekamp and Chao (1972) found similar variation in the force distribution with valgus and varus deformity of the lower limb.

Experimental Testing

The stability of the knee and the effect of various types of loading on the joint has been studied by several researchers. Klein (1962) designed an instrument for testing the medial and lateral collateral ligament stability of the knee. The device was attached to the thigh and lower leg of a subject with cuffs and a machinist's dial attached above the pivot point measured the deviation of the lower leg as a tester adducted or abducted the lower leg. In a later article, Klein (1964), stated that the ability of the

test to demonstrate stability or instability of the ligaments of the joint was dependent upon the experience of the tester.

Degradation of the cartilage in the knee joint has been the subject of recent research. Radin (1973) subjected the knees of adult rabbits to daily intervals of impulse loading to induce cartilage destruction similar to clinically observed degeneration in human knees. Radin's studies and those of Simon, Radin and Paul (1972) investigated the effects of suddenly applied loads or impact loading. Seireg and Gerath (1975) investigated in vivo, the effects of high speed rubbing of the patella joint of rats subjected to a constant static compressive load. The results showed that cartilage damage includes an increase of the skin temperature of the joint, and a change in surface roughness, the cellular structure and mineral content of the cartilage.

The strength of ligaments and tendons has been investigated in animals by Tipton et al. (1967, 1974) who measured the junction strength and ligamentous strength in rats and by Viidik (1966, 1967) who determined the tensile strength of isolated rabbit tendons. A review of literature on this subject has not revealed any studies relating to the strength of the ligaments in man although much literature has been published with respect to the surgical treatment of ligament injuries. (O'Donoghue, 1950)

Exercise and the Knee Joint

Several studies have been made concerning the effects of exercise on the strength of ligaments of the knee joint. Again, these investigations have been confined to animal studies. Adams (1966), Rasch et al. (1967), Tipton et al. (1967, 1975) and Zuckerman and Stull (1969, 1973) all found that the strength of knee ligaments in rats increased after a training program of running. Tipton et al. (1970) made the same observation concerning the strength of the medial collateral ligament of dogs and Viidik (1968) found an increase in strength of the anterior cruciate ligament in rabbits after training.

Although the value of exercise in strengthening ligaments is well documented, Karpovich (1970) and Klein (1971) felt the effect of deep knee bends or deep squat exercises was detrimental to the ligaments of the knee. Klein and associates conducted extensive studies of such exercises and found that football players and weight lifters who included deep squat exercises in their training and competition were subject to ligament and knee instability due to abnormal stretching. Similarly, a study of paratroopers, who used squat jumps in training, showed a high incidence of knee joint instability, especially in the medial and lateral ligaments.

Summary

The review of literature revealed that the biomechanics of the knee joint (Brantigan and Voshell, 1941) are so involved to make a thorough analysis of the forces acting at the joint and within the structures of the joint very difficult. The biomechanical analyses to date (Paul, 1964, 1966; Morrison, 1968, 1970; Seireg and Arvikar, 1973, 1975) have therefore necessarily involved procedures which required reduction of indeterminacy through assumptions of minimizing procedures and linear programming.

There is also a paucity of research with regards the strength of the ligaments of the knee in man although some testing methods have been developed (Klein, 1962) to evaluate the stability of the knee of test subjects. Similar statements can be made about the function and physical properties of the cartilage structure of the knee.

Human locomotion appears to have been thoroughly investigated in terms of kinematics, gait patterns, prosthetic devices, joint forces and muscle involvement but there remains a lack of information directly related to the forces and strains imposed on the joints of the lower extremities of the body in the more dynamic locomotive activities of athletics.

CHAPTER III

METHODS AND PROCEDURES

Anatomy of the Knee Joint

Introduction

The knee joint is a synovial condylar hinge joint that allows flexion and extension in the sagittal plane while restricting valgus and varus rotation about the long axis. The position and structure of the knee makes it an important joint in both weight bearing and locomotion. The stability and equilibrium of the knee is maintained by the supporting structure of muscles and ligaments crossing the joint. The synovial capsule and the menisci deepened articulating surfaces between the femur and tibia also aid in joint stability. Related knee structures are the fibula and the patella.

Bone structure

The femur and tibia are the weight bearing bones of the leg and therefore are directly associated with joint function while the non-weight bearing fibula and patella are only indirectly involved with knee function. (Figure 3.01)

The knee joint has three articulations. The lower end of the femur has two cylindrical shaped condyles which

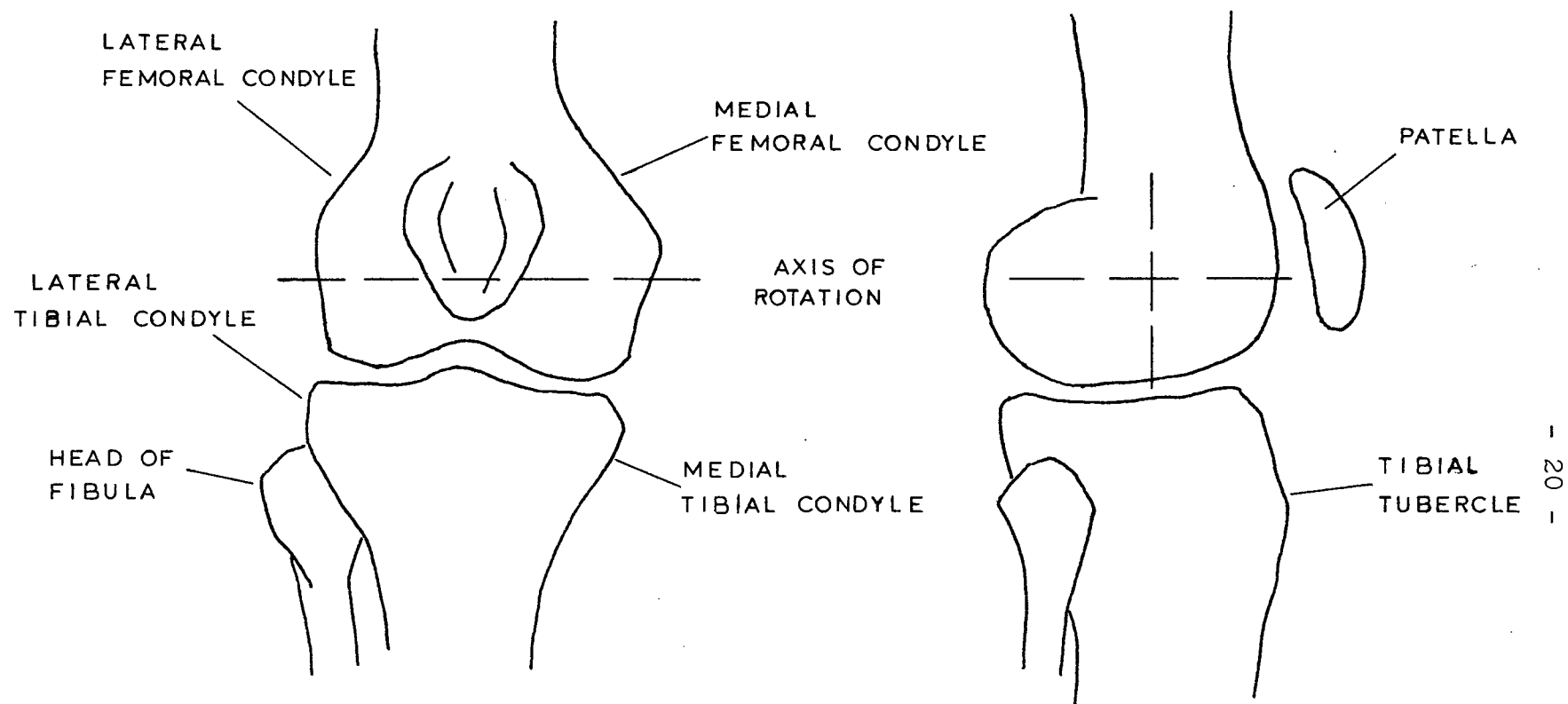


FIG. 3.01 RIGHT KNEE JOINT - BONE STRUCTURE

transmit the body weight to the circular concave condyles of the upper surface of the tibia. (Fig. 3.02) These are referred to as the medial and lateral condylar articulations and are separated by a non-articulating intercondylar notch. The large sesamoid patella bone is embedded in the quadriceps tendon and articulates with the anterior surface of the femoral condyles to form the patellar articulation. (Fig. 3.01)

The fibula, the lateral bone of the leg, is not a functioning part of the joint itself but rather provides sites for muscle and ligament attachments.

Ligamentous Structure

The stability of the knee joint is controlled by two sets of ligaments; the anterior and posterior cruciates and the medial and lateral collaterals. (Fig. 3.03)

The strong cruciates cross each other in the middle of the joint as shown in Fig. 3.04 Their main function is to limit anterior and posterior dislocation of the joint but they also check hyperextension, rotation about the long axis and side to side movement of the joint.

The collateral ligaments prevent abduction and adduction of the joint while allowing a wide range of flexion and extension in the sagittal plane. The medial collateral has a superficial part and a deep part with the deep fibres of ligament adhering to the medial meniscus (Fig. 3.04). The

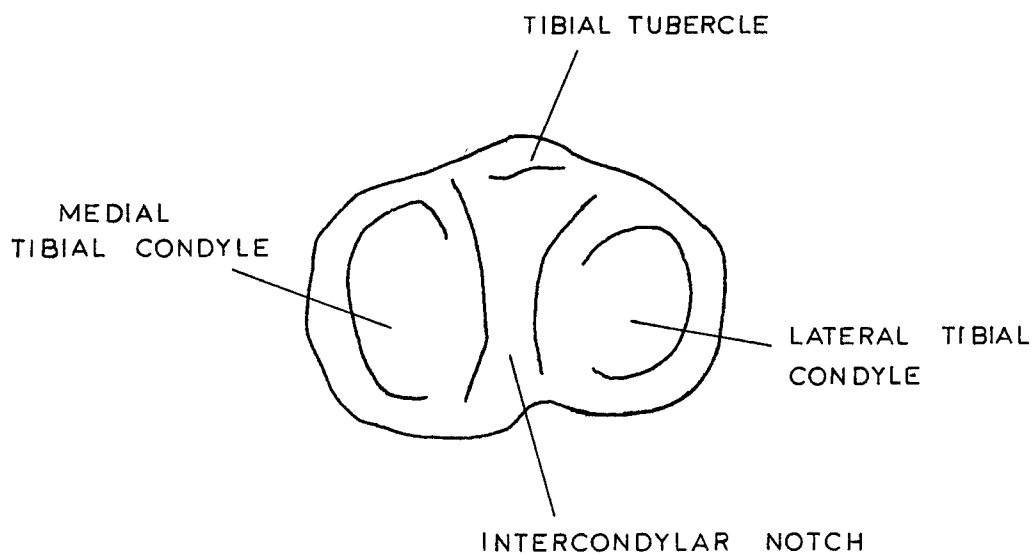


FIG. 3.02 SUPERIOR SURFACE - TIBIA

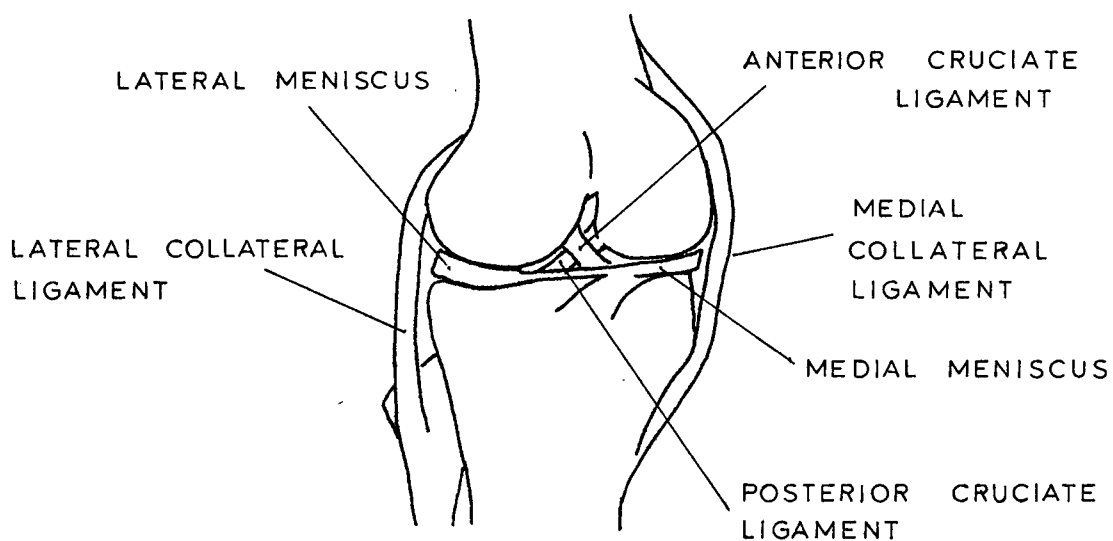


FIG. 3.03 LIGAMENTS OF KNEE JOINT

lateral collateral is a singular cord-like ligament with no adherence to the lateral meniscus. The collaterals are slack in flexion but taut in extension as the distance between the joint surfaces increases. The collateral ligaments along with the cruciates and intercondylar notch restrict rotation of the femur relative to the tibia.

The strong patellar ligament is an extension of the quadriceps tendon and it provides anterior joint stability through its attachment to the tibial tuberosity of the tibia. (Fig. 3.05)

In addition to the main ligaments of the knee, there are two minor ligaments whose function is not well defined. These are the oblique popliteal ligament and the arcuate popliteal ligament situated on the posterior side of the joint.

Menisci and Associated Structures

The menisci deepen the concave condyles of the tibia to aid the articulation of the femoral condyles on the tibial surfaces. The menisci, which are semi-lunar shaped, have a wedge like cross-section with interior borders that taper to thin edges. (Fig. 3.03) The lateral meniscus is smaller in diameter, thicker about the periphery and more circular than the medial meniscus but covers a larger portion of the articular surface as it is wider. (Fig. 3.04) The anterior margins of the two menisci are continuous with the transverse

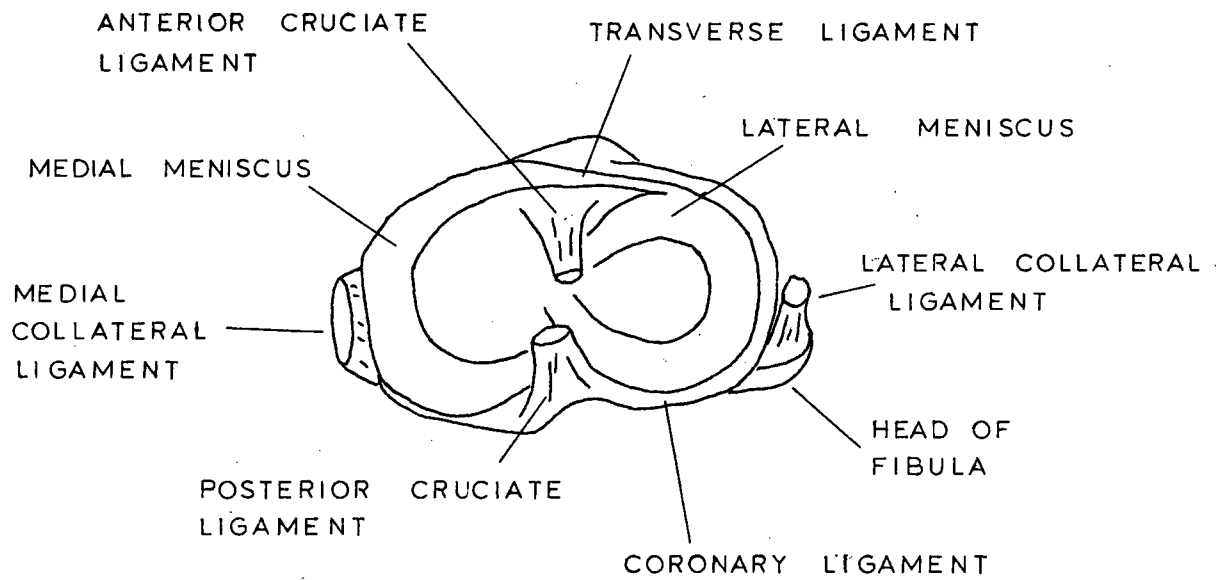


FIG. 3.04 LIGAMENTS OF KNEE JOINT

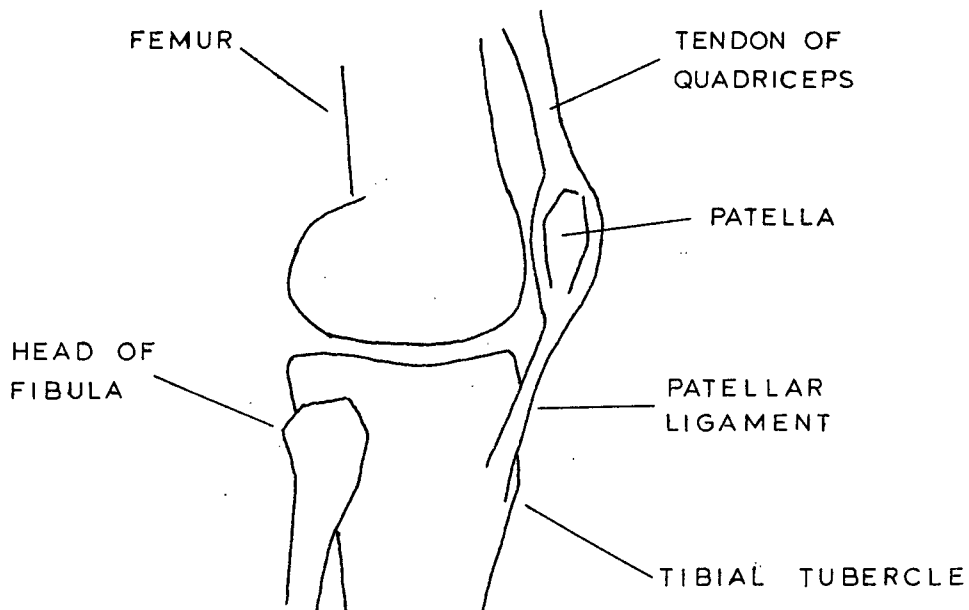


FIG. 3.05 PATELLAR LIGAMENT

ligament while the periphery of the menisci are connected to the tibia by a fibrous portion of the articular capsule known as the coronary ligament (Fig. 3.04). The medial meniscus is attached tightly compared to the lateral meniscus accounting for a difference in mobility.

Muscle System

The muscle groups that control the movements of the knee joint can be divided into extensors and flexors. (Fig. 3.06)

The main extensors form the strong quadriceps femoris group and include rectus femoris, vastus lateralis, vastus medialis and vastus intermedius muscles (Fig. 3.06) which join to form the quadriceps tendon. Some fibres of this tendon insert into the patella while others pass over the patella to blend with the patellar ligament.

The main flexors of the knee form the hamstring group. These include the biceps femoris, the semimembranosus and the semitendinosus (Fig. 3.06). These muscles cross the joint posteriorly to attach to the surfaces of the fibula and the tibia.

The two headed gastrocnemius muscle forms the greater part of the calf and is a weak flexor of the knee. The fibres of the gastrocnemius and the deeper soleus muscle unite to form the tendo calcaneus which attaches to the calcaneus bone of the foot. The small plantaris muscle, the

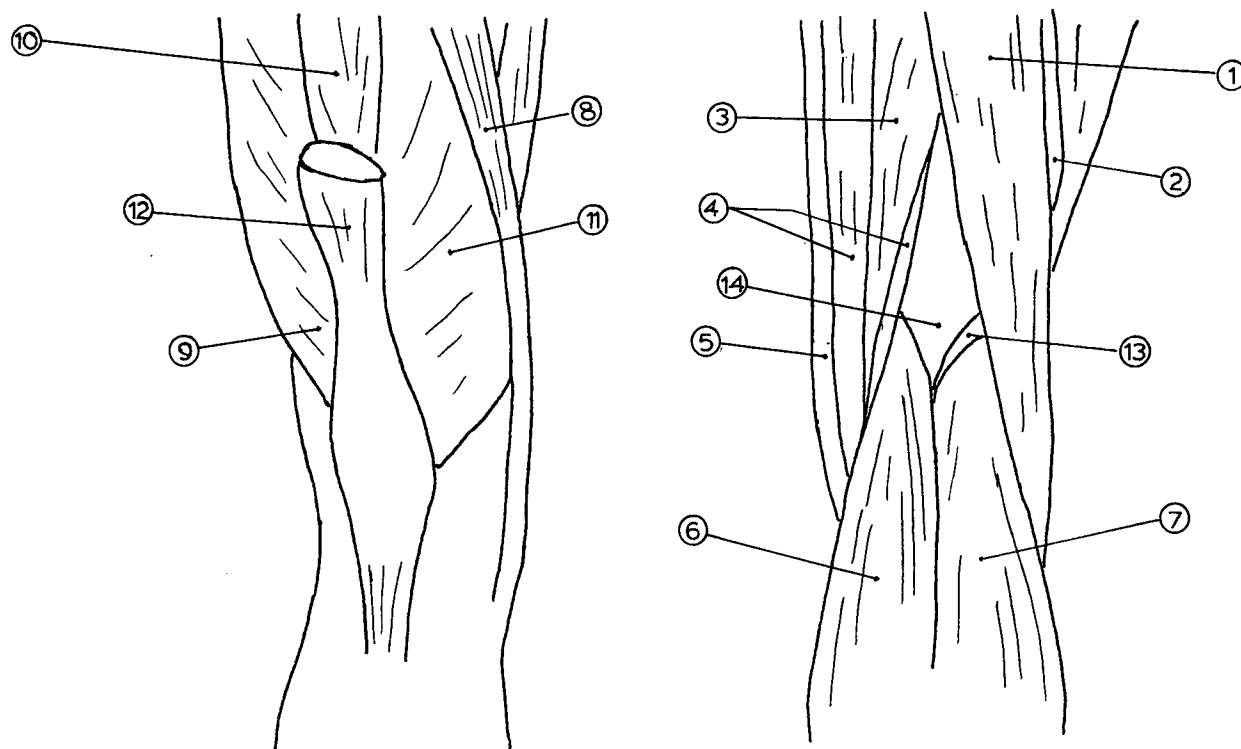


FIG. 3.06 MUSCLES CONTROLLING KNEE JOINT

- | | | |
|----------------------|----------------------------|------------------------|
| 1. BICEPS LONG HEAD | 5. GRACILIS | 9. VASTUS LATERALIS |
| 2. BICEPS SHORT HEAD | 6. GASTROCNEMIUS MED. HEAD | 10. VASTUS INTERMEDIUS |
| 3. SEMITENDINOSUS | 7. GASTROCNEMIUS LAT. HEAD | 11. VASTUS MEDIALIS |
| 4. SEMIMEMBRANOSUS | 8. SARTORIUS | 12. RECTUS FEMORIS |
| 13. PLANTARIS | 14. POPLITEAL FOSSA | |

soleus and the gastrocnemius are the main plantar flexors of the foot (Fig. 3.06).

Other weak flexors of the knee are the long sartorius muscle, the thin flat gracilis muscle, the plantaris and the triangular popliteus muscle (Fig. 3.06). The sartorius and gracilis assist medial rotation of the tibia in flexion while the popliteus aids in unlocking the joint at the onset of flexion.

Concepts of Analysis

Reference Axes of Knee

To analyze the forces acting at the knee joint, Morrison's (1973) reference axes were adopted. These Xs, Ys, Zs axes are referenced with respect to the tibia and have their origin at the assumed joint centre of the knee. (Fig. 3.07) The horizontal Xs axis coincides with the medial-lateral axis of the tibial condyle surfaces, the anterior-posterior Ys axis coincides with the mid-axis of the intercondylar notch while the Zs axis represents the vertical axis of the tibia. (Fig. 3.08)

Axes of Femur and Pelvis

In order to calculate the muscle and ligament attachments to the femur and pelvis, two additional reference axes are required.

Morrison's (1973) femoral reference axes Xf, Yf, Zf

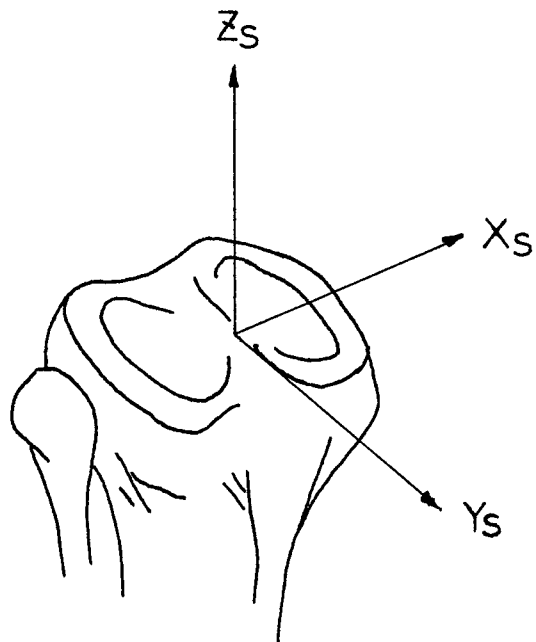


FIG. 3.07 TIBIAL REFERENCE AXES

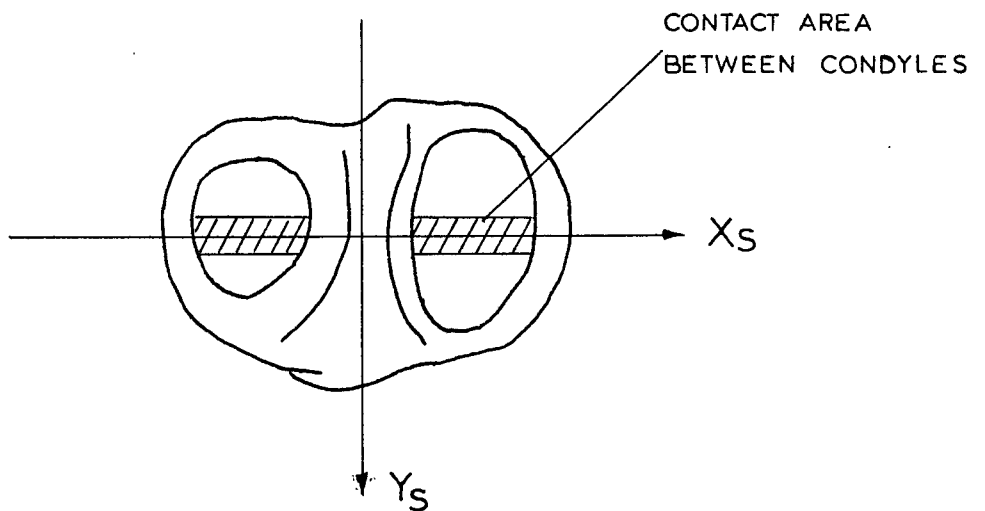


FIG. 3.08 TIBIAL CONDYLES

were adopted (Fig. 3.09). The Xf axis coincides with the centre line of the femoral condyles and is parallel to the Xs axis of the tibia and the Yf axis is parallel to the Ys axis of the tibia. The Zf axis is coincident with the Zs axis of the tibia but only in 180° extension.

The intersection of the centre line of the femoral condyles and the Zs axis determines the origin of the femoral reference axes. This origin is not fixed in flexion relative to the tibial axes (Fig. 3.10) due to the character of joint articulation discussed below.

The reference axes of the pelvis, Xp, Yp, Zp were chosen with origin at the centre of the acetabulum (Fig. 3.11). The Xp axis is parallel to the line joining the anterior superior spines of the hip bones, the Yp axis lies in the sagittal plane and the Zp axis is perpendicular.

Movements of the Knee Joint

The main movements of the knee joint are flexion and extension through about 135 degrees. These movements are governed by the shape of the joint articular surfaces and the resistance of the ligaments and muscles that cross the joint. For the greater part of the joint's range of motion, the cylindrical femoral condyles slide on the tibia with a fixed line contact on the concave tibial condyles. However, in the last 10 to 20 degrees of extension the femoral condyles roll forward on the tibial surface. Similarly the

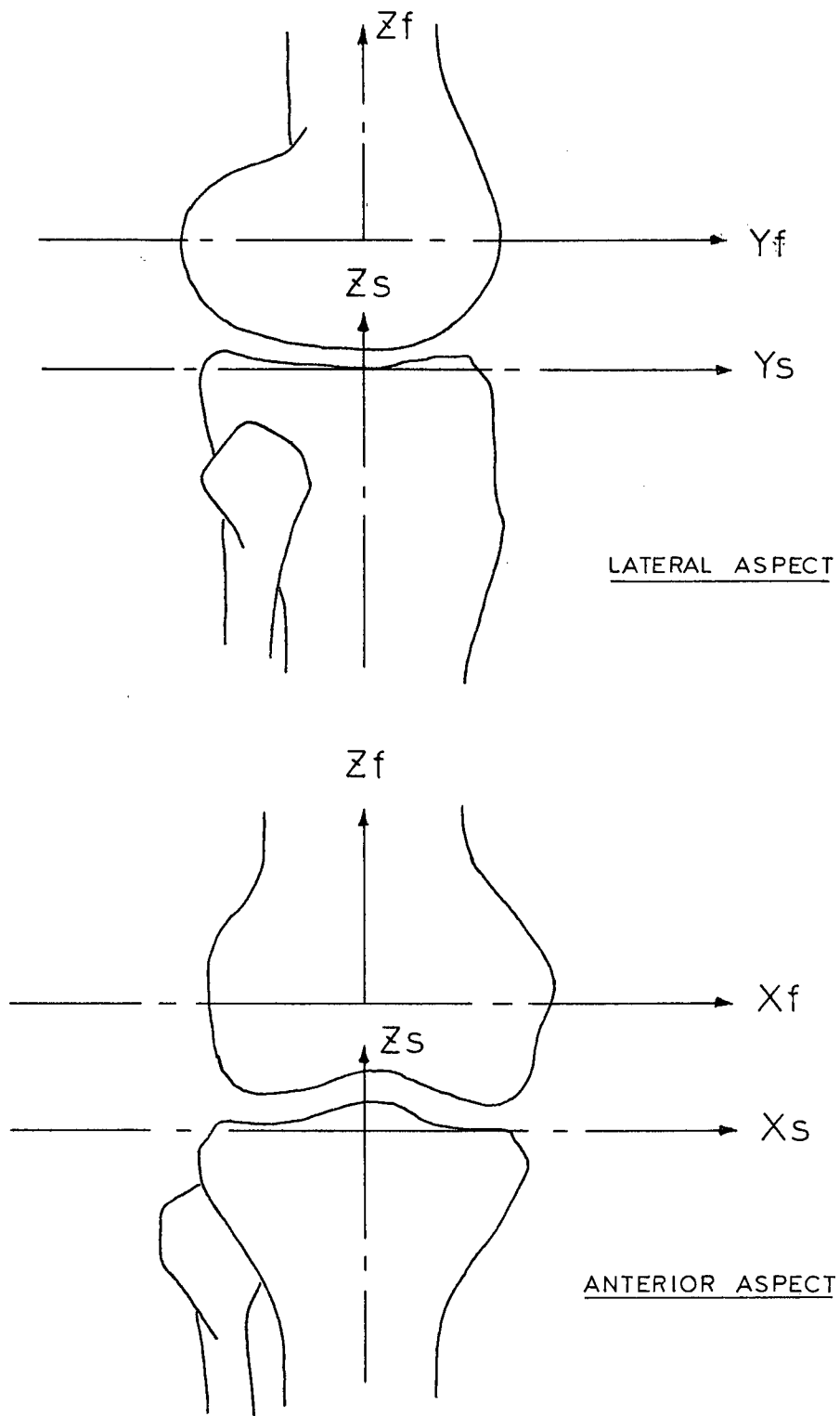


FIG. 3.09 REFERENCE AXES - FEMUR, TIBIA

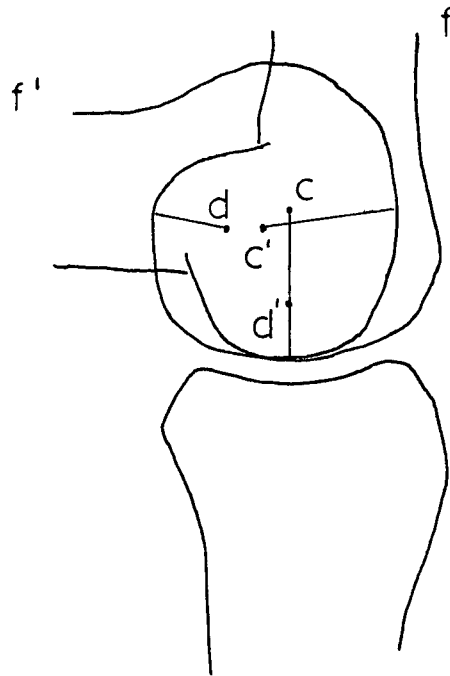


FIG. 3.10 ERROR IN ASSUMED CENTRE
OF ROTATION OF FEMUR IN
90° FLEXION - cc'

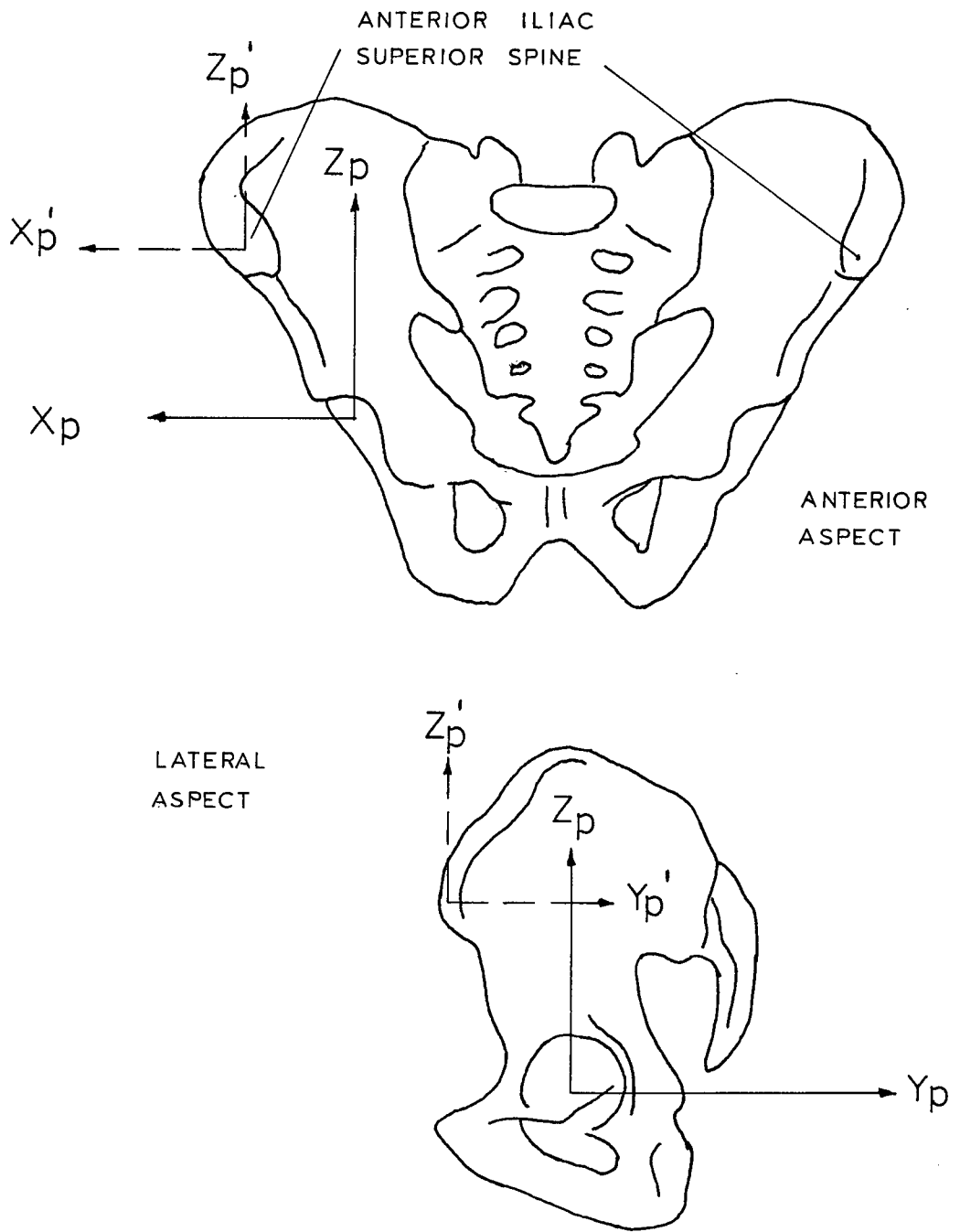


FIG. 3.11

PELVIC REFERENCE AXES

first 10 to 20 degrees of flexion involve a backward rolling of the femoral condyles. The line contact of the joint surfaces is assumed to be coincident with the Xs axis of the tibia (Fig. 3.08). The rolling of the femoral condyles causes an anterior or posterior displacement of this contact line during articulation and introduces an error in the above assumption.

The final 10 to 15 degrees of knee extension are accompanied by an outward rotation of the tibia relative to the femur. This movement is known as "locking" of the joint and a similar "unlocking" action occurs at the onset of flexion. The locking and unlocking actions coincide with the rolling phase of joint movement.

In full extension, rotation of the joint about the long axis is restricted but up to 25 degrees of rotation can occur in flexion as the ligaments across the joint begin to slack. Also some lateral motion at the joint surfaces is allowable between 30 and 50 degrees flexion.

Muscle and Ligament System

In order to complete an analysis of the forces imposed at the knee, a simplified muscle and ligament system after Morrison (1970:34) was adopted. In this simplified anatomical model, the four main ligaments of the joint, the cruciates and the collaterals, are assumed to have individual force actions. The muscles that cross the joint were divided into

three separate groups so that the muscles of each group act synchronously. The complete system is defined as follows: (Fig. 3.12)

- (1) Hamstrings; including biceps femoris, semitendinosus and semimembranosus.
- (2) Gastrocnemius; including lateral and medial heads of gastrocnemius and plantaris.
- (3) Quadriceps femoris; including rectus femoris, vastus medialis, vastus intermedius and vastus lateralis.
- (4) Cruciate Ligaments; anterior and posterior.
- (5) Collateral Ligaments; medial and lateral.

The four muscles of the knee not accounted for in the above model, tensor fascia latae, gracilis, sartorius and popliteus are assumed to be of insignificant importance for this study and are therefore excluded from the analysis. In actual fact, the tensor fascia latae acts with the quadriceps group, gracilis and sartorius aid the hamstrings group and popliteus is associated with the "unlocking" action of the knee.

Anthropometry

Introduction

In order to calculate the lines of force action of the muscle groups and ligaments at the knee, the co-ordinates of their skeletal attachments are required.

The present analysis utilizes Morrison's (1970) anthro-

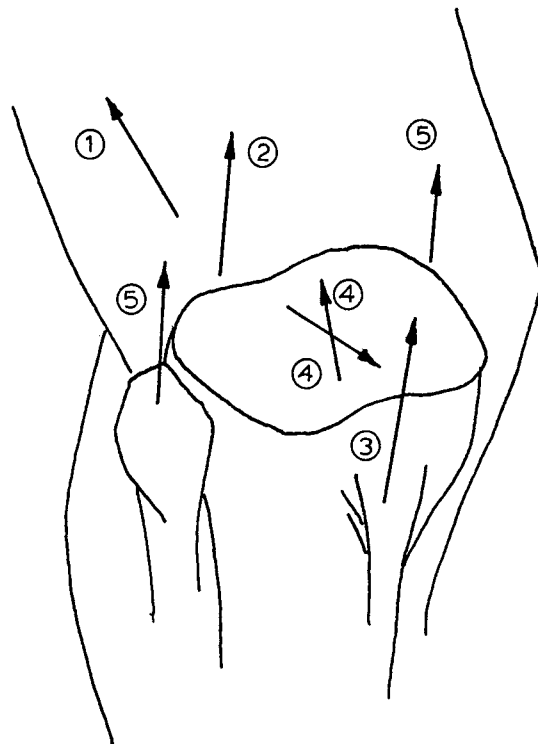


FIG. 3.12 SIMPLIFIED MUSCLE AND LIGAMENT
SYSTEM ACTING AT KNEE JOINT

- | | |
|-----------------------|-------------------------|
| 1. HAMSTRINGS | 4. CRUCIATE LIGAMENTS |
| 2. GASTROCNEMIUS | 5. COLLATERAL LIGAMENTS |
| 3. QUADRICEPS FEMORIS | |

pometric measurements to determine the co-ordinates of attachment for the test subject.

Measurements

Morrison (1970) determined the co-ordinates of muscle and ligament attachment for a dissected male limb. These measurements, which were made in inches relative to the tibial (s) and femoral (f) axes of the amputated limb, are given in Table No. 1. Muscle origin co-ordinates for the pelvis represent measurements relative to Morrison's pelvic (p) axis with centre at the anterior superior spine of the right hip bone (Fig. 3.11). For the hamstrings group a common muscle origin was assumed for the biceps femoris, semimembranosus and semitendinosus muscles. Also, since the gastrocnemius muscle group has a medial and lateral head, an equivalent common insertion on the femur was assumed so that its line of action passed through the tendo calcaneus to the mid-point of the posterior surface of the femoral condyles.

Since the line of action of the quadriceps femoris muscle group is continuous with the line of action of the patellar ligament, Morrison (1970) developed a relationship between the angle of the patellar ligament and the angle of knee flexion (Fig. 3.13).

$$\begin{aligned} \theta_q = & 0.31 \times 10^{-4} (\phi) - 8.4 \times 10^{-3} (\phi)^2 \\ & + 0.37 \times 10^{-2} (\phi) + 15.3.01 \end{aligned}$$

TABLE NO.1 ANTHROPOMETRIC DATA

Xsq	0.0	Xsl	1.65	Xffa	0.15
Ysq	-1.3	Ysl	1.0	Yffa	0.4
Zsq	-1.55	Zsl	-1.1	Zffa	0.2
Xsh	0.0	Xffl	1.6	Xsp	0.0
Ysh	1.0	Yffl	0.2	Ysp	0.65
Zsh	-1.05	Zffl	0.25	Zsp	-0.25
Xph	-2.24	Xsm	-0.85	Xffp	-0.3
Yph	4.35	Ysm	0.3	Yffp	-0.3
Zph	-3.95	Zsm	2.35	Zffp	-0.2
Xsg	0.0	Xffm	-1.8	Xpfh	-1.1
Ysg	2.0	Yffm	0.1	Ypfh	2.0
Zsg	-16.0	Zffm	0.65	Zpfh	-2.4
Xsfg	0.0	Xsa	-0.15	Xl	0.72
Ysfg	1.1	Ysa	-0.4	Zsfc	0.8
Zsfg	1.1	Zsa	0.15		
KNEE SCALING DIMENSIONS			PELVIC SCALING DIMENSIONS		
X	Y	Z	X	Y	Z
3.5	3.35	16	8.7	4.35	5.0

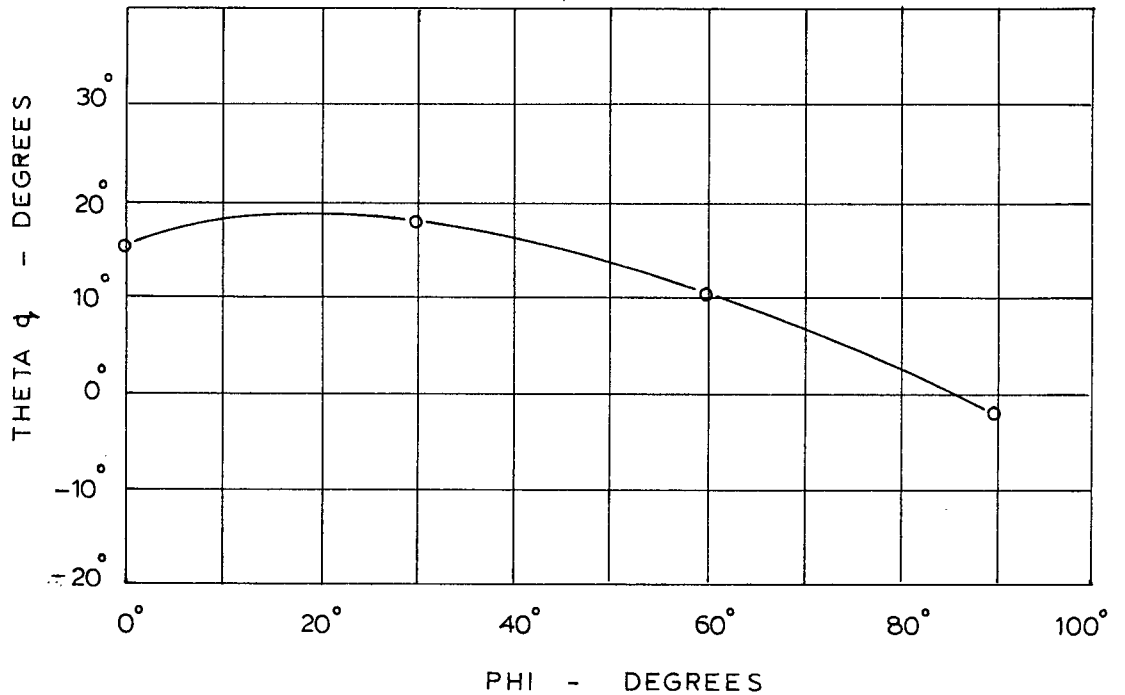


FIG. 3.13 ANGLE OF PATELLAR
LIGAMENT RELATIVE TO
ANGLE OF KNEE FLEXION

THETA q - ANGLE BETWEEN LINE OF
PATELLAR LIGAMENT AND LONG
AXIS OF TIBIA (Z_5)

PHI - - - ANGLE OF FLEXION OF KNEE
JOINT

where,

theta q = angle between the line of patellar ligament and
the vertical axis of the tibia (Zs).

phi = angle of flexion of the knee joint

Scaling Factors

The co-ordinates of muscle and ligament attachment for the test subject were obtained by using Morrison's anthropometric measurements of Table No. 1 and appropriate scaling factors. To determine the scaling factors for the test subject, the knee and pelvic scaling dimensions of the test subject were compared to the corresponding measurements from the amputated limb and skeleton of Morrison's (1970) study. The scaling dimensions are listed in Table No. 2 of the results section along with additional anthropometric data for the test subject while the scaling factor calculations are given in Appendix A.

Testing Procedures

Introduction

The test subject for the study was an experienced and accomplished ice hockey player. The testing was conducted in laboratories of the University of Washington and the University of British Columbia. Synchronized film records and oscilloscope force records were obtained with the force plate apparatus at the University of Washington for a simu-

lated skating stride. Electromyograph tests were completed at the University of British Columbia to compare the phasic muscle activity of a simulated skating stride in the laboratory with an actual on-ice skating stride. The electromyograph data was necessary to allow for a solution of the indeterminate equations of the force system.

Cinematography Procedures

The test subject was filmed in the sagittal and frontal planes while executing a simulated skating stride.

To determine limb movement, the test subject wore swimming trunks and white circular reference markers, 0.75 inches in diameter, were placed on the lower right limb and pelvis. The locations of the reference markers, shown in Fig. 3.14 were as follows:

- (1) at the hip joint centre over the femoral head of the acetabulum articulation on the lateral and frontal sides of the hip
- (2) at the knee joint centre over the lateral epicondyle of the femur and at the corresponding frontal location
- (3) at the ankle joint centre on the front and lateral sides
- (4) at the centre of gravity of the shank on the front and lateral sides (see Appendix A)
- (5) at the centre of gravity of the foot and skate on

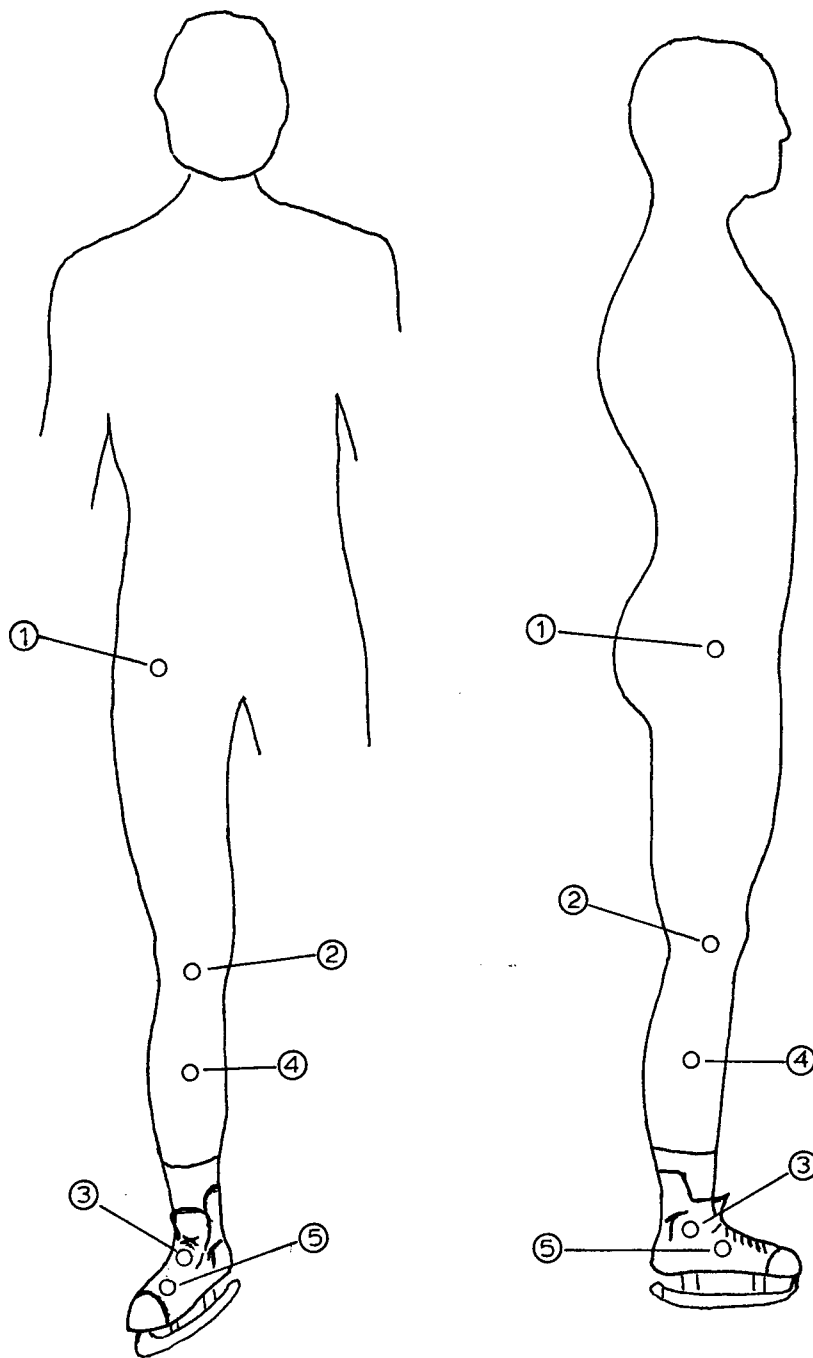


FIG. 3.14 LOCATION OF REFERENCE MARKERS

the front and lateral sides (see Appendix A)

Two 16 mm motion picture cameras detailed in Appendix B, were used to record the skating stride at a filming speed of 64 frames per second. The film records and the reference markers allowed location in time of the X, Y, Z co-ordinates of the joint centres and of the centres of gravity of the lower right limb.

The experimental set-up with the location of the cameras is shown in Fig. 3.15.

Force Measurements

A force analysis of a movement during any activity involves the use of precise and sophisticated measuring equipment. A KISTLER piezo-electric force plate with a six-component force measuring system (Appendix B) was utilized to determine the reaction forces developed during the simulated skating stride. The six-channel output of the force plate was stored as continuous traces on three oscilloscopes. A 35 mm camera with suitable oscilloscope attachment was then used to photograph these traces for later digitization. The force record obtained from the force plate output is expressed as the three orthogonal force components (F_{xp} , F_{yp} and F_{zp}) at the plate, the moment about the Z-axis (M_{zp}) and the co-ordinates of the point of application (A_x , A_y) of the force (Fig. 3.16).

The synchronization of the force plate oscilloscope

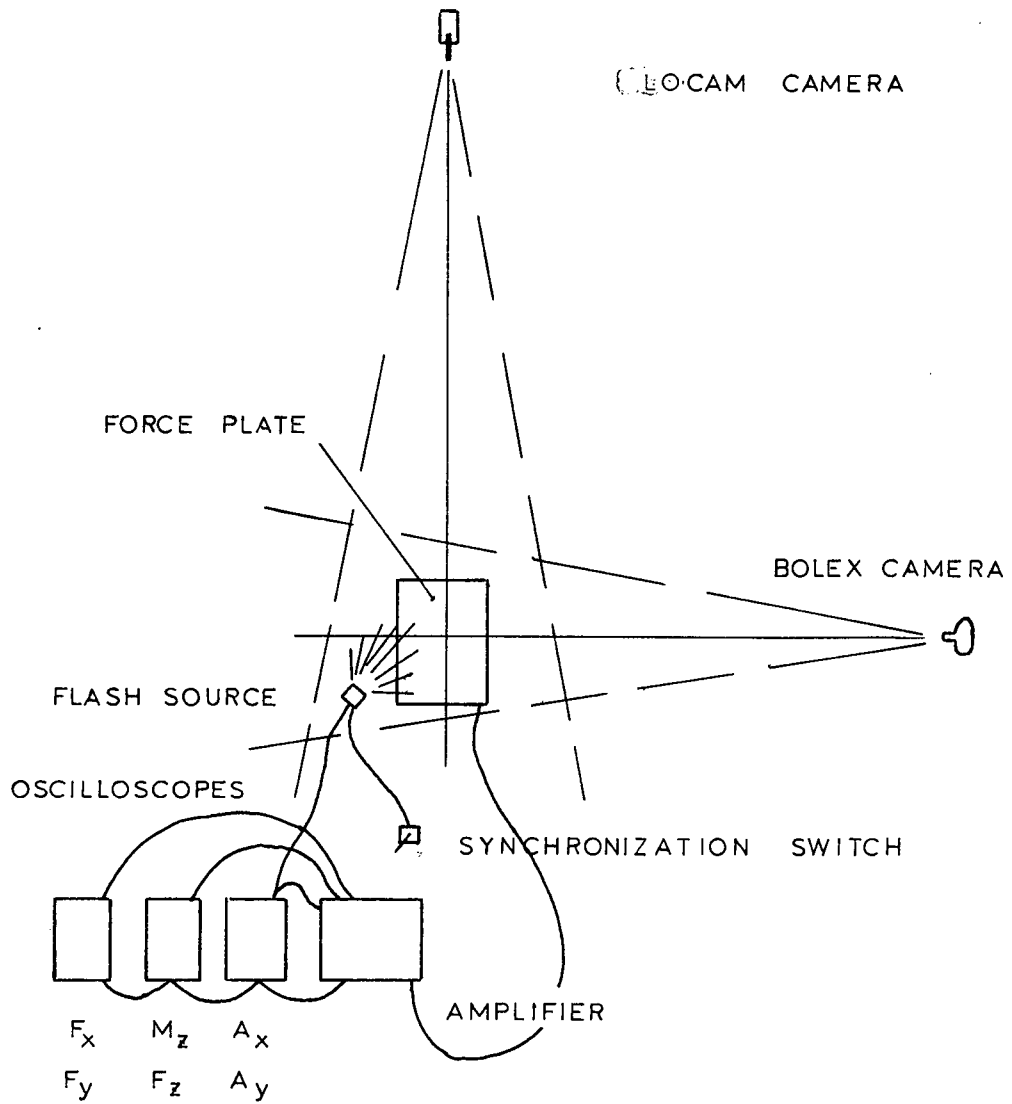


FIG. 3.15 EXPERIMENTAL SET-UP

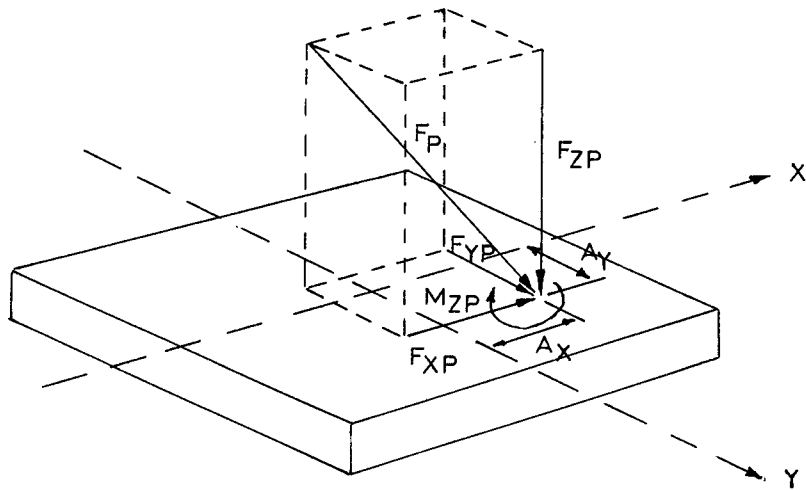


FIG.3.16 FORCE RECORD OF FORCE
PLATE EXPRESSED AS SIX
MEASURED VARIABLES

F_{XP}, F_{YP}, F_{ZP} — ORTHOGONAL FORCE COMPONENTS
OF FORCE , F_P

M_{ZP} — MOMENT ABOUT VERTICAL AXIS

A_X, A_Y — POINT OF APPLICATION OF FORCE , F_P

traces with the 16 mm film record was achieved with a flash source as shown in Fig. 3.15. The flash source was placed in the field of the 16 mm cameras and was connected in series to a control switch and the external trigger source of the oscilloscope. Closing the switch initiated the oscilloscope trace and illuminated the flash simultaneously thereby synchronizing the force plate output with the film record.

Electromyography

To compare the muscle activity of a simulated skating stride to an actual skating thrust, electromyograph tests were conducted both in the laboratory and on ice. Therefore, independent electromyograph tests were conducted at the exercise physiology laboratory of the University of British Columbia and on ice at the Thunderbird Winter Sports Centre.

Surface electrodes were attached over the belly of the rectus femoris, biceps femoris and gastrocnemius muscles to record the electrical activity of the quadriceps femoris, hamstrings and gastrocnemius muscle groups respectively. A two-channel Sanborn Recorder (Appendix B) was used to monitor the electrical signals.

The electromyograph records were synchronized with 16 mm film records by means of a flash source in the field of the camera triggered simultaneously with the Sanborn Recorder. Since the muscle groups were connected to the two-channel recorder in pairs, before each test the output

signal of one muscle group was checked for interference from the output signal of the other monitored muscle group.

Simulated Skating Thrust

The normal skating stride has three distinct movements which can be described as follows:

- (1) the thrust extension by the pushing leg,
- (2) the weight shift to the glide leg and
- (3) the glide on the supporting glide leg.

The present study is concerned with an analysis of the forces acting at the knee during the thrust extension phase of a simulated skating stride executed in a laboratory environment.

The test subject performed the skating thrust from a stationary position with the right skate blade placed at the centre of a force plate and pointing in the positive Y-direction. (Fig. 3.17). The subject initiated movement by shifting the body weight from the rear left foot to the right foot and then driving off the right foot to land on the left foot in front of the force plate. To allow the skater to develop the required thrusting force on the force plate, rubber skate blade guards were placed on both of the subject's skates. The test subject performed the skating thrust in the laboratory using a hockey stick to duplicate the arm action of a hockey player's stride.

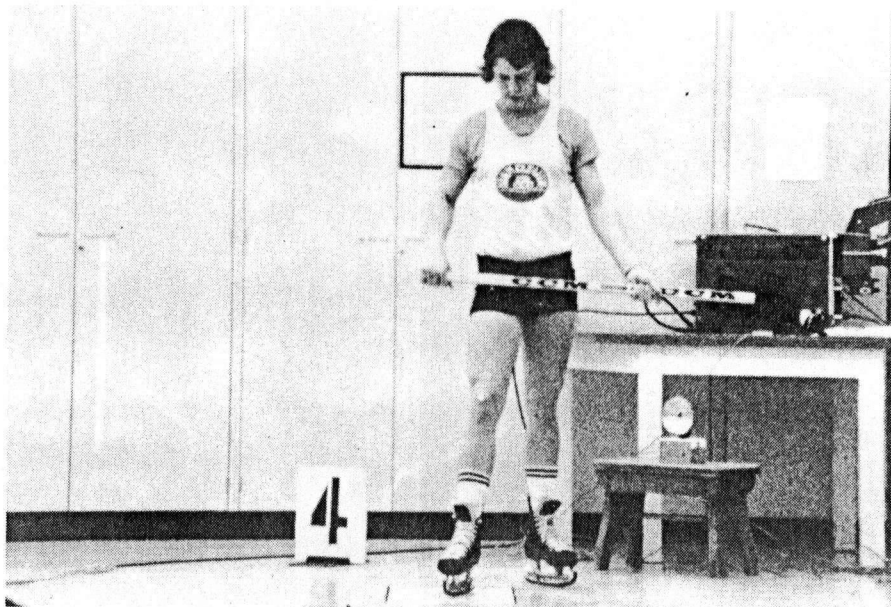


FIG.3.17 EXPERIMENTAL SET-UP SHOWING
TEST SUBJECT ON FORCE PLATFORM

Data Reduction

For each test trial, the co-ordinates for the lower limb were obtained from the developed 16 mm film and the force plate output was obtained from the developed 35 mm photographs of the respective oscilloscope traces. A Vanguard Motion Analyzer of the Institute of Animal Resource Ecology (I.A.R.E.) was used to digitize the film data. For each frame of the 16 mm film describing the skating stride, the co-ordinates of each limb reference marker relative to an origin located at the centre of the force plate were measured. The skating stride was adequately represented by 50 frames of the 16 mm film. The X, Y and Z co-ordinate readings were made to the nearest 0.001 inch with respect to the scale of the Vanguard projected image. The actual readings were obtained by multiplying the Vanguard measurements by an appropriate scaling factor, the scale determined from the film image of a five foot length surveyor's range pole held at the centre of the force plate. (Appendix C)

The synchronized force plate records on 35 mm film were also digitized with the Vanguard Motion Analyzer by dividing the traces into 50 equal horizontal increments corresponding to the 50 frames of the 16 mm film. The actual force readings were then determined by applying the suitable force plate and oscilloscope calibration factors (Appendix C) to the vertical co-ordinate measure of the Vanguard image. The force plate readings were taken for each frame of film at a film speed of 64 frames/sec or for every 0.16 sec time interval.

The electromyographic output was examined with respect to the time interval used to describe the skating stride (50 frames or 0.80 sec) to determine the phasic activity of the muscle groups involved. The period of activity for each muscle group was defined relative to the film frames.

A general computer program, DIFRN, was written to calculate the external force system acting at the knee and the corresponding muscle and ligament forces for each frame of film analyzed. Input data included limb co-ordinates, joint co-ordinates, force plate reactions, anthropometric measurements and electromyograph information.

Analysis

Introduction

The analysis of the film and force plate data to determine the muscle, ligament and joint forces acting at the knee is outlined in the flow chart of Fig. 3.18. The following text summarizes the steps involved in the analysis while a more detailed description is given in the Appendices.

Limb and Joint Co-ordinates

The co-ordinates of the joints and mass centres of the lower limb were determined from the location of the corresponding reference markers in the frontal and sagittal planes. The actual co-ordinates were corrected for the distance of the reference markers from the respective joint centre or

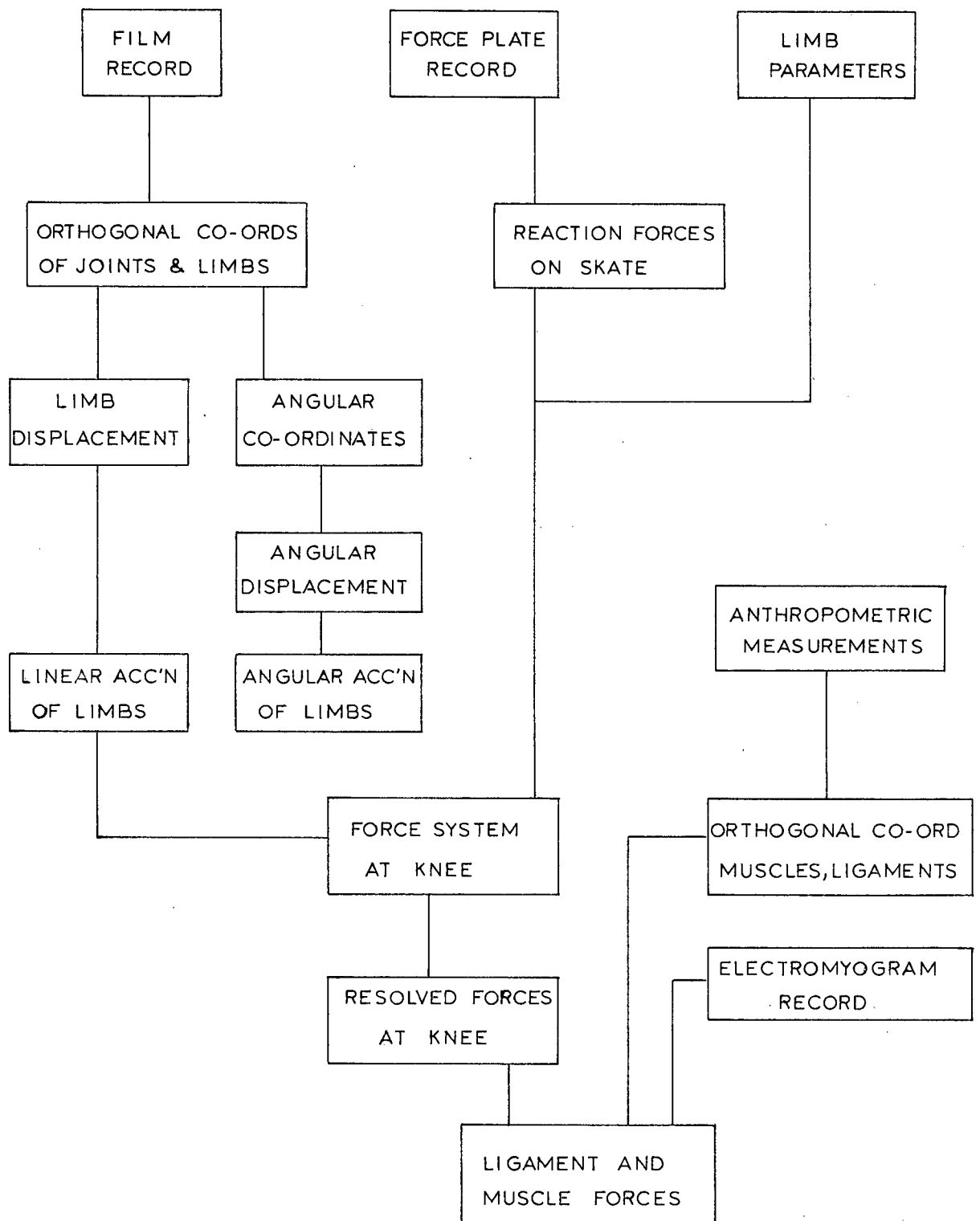


FIG. 3.18 ANALYSIS OF DATA

centre of mass and for the rotation of the limb. (Appendix D) The angular co-ordinates of the axes of the thigh, the tibial axes and the axes of the foot were also determined.

Limb Acceleration

The displacements in time of the centres of mass of the lower limb were determined from the limb co-ordinates for each frame of film analyzed. A nine-point numerical differentiation technique developed by Lanczos (1957) was then used to calculate the linear acceleration of the mass centres of the shank and foot from the displacement data. Linear accelerations were calculated for the respective X, Y and Z directions. Similarly the angular accelerations of the shank and foot about the X, Y and Z axes were determined from the corresponding angular co-ordinates and angular displacements.

The numerical differentiation technique which is based on the theory of finite differences is described in Appendix H.

External Force System at the Knee

The six component external force system acting at the knee joint centre, Fig. 3.19 represents the orthogonal summation of all moments and forces acting on the lower limb, Fig. 3.20. The forces acting on the limb are:

- (a) the force plate reactions

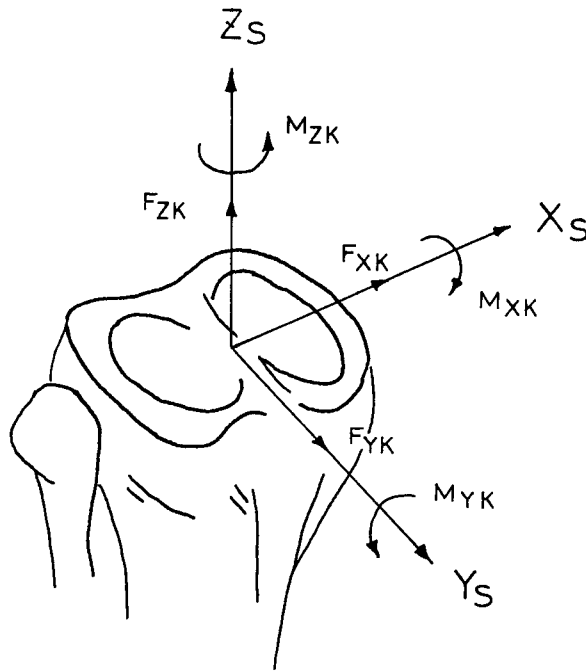


FIG.3.19 EXTERNAL FORCE SYSTEM
AT KNEE. EXPRESSED IN
TERMS OF TIBIAL REFERENCE
AXES OF RIGHT KNEE

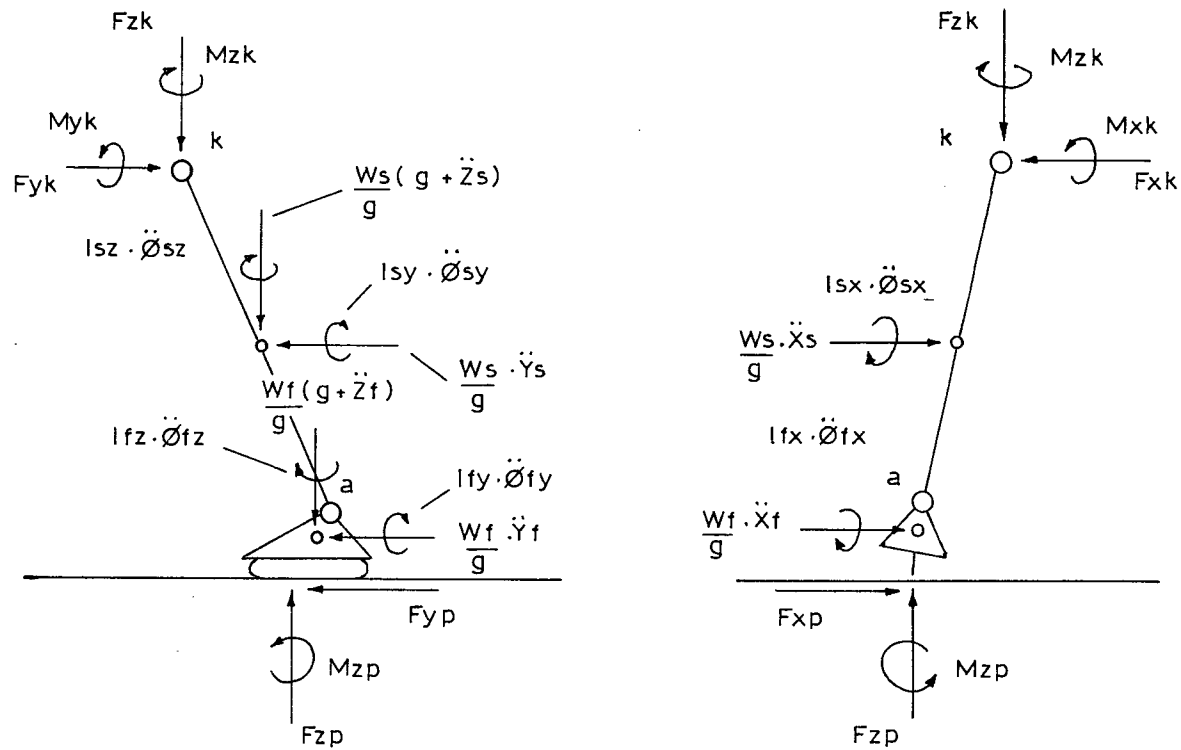


FIG.3.20 FORCES ACTING ON LOWER LIMB INCLUDING
REACTION FORCES, GRAVITY FORCES AND
ACCELERATION FORCES

- (b) the gravitational forces and
- (c) the inertial forces of the foot and shank.

The gravitational forces represent the weight of the foot and shank while the inertial forces are due to the acceleration of the foot and shank masses. The mass of the subject's shank and foot was determined from Dempster's (1955) percentage figures and the moments of inertia of the shank and foot were calculated from Braune and Fischer's (1889) coefficients C_3 and C_4 . (Appendix A)

By considering the lower limb as a free body and by summing the forces and moments acting on the limb (Fig. 3.20) in terms of the knee reference axes, six equations expressing the equilibrium conditions of the lower limb are derived.

$$F_{xk} = F_{xp} + \frac{W_s}{g} \cdot \ddot{X}_s + \frac{W_f}{g} \cdot \ddot{X}_f \dots \dots \dots 3.02a$$

$$F_{yk} = F_{yp} + \frac{W_s}{g} \cdot \ddot{Y}_s + \frac{W_f}{g} \cdot \ddot{Y}_f \dots \dots \dots 3.02b$$

$$F_{zk} = F_{zp} - \frac{W_s}{g}(g + \ddot{Z}_s) - \frac{W_f}{g}(g + \ddot{Z}_f) \dots \dots \dots 3.02c$$

$$\begin{aligned} M_{xk} = & F_{zp}(Y_k - A_y) - F_{yp}(Z_k) - \frac{W_f}{g} \cdot \ddot{Y}_f(Z_k - Z_f) \\ & - \frac{W_s}{g} \cdot \ddot{Y}_s(Z_k - Z_s) - \frac{W_f}{g}(g + \ddot{Z}_f)(Y_k - Y_f) \\ & - \frac{W_s}{g}(g + \ddot{Z}_s)(Y_k - Y_s) \\ & + I_{sx} \cdot \ddot{\theta}_{sx} + I_{fx} \cdot \ddot{\theta}_{fx} \dots \dots \dots 3.02d \end{aligned}$$

$$M_{yk} = - F_{zp}(X_k - A_x) + F_{xp}(Z_k) + \frac{W_f}{g} \cdot \ddot{X}_f(Z_k - Z_f)$$

$$\begin{aligned}
 & + \frac{W_s}{g} \cdot \ddot{X}_s(Z_k - Z_s) + \frac{W_f}{g}(g + \ddot{Z}_f)(X_k - X_f) \\
 & + \frac{W_s}{g}(g + \ddot{Z}_s)(X_k - X_s) \\
 & - I_{sy} \cdot \ddot{\theta}_{sy} - I_{fy} \cdot \ddot{\theta}_{fy} \dots \dots \dots 3.02e
 \end{aligned}$$

$$M_{zk} = M_{zp} + F_{yp}(X_k - A_x) - F_{xp}(Y_k - A_y)$$

$$\begin{aligned}
 & - \frac{W_f}{g} \cdot \ddot{X}_f(Y_k - Y_f) - \frac{W_s}{g} \cdot \ddot{X}_s(Y_k - Y_s) \\
 & + \frac{W_s}{g} \cdot \ddot{Y}_s(X_k - X_s) + \frac{W_f}{g} \cdot \ddot{Y}_f(X_k - X_f) \\
 & - I_{fz} \cdot \ddot{\theta}_{fz} - I_{sz} \cdot \ddot{\theta}_{sz} \dots \dots \dots 3.02f
 \end{aligned}$$

The calculated forces (F_{xk} , F_{yk} , F_{zk}) and moments (M_{xk} , M_{yk} , M_{zk}) represent the complete external force system acting at the knee joint centre, k , in terms of reference axes at the knee perpendicular to the force plate surface. To determine the associated muscle, ligament and joint forces, the force system at the knee must be resolved with respect to the tibial axes X_s , Y_s , Z_s . See Appendix G.

Muscle and Ligament Co-ordinates

For the test subject, the co-ordinates of muscle and ligament attachment to the tibia, femur and pelvis were obtained by multiplying Morrison's anthropometric measurements of Table No. 1 by the appropriate scaling factor. (Appendix A) The co-ordinates of attachment were determined relative to the tibial axes for each frame of film describing the

skating thrust and were corrected for rotations of the lower limb. These calculations are described in Appendix E.

Muscle and Ligament Forces

In order to determine the muscle and ligament forces, the lines of force action of the respective muscle groups and ligaments were calculated from the co-ordinates of muscle and ligament attachment. The lines of force action were expressed as the angles of the line of action relative to the tibial axes and with corrections for rotation of the lower limb. These calculations are given in Appendix F. The line of action of the quadriceps femoris muscle group was calculated from equation 3.01 where the angle calculated represents the angle of the patellar ligament with respect to the long axis of the tibia.

A knowledge of the lines of action of the muscles and ligaments allowed determination of the forces acting in these tissues from the known equilibrium conditions that exist at the knee. The external force system acting at the knee is balanced by

- (a) the force acting between the articulating surfaces of the femur and tibia (condyles) and
- (b) the forces developed in the muscle groups and ligament structures of the knee.

Since the number of muscle groups (3) and ligament structures (4) is greater than the number of available equi-

ilibrium equations, the analysis is essentially indeterminate. Therefore a number of assumptions based on the known functional anatomy of the knee and the determined phasic activity of the muscle groups (EMG record) were made to obtain a complete solution. Following Morrison's (1970) procedure, each action of the external force system, Fig. 3.19, was considered separately in terms of the particular muscle or ligament action involved.

Forces in Muscle Groups

The moment action, M_{xk} , in the anterior-posterior plane of the tibial axes is equilibrated by muscle action in the muscle groups in that plane, i.e.,

- (1) hamstrings group
- (2) gastrocnemius group
- (3) quadriceps femoris group

A positive M_{xk} corresponds to a force action on the lower limb that tends to flex the knee and equilibrium is obtained by muscle force in the quadriceps group, the extensors of the lower limb. EMG records, Fig. 4.02, show that both quadriceps and gastrocnemius groups were active during this period while hamstrings were inactive. To reduce the indeterminacy of this situation the antagonistic effect of the gastrocnemius group on equilibrium conditions at the knee was assumed to be small. The force acting in the quadriceps femoris group, P_q , was therefore determined from Fig. 3.21

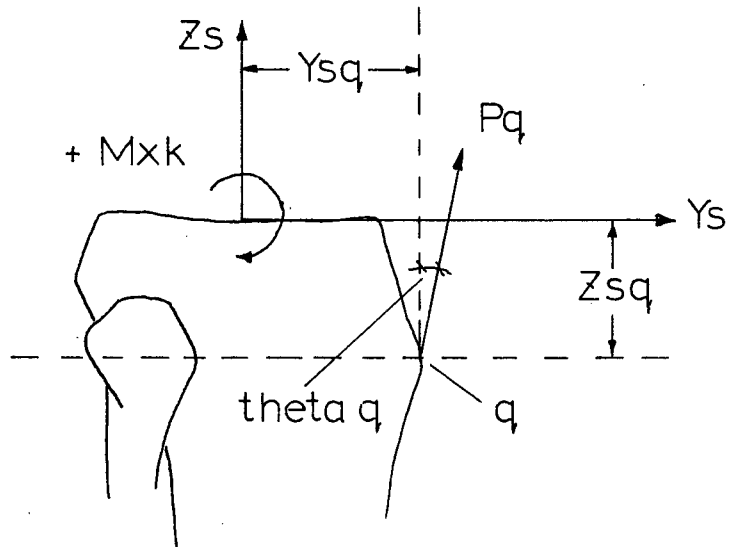


FIG.3.21 MUSCLE FORCE IN QUADRICEPS
TO BALANCE MOMENT $+M_{xk}$

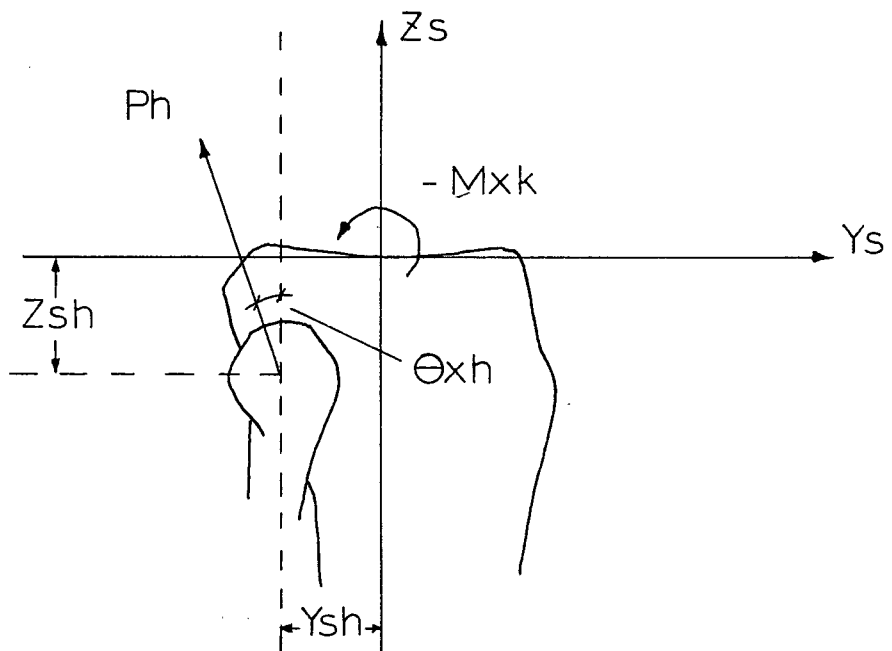


FIG.3.22 MUSCLE FORCE IN HAMSTRINGS
TO BALANCE MOMENT $-M_{xk}$

and equilibrium equation 3.03 as,

$$P_q = M_{xk} / (\cos \theta_q \cdot Y_{sq} + \sin \theta_q \cdot Z_{sq}) \dots \dots \dots 3.03$$

where,

θ_q = angle between line of action of patellar ligament and
long axis of tibia.

X_{sq}, Y_{sq} = co-ordinates of patellar ligament attachment to
tibia.

Since the hamstrings are inactive and the antagonistic action
of the gastrocnemius force on the knee is discounted for this
phase

$$P_h = P_g = 0 \dots \dots \dots 3.04$$

The horizontal component of muscle force, F_{ym} , and
the vertical component of muscle force, F_{zm} , are then

$$F_{ym} = P_q \cdot \sin \theta_q \dots \dots \dots 3.05a$$

$$F_{zm} = P_q \cdot \cos \theta_q \dots \dots \dots 3.05b$$

A negative M_{xk} represents an extension force action
on the lower limb which is equilibrated by muscle force
action in the hamstrings group and/or the gastrocnemius
group, the flexors of the lower limb. The moment, M_{xk} , was
negative for the first half of the skating thrust, Fig. 4.06
and for the final push-off of the thrust. EMG records show

that the hamstrings were active for the first portion of the thrust while the gastrocnemius group was active for the final portion. The quadriceps muscle group, which has an antagonistic effect relative to both the hamstring and gastrocnemius groups, was also intermittently active during these periods, Fig. 4.02. In order to obtain a singular solution for the forces acting in the hamstring and gastrocnemius groups, the antagonistic action of the quadriceps was ignored.

For the first phase of the skating thrust, the force acting in the hamstrings group, Ph , was determined from Fig. 3.22 and equilibrium equation 3.06.

$$Ph = Mxk / (\cos \theta_{xh} \cdot Ysh + \sin \theta_{xh} \cdot Zsh) \dots \dots \dots 3.06$$

where,

θ_{xh} = angle between line of action of the hamstrings muscle group and long axis of the tibia

Ysh, Zsh = co-ordinates of hamstring attachment to the tibia

Since the quadriceps antagonistic force is not included in the calculation, the force in the hamstrings group represents a lower limit value where in

$$Pg = Pq = 0 \dots \dots \dots 3.07$$

and the horizontal and vertical components of muscle force are

$$F_{ym} = -Ph \cdot \sin \theta_{xh} \dots \dots \dots 3.08a$$

$$F_{zm} = P_h \cdot \cos \theta_{xh} \dots \dots \dots 3.08b$$

For the final push-off phase of the skating thrust, the force acting in the gastrocnemius group, P_g , was determined from Fig. 3.23 and equilibrium equation 3.09 so that,

$$P_g = M_{xk} / (\cos \theta_{xg} \cdot Y_{sg} + \sin \theta_{xg} \cdot Z_{sg}) \dots \dots \dots 3.09$$

where,

θ_{xg} = angle between line of action of the gastrocnemius group and the long axis of the tibia

X_{sg}, Z_{sg} = co-ordinates of gastrocnemius muscle attachment to the tibia.

Once again the calculated value of gastrocnemius muscle force is lower limit and

$$P_h = P_q = 0 \dots \dots \dots 3.10$$

and the vertical and horizontal muscle components are

$$F_{ym} = -P_g \cdot \sin \theta_{xg} \dots \dots \dots 3.11a$$

$$F_{zm} = P_g \cdot \cos \theta_{xg} \dots \dots \dots 3.11b$$

Forces in Cruciate Ligaments

Anterior-posterior force action in the y-direction at the joint is equilibrated by tension in the cruciate ligaments as noted by Brantigan and Voshell (1941) and Steindler (1955). It was further assumed that a force action directed

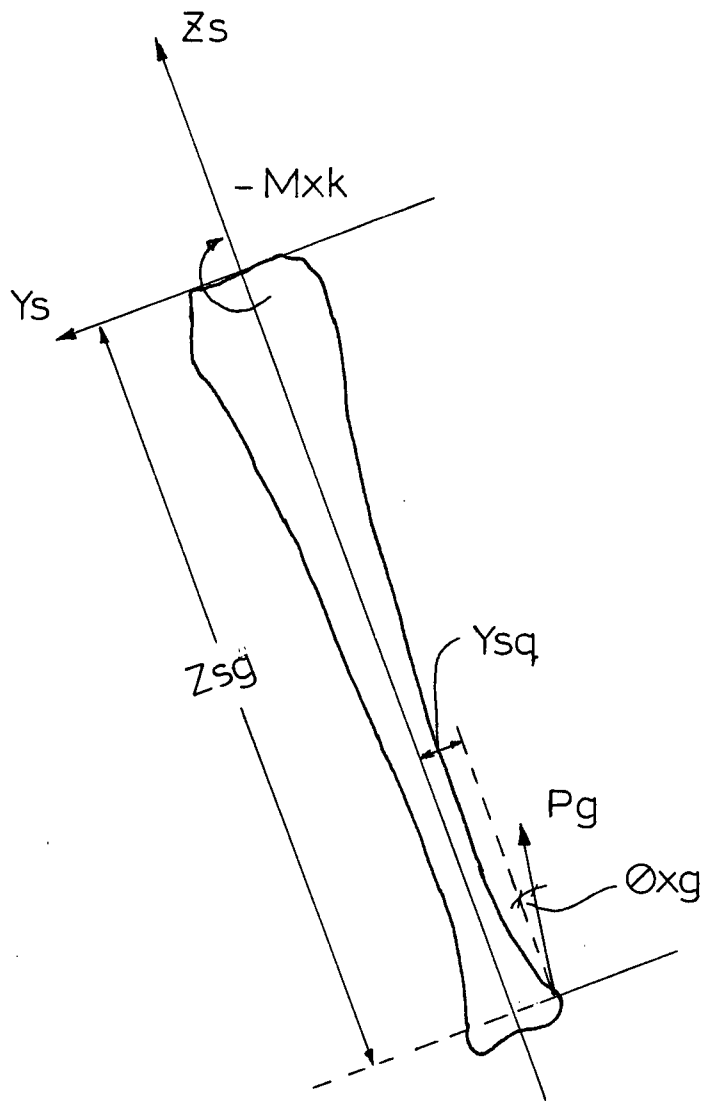


FIG.3.23 MUSCLE FORCE IN GASTROCNEMIUS
TO BALANCE MOMENT $-M_{xk}$

forwards develops tension only in the anterior cruciate and a backwards force causes tension only in the posterior cruciate. See Fig. 3.24 after Morrison (1970).

The equilibrium equation for the anterior-posterior force actions is

$$F_{yk} + F_{ym} = P_a \cdot \cos \theta_{xa} + P_p \cdot \cos \theta_{xp} \dots \dots \dots 3.12$$

where,

F_{yk} = y-component of external force system

F_{ym} = y-component of muscle force

P_a = force acting in the anterior cruciate ligament

P_p = force acting in the posterior cruciate ligament

θ_{xa} = angle between line of action of anterior cruciate and tibial axis

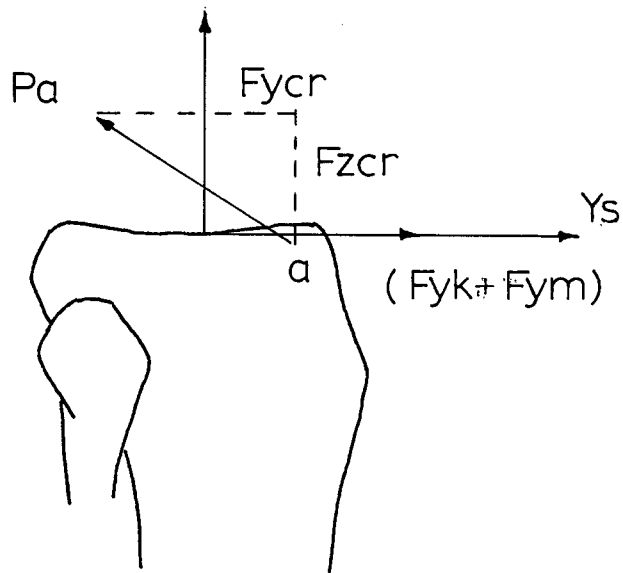
θ_{xp} = angle between line of action of posterior cruciate and tibial axis

For a forward directed force action, the force, P_a , developed in the anterior cruciate ligament was calculated from equation 3.12 by setting

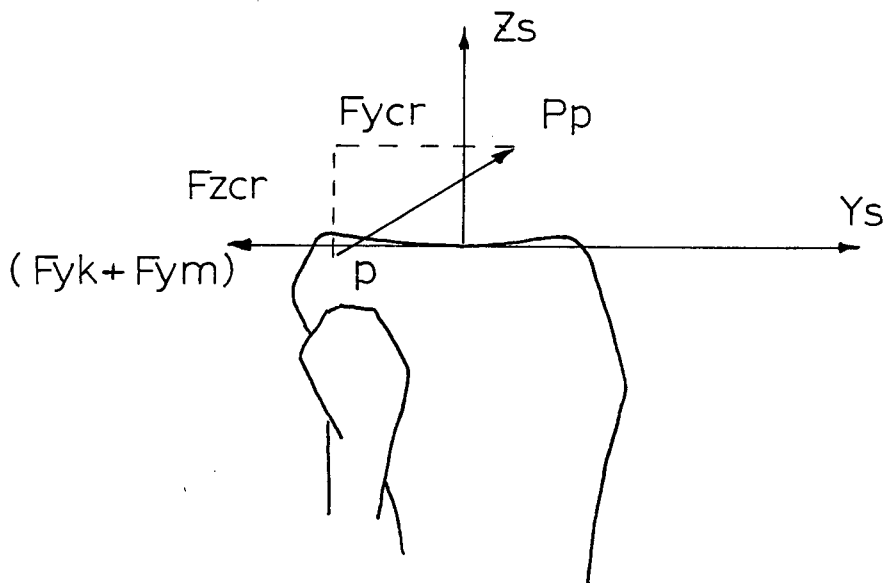
$$P_p = 0 \dots \dots \dots 3.13a$$

$$P_a = -(F_{yk} + F_{ym}) / \cos \theta_{xa} \dots \dots \dots 3.13b$$

The horizontal and vertical components of the anterior cruciate ligament force relative to the tibial axes are



(a) FORCE IN ANTERIOR CRUCIATE FOR
 $(F_{yk} + F_{ym})$ IN FORWARD DIRECTION



(b) FORCE IN POSTERIOR CRUCIATE FOR
 $(F_{yk} + F_{ym})$ IN BACKWARD DIRECTION

FIG. 3.24 FORCE IN POSTERIOR CRUCIATE AND
ANTERIOR CRUCIATE LIGAMENTS

$$F_{ycr} = P_a \cdot \cos \theta_{xa} \dots \dots \dots 3.14a$$

$$F_{zcr} = P_a \cdot \sin \theta_{xa} \dots \dots \dots 3.14b$$

For a backward directed force action at the knee, the force, P_p , developed in the posterior cruciate ligament was calculated from equation 3.12 by setting

$$P_a = 0 \dots \dots \dots 3.15a$$

$$P_p = - (F_{yk} + F_{ym}) / \cos \theta_{xp} \dots \dots \dots 3.15b$$

The horizontal and vertical components of the posterior cruciate ligament force are

$$F_{ycr} = P_p \cdot \cos \theta_{xp} \dots \dots \dots 3.16a$$

$$F_{zcr} = P_p \cdot \sin \theta_{xp} \dots \dots \dots 3.16b$$

Forces in Collateral Ligaments and Joint Force

The moment, M_{yk} , tends to bend the knee laterally and medially in the frontal plane. Morrison (1970) interprets the equilibrium conditions at the knee for these force actions as follows.

When there is a compressive force, R_z , between the femoral and tibial condyles, the force action of M_{yk} shifts the centre of pressure of this force medially or laterally depending on the direction of M_{yk} .

If the shift of weight is sufficient to reduce the pressure at the periphery of the condyle to zero then any

further increase in My_k must be balanced by a tension in the collateral ligament at that side of the joint. (Fig. 3.25) Morrison (1970) determined a limiting valve, X_l , for the shift of the centre of pressure that reduces the pressure at the periphery of the condyle bearing area to zero. See Fig. 3.13.

Essentially there are two equilibrium equations that describe the force action of moment, My_k .

$$R_z = F_{zk} + F_{zm} + F_{zcr} + P_m \cdot \cos \theta_{ym} \cdot \cos \theta_{xm} \\ + P_l \cdot \cos \theta_{yl} \cdot \cos \theta_{xl} \dots \dots \dots 3.17$$

$$0 = My_k - P_l \cdot \cos \theta_{yl} \cdot X_{sl} + P_l \cdot \sin \theta_{yl} \cdot Z_{sl} \\ + P_m \cdot \cos \theta_{ym} \cdot X_{sm} + P_m \cdot \sin \theta_{ym} \cdot Z_{sm} \\ + R_z \cdot X_o \dots \dots \dots 3.18$$

where,

F_{zk} = Z-component of external force system

F_{zm} = Z-component of muscle force

F_{zcr} = Z-component of cruciate ligament force

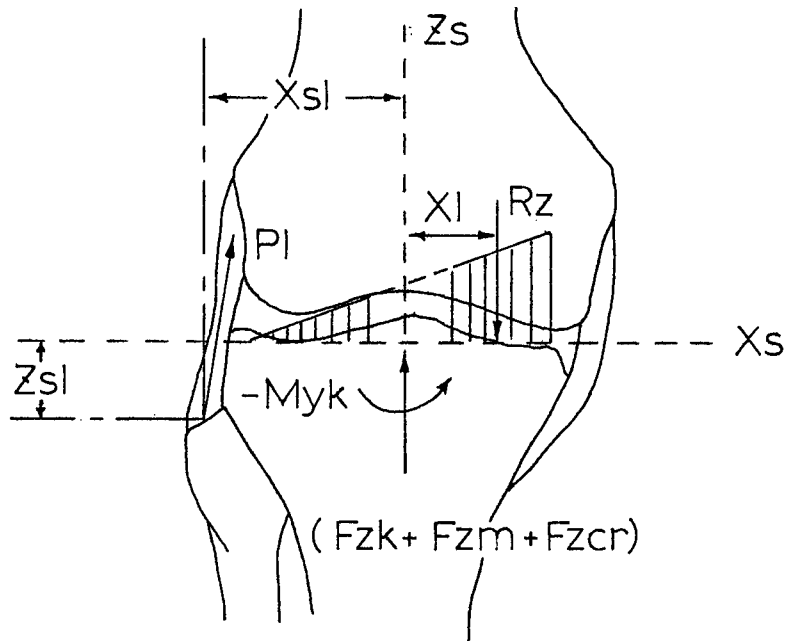
P_m = force acting in medial ligament

P_l = force acting in lateral ligament

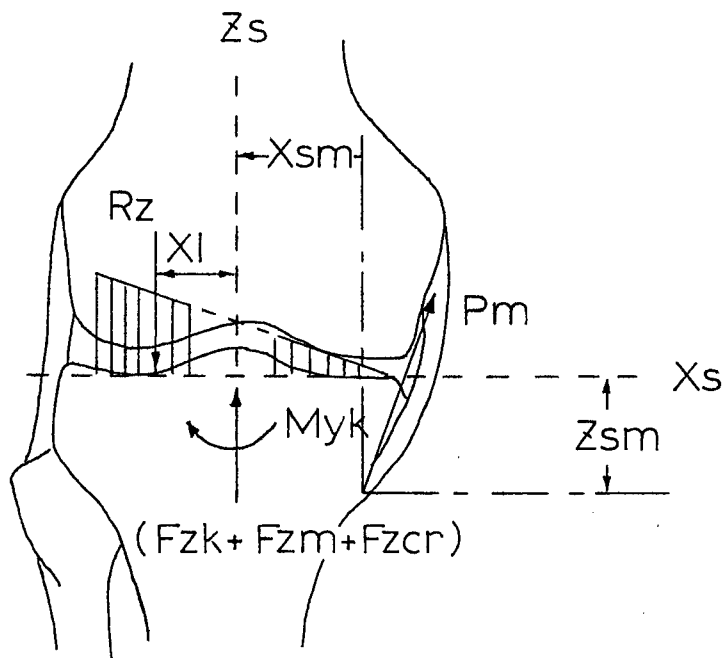
R_z = compressive force between tibial and femoral condyles

X_o = offset of centre of pressure from joint centre

These two equations are indeterminant in that they contain four unknowns, R_z , X_o , P_m and P_l . However, a solution can be obtained by reducing the number of unknowns to



(a) FORCE IN LATERAL COLLATERAL DUE TO ADDUCTION FORCE $-My_k$



(b) FORCE IN MEDIAL COLLATERAL DUE TO ABDUCTION FORCE $+My_k$

FIG. 3.25 COLLATERAL LIGAMENT FORCES

two by considering specific loading conditions.

Condition 1:

Pressure exists between the condyles of the joint so that

$$F_{zk} + F_{zm} + F_{zcr} > 0$$

$$P_m = P_l = 0$$

For these loading conditions, Fig. 3.26, R_z is calculated directly from equation 3.17

$$R_z = F_{zk} + F_{zm} + F_{zcr} \dots \dots \dots 3.19$$

and X_o can be evaluated by substitution for R_z in equation 3.18

$$X_o = - M_{zk} / (F_{zk} + F_{zm} + F_{zcr}) \dots \dots \dots 3.20$$

Condition 2:

The calculated value of X_o is greater than the limiting value of X_l and M_{yk} acts in a positive direction medially.

For these loading conditions, Fig. 3.25, a solution is obtained for R_z and P_l by substituting $P_m = 0$ and $X_o = X_l$ into equations 3.17 and 3.18 so that,

$$P_l = (M_{yk} + [F_{zk} + F_{zm} + F_{zcr}] \cdot X_l) / (\cos \theta_{y1} \cdot X_{s1} - \sin \theta_{y1} \cdot Z_{s1} - \cos \theta_{y1} \cdot X_l) \dots \dots \dots 3.21$$

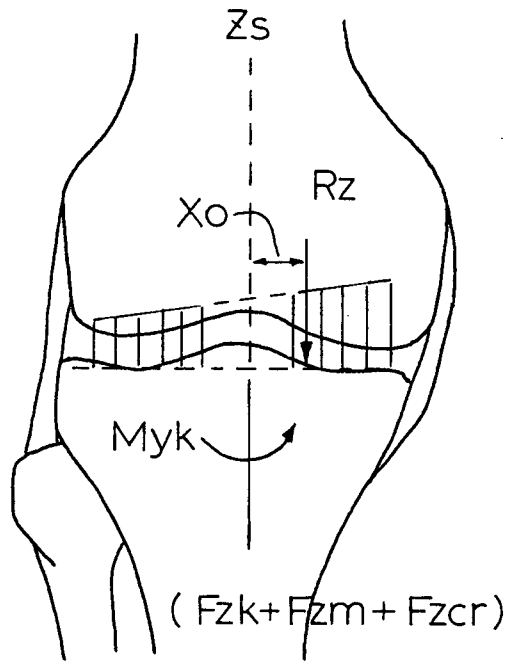


FIG. 3.26 COMPRESSIVE JOINT FORCE, R_z

$$R_z = F_{zk} + F_{zm} + F_{zcr} + P_l \cdot \cos \theta_{yl} \cdot \cos \theta_{xl} \dots \dots \dots 3.22$$

Therefore for a positive My_k , such that $X_o > X_l$, a tensile force, P_l , acts in the lateral ligament and the centre of pressure of the compressive force between the joint condyles is shifted a distance X_l medially from the joint centre.

Condition 3:

The calculated value of X_o is greater than X_l and My_k acts in a negative direction laterally.

For these loading conditions, Fig. 3.25, a solution is obtained for R_z and P_m by substituting $P_l = 0$ and $X_o = X_l$ into equations 3.17 and 3.18 so that

$$P_m = (My_k + [F_{zm} + F_{zk} + F_{zcr}] \cdot X_l) / (\cos \theta_{ym} \cdot X_{sm} + \sin \theta_{ym} \cdot Z_{sm} - \cos \theta_{ym} \cdot X_l) \dots \dots \dots 3.23$$

$$R_z = F_{zk} + F_{zm} + F_{zcr} + P_m \cdot \cos \theta_{ym} \cdot \cos \theta_{xm} \dots \dots \dots 3.24$$

Therefore, for a negative My_k such that $X_o > X_l$, a tensile force, P_m , acts in the medial ligament and the centre of pressure of the compressive force at the joint is displaced a distance, X_l , laterally from the joint centre.

Shear Force and Torque

The shear force at the joint in the medial-lateral direction is determined by summing the X component of the external force, the muscle force and the ligament forces.

$$R_x = F_{xk} + F_{xm} + F_{xcol} \dots \dots \dots 3.25$$

where F_{xcol} is the summation of the X components of P_m , the medial ligament force.

$$F_{xcol} = P_l \cdot \sin \theta_{yl} + P_m \cdot \sin \theta_{ym} \dots \dots \dots 3.26$$

The torque acting on the joint is equal to the summation of the twisting forces acting on the joint.

$$\begin{aligned} M_z = M_{zk} + F_{xlc} \cdot Y_{sl} + F_{xmc} \cdot Y_{sm} \\ + F_{ylc} \cdot X_{sl} + F_{ymc} \cdot X_{sm} \dots \dots \dots 3.27 \end{aligned}$$

where,

F_{xlc} = x-component of lateral ligament force

F_{ylc} = y-component of lateral ligament force

F_{xmc} = x-component medial ligament force

F_{ymc} = y-component of medial ligament force

The complete solution for the muscle, ligament and joint forces at the knee includes,

R_z - compressive force between joint condyles

Z_o - centre of pressure of compressive force with respect to the knee joint centre

R_x - shear force on joint

P_h - force acting in hamstring muscle group

P_g - force acting in gastrocnemius muscle group

P_q - force acting in quadriceps muscle group

Pa - force acting in anterior cruciate ligament
Pp - force acting in posterior cruciate ligament
Pm - force acting in medial collateral ligament
Pl - force acting in lateral collateral ligament
Mz - torque on joint

CHAPTER IV

RESULTS AND DISCUSSION

Results

Force plate output and limb displacement data were collected for a total of 15 trials. From these data the linear and angular accelerations of the lower limb were determined, the external force system acting at the knee was calculated and finally the muscle, ligament and joint forces were calculated for each trial.

These results are reviewed in the following section with reference to trial No. 4 which is considered to be representative of the 15 trials made.

Anthropometric Measurements

The body parameters for the test subject are listed in Table No. 2. The calculations of these anthropometric measures are shown in Appendix A.

In order to scale the basic co-ordinates of muscle and ligament attachments of Table No. 1 to the test subject, the test subject's knee and pelvic scaling dimensions were obtained. These measurements are given in Table No. 2 along with the additional anthropometric data from the test subject. All measurements are in inches and represent the average

TABLE NO.2 ANTHROPOMETRIC DATA

Foot		Shank	
Lf	10.50	Ls	16.50
Rf	2.07	Rs	2.31
rfx	1.45	rsx	4.15
rfy	3.15	rsy	4.15
rfz	3.15	rsz	1.62
lfx	0.15	lsx	3.92
lfy	0.71	lsy	3.92
lfz	0.71	lsz	0.60
Wf	2.37	Ws	7.43
Knee		Ankle	
Rxk	1.90	Ra	2.02
Ryk	2.44		

Knee Scaling Dimensions			Pelvic
X	Y	Z	X
3.78	3.64	16.16	8.2

value of at least five independent measuring trials. The knee and pelvic dimensions were used to calculate the scaling factors for the subject. The scaling factors are listed in Appendix A with calculations.

Force Plate Results

The force plate output in the form of six separate oscilloscope traces is shown in Fig. 4.01 for a trial No. 4. These traces represent the three orthogonal plate reaction forces, the torque about a vertical axis through the point of application of the resultant force of the plate and the co-ordinates of the point of application of the resultant force, Fig. 3.16. The vertical amplitude of each trace was measured with the Vanguard Motion Analyzer at intervals corresponding to the 50 frames of the synchronized cine film of the skating thrust. The actual values of the forces, torque and co-ordinates of point of application were obtained by applying the appropriate calibration factors to the measured trace values. See Appendix C.

Electromyograph Results

Fig. 4.02 shows representative electromyograms for the three muscle groups instrumented and indicates the phasic activity of these muscle groups during the skating thrust. The quadriceps muscle group was active throughout the entire cycle, the hamstrings were active for the first portion of the thrust and the gastrocnemius group showed activity during

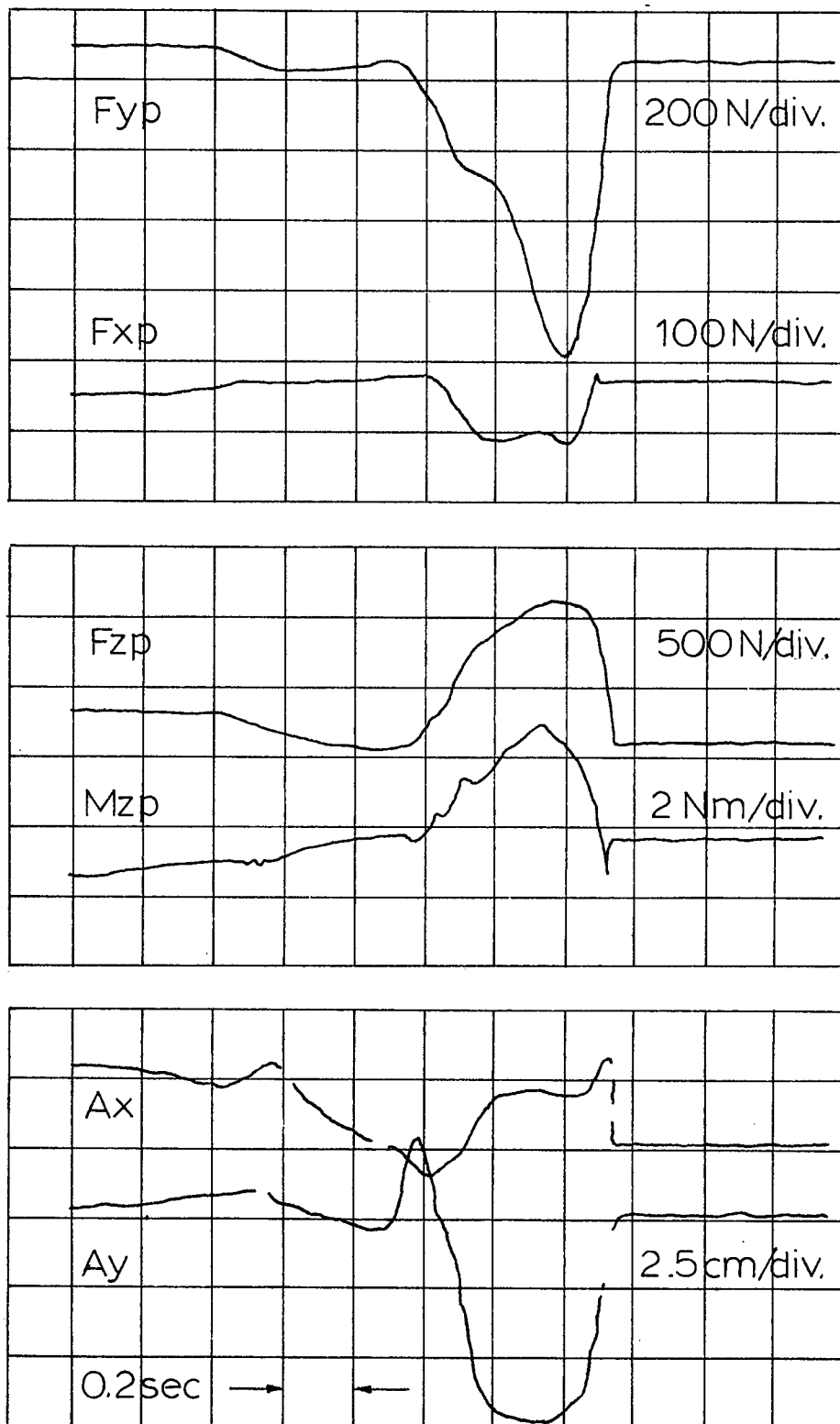


FIG.4.01 FORCE PLATE OUTPUT IN FORM
OF OSCILLOSCOPE TRACE - TRIAL NO.4

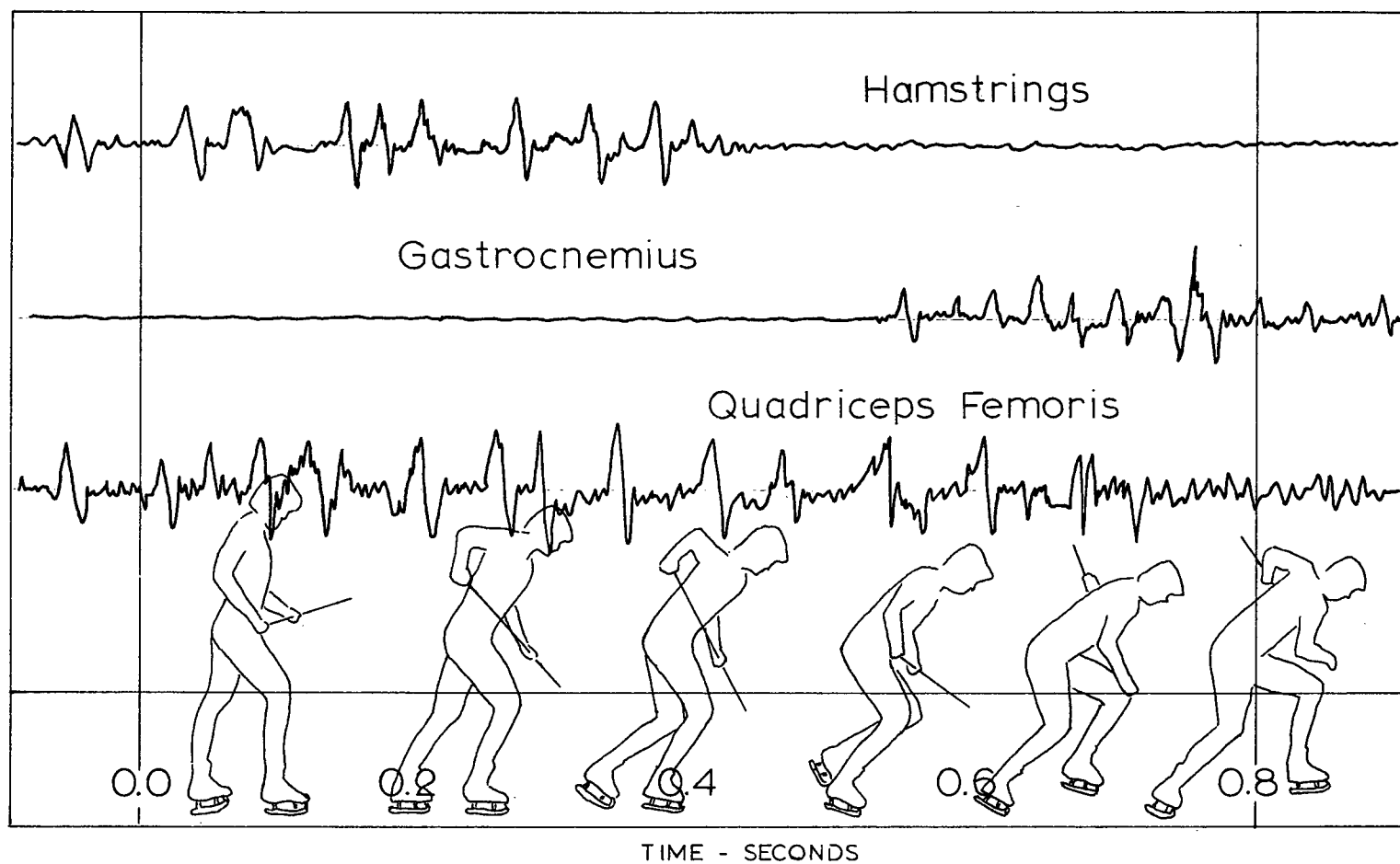


FIG. 4.02 ELECTROMYOGRAM - SKATING THRUST ON ICE

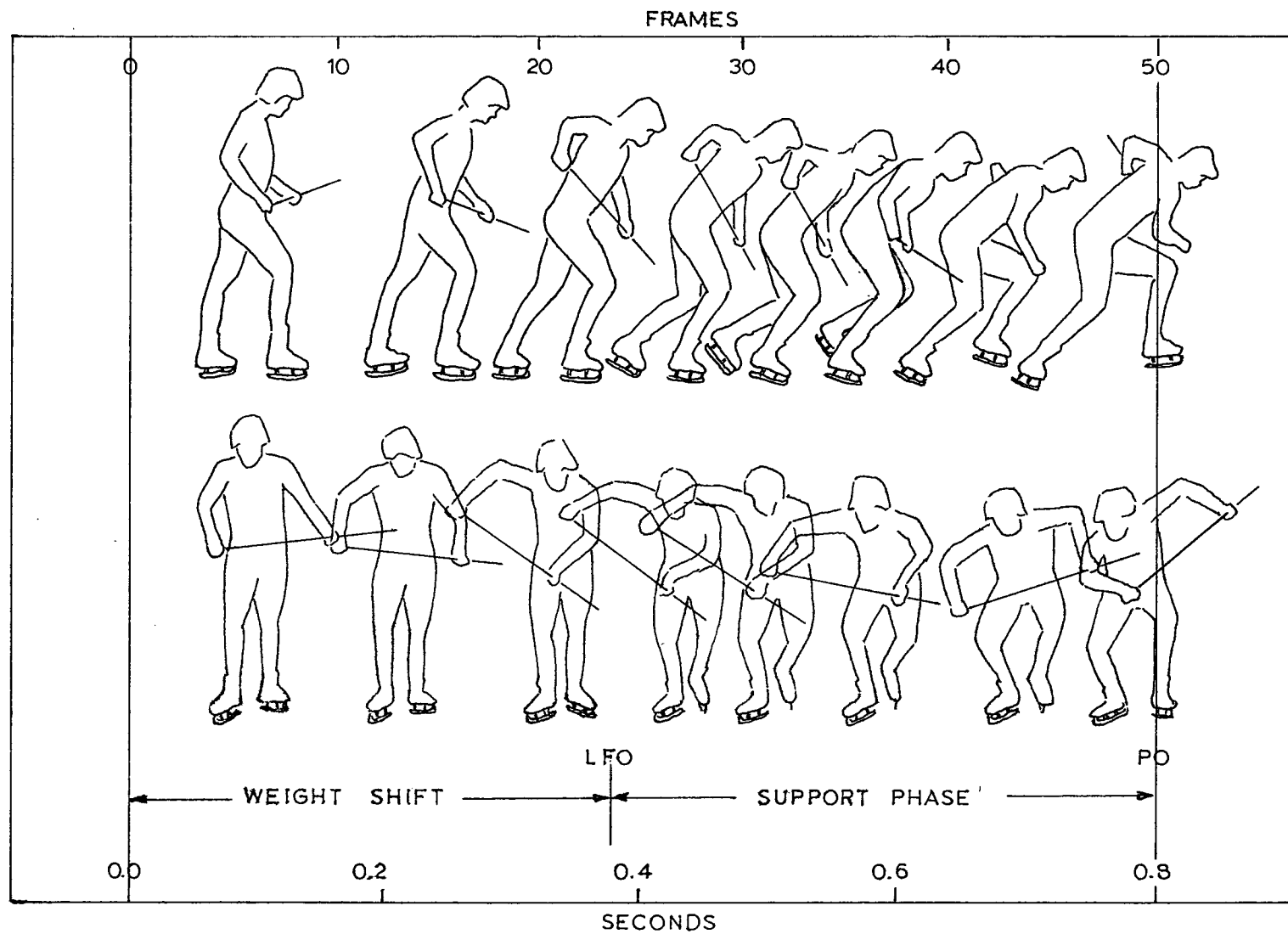


FIG. 4.03 ILLUSTRATED SEQUENCE OF SKATING THRUST

the later phase. The electromyograph results for a simulated skating thrust in the laboratory were closely related to on-ice electromyograph results indicating comparable muscle activity.

Linear Limb Accelerations

The linear accelerations of the shank and foot for the X, Y and Z directions are plotted in Fig. 4.04. As shown, the linear accelerations of the shank and foot are small until push off. The dramatic positive increase in the values of AXS, AYS and AZS at push off correspond to an abrupt inward, forward and upward acceleration of the shank. The foot accelerates upward and backward in plantar flexion at push off as indicated by a positive AZF and a negative AYF. The inward acceleration of the foot at push off as indicated by the positive increase in AXF is accompanied by an outward rotation of the shank.

Angular Limb Accelerations

The angular accelerations of the shank and foot about the X, Y and Z axes are plotted in Fig. 4.05. Similar to the linear limb accelerations, the angular accelerations are minimal for the first portion of the skating thrust but increase rapidly during push off. The large negative values of AASZ and AAFZ at push off represent a sharp outward rotation of the shank and foot about the vertical axis while the positive increase in AASY and AAFY at push off

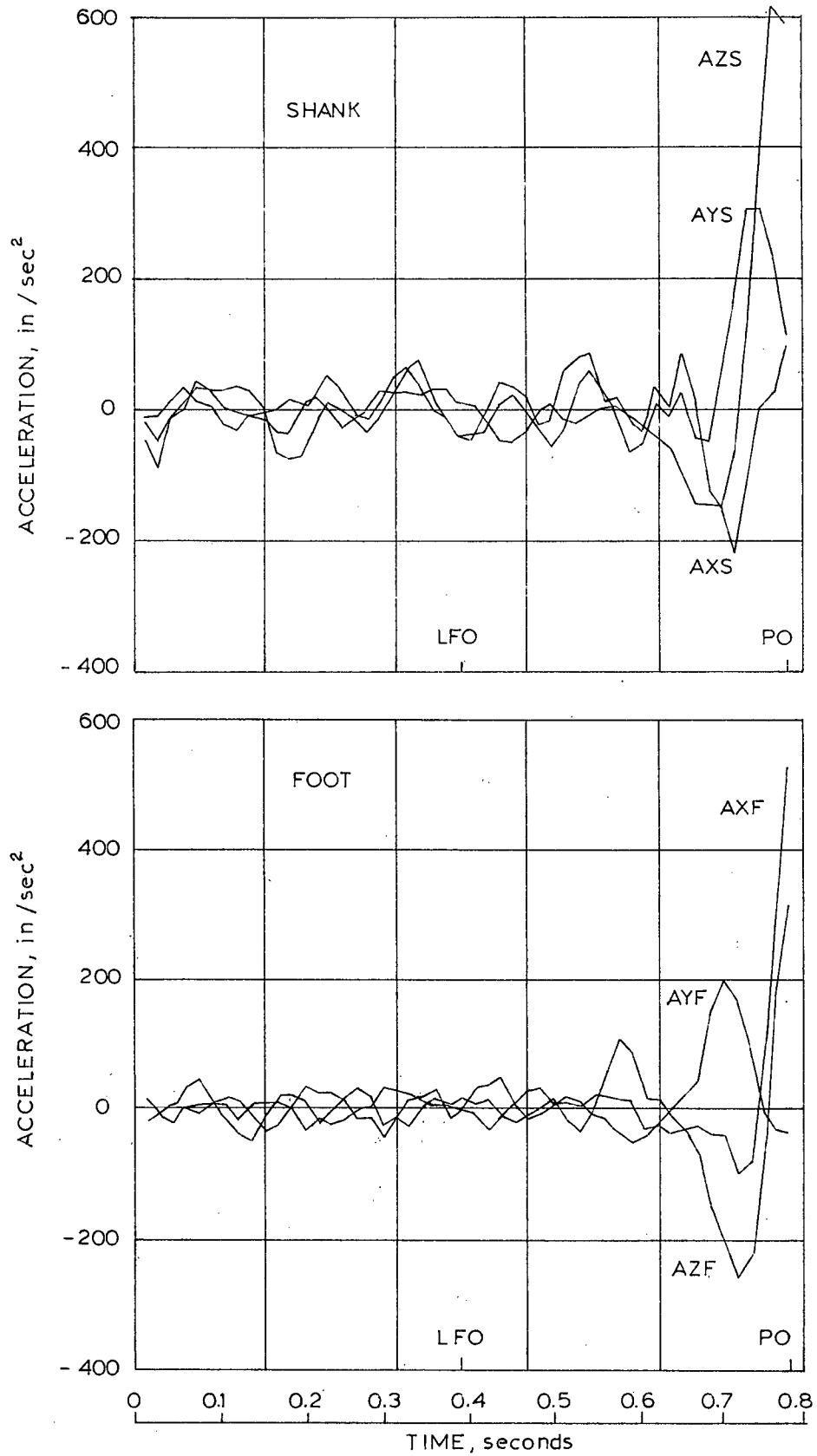


FIG.4.04 LIMB LINEAR ACCELERATIONS

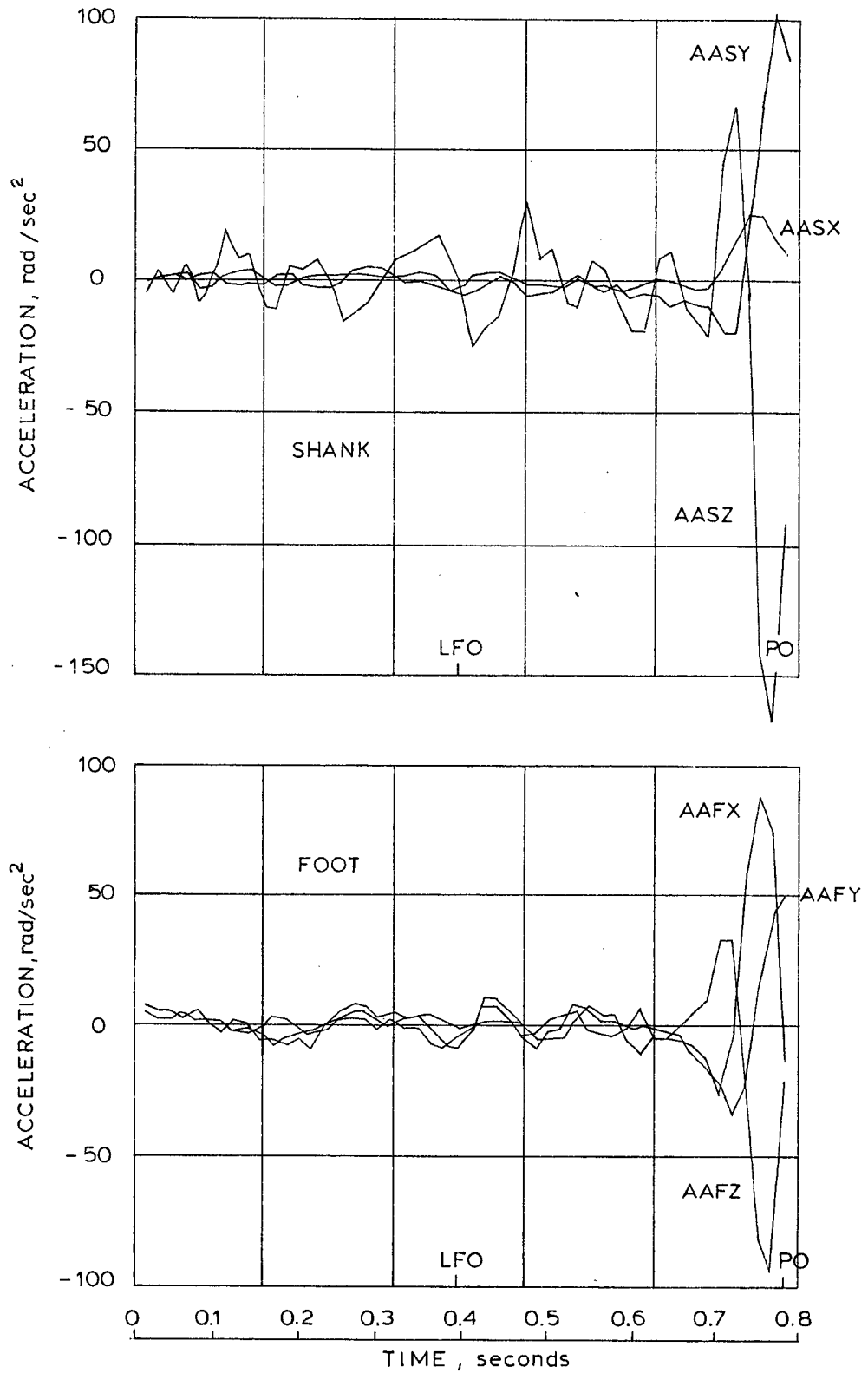


FIG. 4.05 LIMB ANGULAR ACCELERATIONS

indicate an inward rotation of the shank and foot about the axis of progression. The foot rotates forward in plantar flexion at push off as shown by the positive increase in AAFX while the shank also appears to have some forward rotation as indicated by the positive value of AASX at push off.

External Force System at Knee

The variations in the external force system during one skating stride in terms of the three forces and three moments acting at the knee are plotted in Fig. 4.06. The length of the support phase in the skating stride as indicated on the time base of Fig. 4.03 is approximately 0.4 seconds from the time the skater's left foot lifted off the force plate (LFO) until the final push off (PO) with the right foot. The commencement of the support phase is coincident with a positive increase in the vertical force F_{zk} and a change of sign of the moment M_{xk} in the plane of progression from negative to positive. A negative M_{xk} tends to extend the knee while a positive M_{xk} tends to flex the knee joint.

Moment M_{yk} is initially positive and then negative during the support phase, a positive M_{yk} representing a valgus effect on the knee joint and a negative M_{yk} a varus effect. The torque on the joint about the long axis of the limb, M_{zk} , is positive for the entire support phase indicating a constant counter-clockwise torque on the joint.

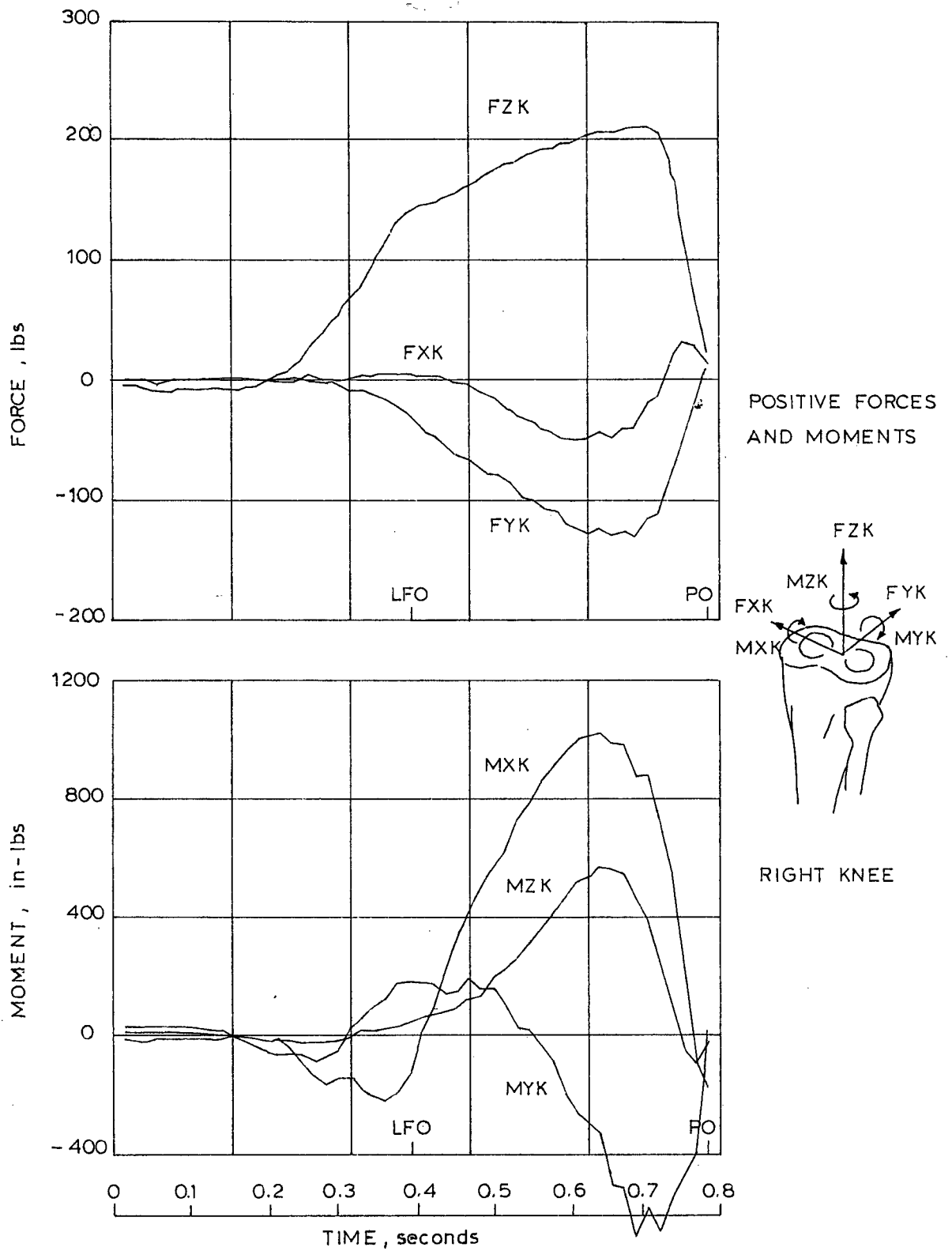


FIG.4.06 RESOLVED FORCE COMPONENTS
AT KNEE - TRIAL NO.4

The force F_{zk} , through the long axis of the joint, remains positive upward for the duration of the support phase but the shear force F_{xk} is initially negative in a lateral direction and then becomes positive medially. The anterior-posterior force, F_{yk} , is negative and therefore directed posteriorly for the duration of the skating thrust.

Muscle and Ligament Forces

Muscle and ligament forces corresponding to the external force system of Fig. 4.06 and the electromyograms of Fig. 4.02 are plotted in Fig. 4.07 for one complete skating thrust. Muscle and ligament forces for the 15 trials of the study are superimposed in Fig. 4.08 to indicate the variation in the results obtained while maximum forces developed during each of the 15 trials are given in Table No. 3.

Peak forces determined in the quadriceps femoris, hamstrings and gastrocnemius muscle groups were 665, 273 and 118 pounds respectively. As indicated in Fig. 4.08, peak quadriceps forces occurred during the support phase as the skater extended the support leg to drive forward whereas maximum hamstrings forces were recorded immediately before the commencement of the support phase. The gastrocnemius muscle, active only at push off, developed considerably smaller muscle forces.

Maximum forces acting in the ligaments were respectively 240 and 62 pounds in the posterior and anterior cru-

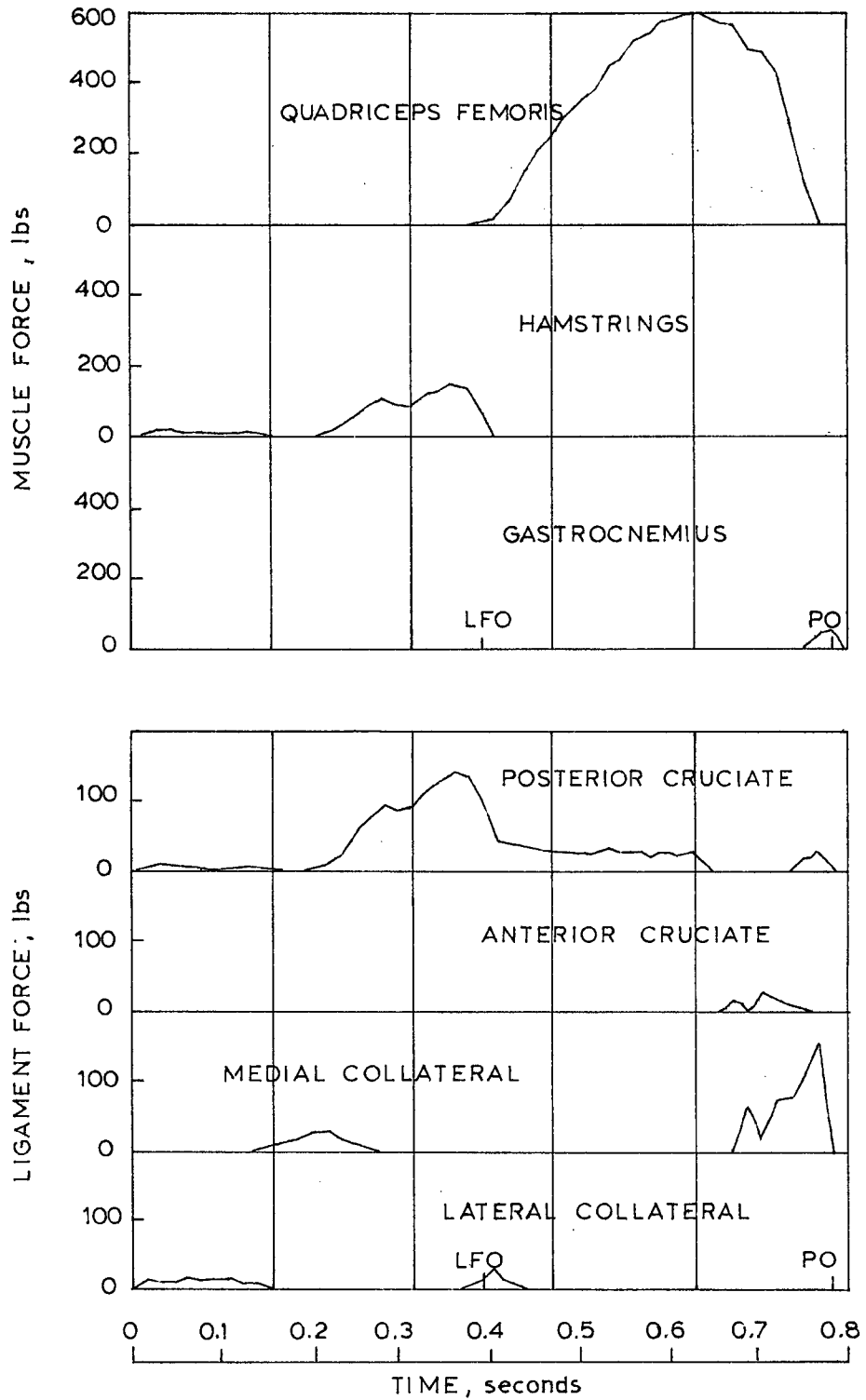


FIG. 4.07 MUSCLE AND LIGAMENT FORCES
FOR TRIAL NO.4

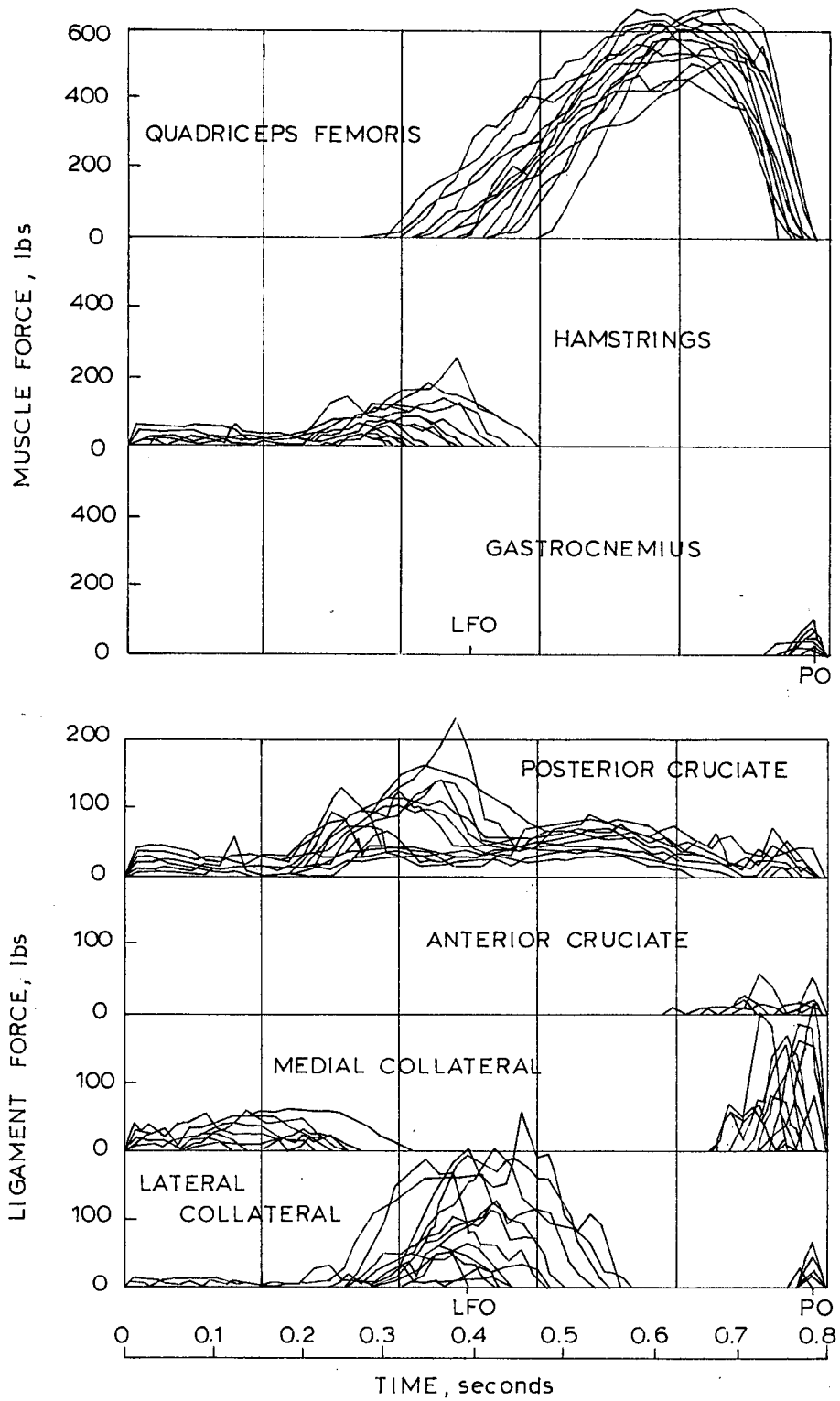


FIG. 4.08 . MUSCLE AND LIGAMENT FORCES

ciates and 289 and 258 pounds in the medial and lateral collaterals. The posterior cruciate ligament was tense for the duration of the skating thrust with peak forces occurring at the onset of the support phase while the anterior cruciates were slack until push off. The maximum medial collateral forces were recorded at push off as opposed to peak lateral collateral forces which occurred during the initial portion of the support phase as the skater moved forward and laterally.

It is interesting to observe that peak hamstrings muscle forces were coincident sequentially with maximum posterior cruciate ligament forces and maximum gastrocnemius muscle forces were coincident with maximum medial collateral ligament forces. On the other hand, at that time of peak quadriceps force, the collateral ligaments were slack, no force was recorded in the anterior cruciate ligament and only minimal forces were indicated in the posterior cruciate ligament.

Articular Forces

The magnitude of the normal joint force R_z acting at the knee during the skating thrust is plotted in Fig. 4.09. The maximum values of R_z varied between 666 pounds and 888 pounds for the 15 test trials with the peak value of R_z coincident in time with the maximum quadriceps force recorded. The maximum values of R_z developed represent joint forces 4.2 to 5.6 times the 165 pound body weight of the

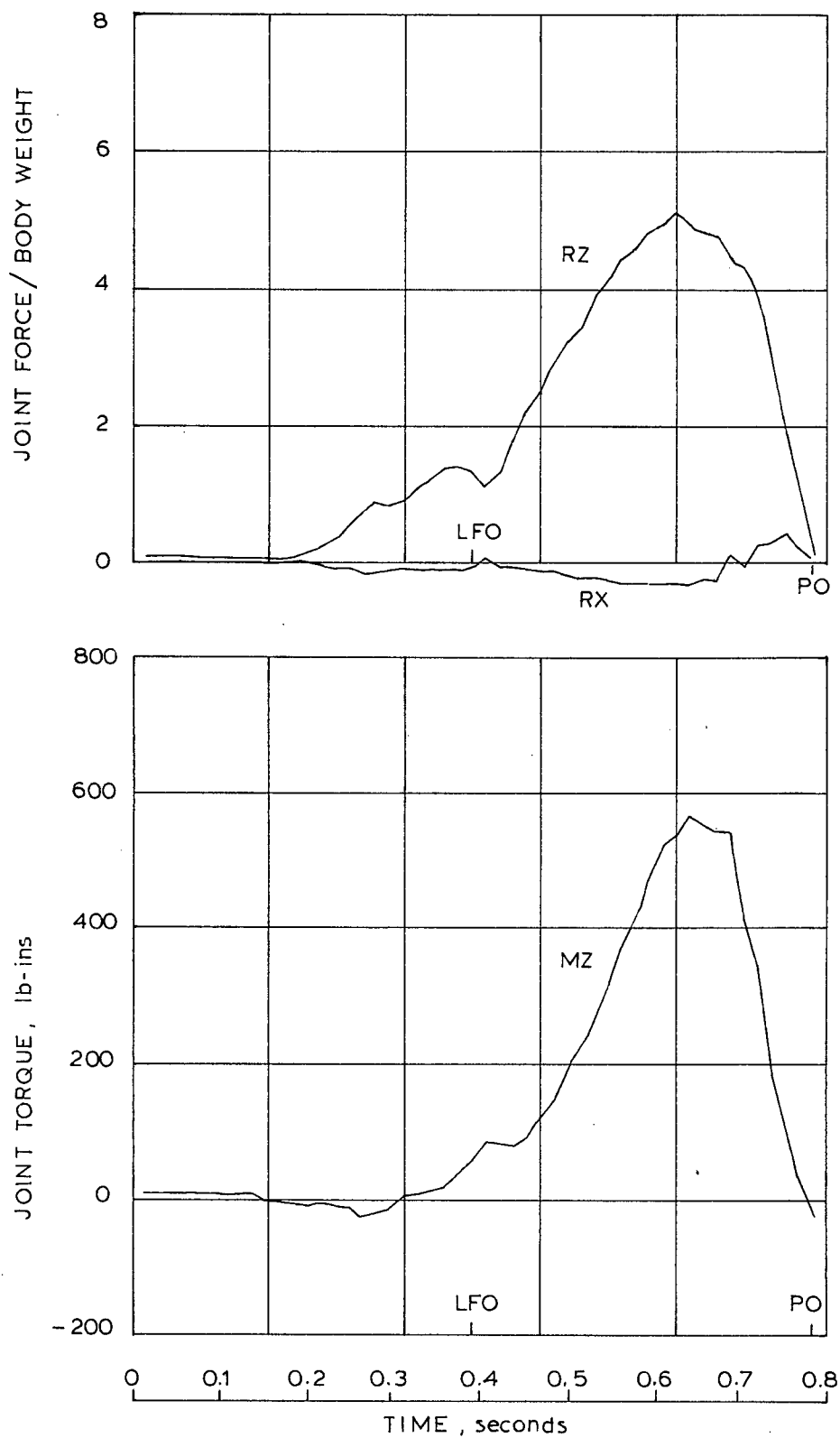


FIG.4.09 JOINT FORCES ACTING AT KNEE

test subject.

The variation of the medial-lateral shear force R_x on the articular surfaces of the joint is shown in Fig. 4.09. The shear force acts medially during the support phase of the skating thrust but is lateral at push off. The maximum medial and lateral shear forces recorded were 96 and 57 pounds respectively.

The anterior-posterior force, R_y , on the knee joint is assumed to be equilibrated by the forces developed in the cruciate ligaments, either the posterior cruciate or the anterior cruciate dependent upon the direction of the force, R_y . Fig. 3.24.

The maximum values of M_z , the torque on the joint about the long axis of the tibia, were developed during the support phase of the skating thrust and were coincident with peak quadriceps muscle forces. A plot of M_z is given in Fig. 4.09 for Trial No. 4 with peak values of torque for each test trial given in Table No. 3. The maximum values of torque on the joint varied from 455 to 735 pound-inches and were directed medially inward.

Discussion

The summary of results as shown in Fig. 4.08 and as tabulated in Table No. 3 indicates that although the cyclic pattern of muscle and ligament forces was quite consistent from trial to trial, there was considerable variation in

TABLE NO. 3

MAXIMUM MUSCLE LIGAMENT AND JOINT FORCES
FOR THE SIMULATED SKATING THRUST

TR	Ph	Pq	Pg	Pp	Pa	Pm	Pl	Rz	Rx	Mz
2	193.67	618.40	118.62	165.01	6.95	2.69	36.39	843.45	54.01	486.78
3	272.92	613.89	20.31	239.51	20.64	37.04	131.11	822.28	-50.95	573.90
4	144.35	601.38	24.55	140.86	25.03	159.69	30.89	802.06	64.54	566.34
5	100.94	506.99	50.69	111.34	21.52	17.80	202.11	707.34	61.83	521.60
6	116.42	518.75	60.81	103.25	8.30	59.48	69.95	721.24	-50.39	413.81
7	30.75	633.39	57.51	73.01	4.99	86.01	15.05	855.18	68.84	510.59
9	20.54	453.08	24.19	90.42	17.44	207.42	102.61	666.44	82.97	455.37
10	87.43	639.42	106.15	75.56	4.74	178.71	51.06	872.22	64.53	497.96
11	74.06	545.16	29.10	86.76	9.28	79.13	52.68	767.69	-56.87	522.78
12	95.98	582.18	18.86	74.61	14.96	158.15	56.57	803.88	96.09	610.95
13	151.36	540.24	24.43	131.60	12.47	221.60	172.85	765.80	-61.27	590.76
14	40.08	665.52	21.59	43.99	29.99	145.26	109.83	878.11	-55.52	735.62
15	78.89	660.43	25.14	74.99	61.76	164.33	194.21	888.29	47.63	675.50
16	130.25	663.77	43.11	139.83	17.92	288.88	258.81	885.78	96.74	700.47
17	111.01	625.56	25.34	95.57	12.81	41.50	191.53	852.17	-56.16	674.23

muscle, ligament and joint forces = pounds

joint torque = pound-inches

the peak forces recorded. The variance in the results can be largely attributed to the fact that it was extremely difficult for the test subject to exactly duplicate the simulated skating thrust for each trial. Morrison (1970) also found some variation in the muscle and joint forces of a single test subject when tested twice for simple level walking.

Due to the limitations of the analysis, the antagonistic muscle actions (Fig. 4.02) could not be considered and therefore the values of muscle force calculated are the minimum required for equilibrium of the external force system. These minimum values are also reflected in the values of ligament forces and articular forces.

Muscle Forces

The forces developed in the three muscle groups can be explained with reference to the actions of the skating thrust and the assumptions made in the analysis. The initial movement of the skating thrust is a shift of weight from the rear foot to the forward support or thrusting foot. Since the support foot is anterior to the knee at this point, Fig. 4.03, the vertical force, F_{zp} , on the support foot, Fig. 3.20, produces a negative moment M_{xk} on the knee that tends to extend the joint. This moment action is resisted by force action in the hamstrings, to stabilize the knee joint as the forward leg assumes the body weight. The electromyogram of Fig. 4.02 shows that both quadriceps and hamstrings muscle

groups are active during this phase but the magnitude of quadriceps force could not be evaluated due to the indeterminacy of the analysis. Since the force action of the quadriceps is antagonistic to the force action of the hamstrings, the value of hamstrings force calculated is by definition the minimum muscle force required to balance the external moment, M_{xk} . The actual force acting in the hamstrings is equal to the sum of

- (a) the force action required to resist the external moment, M_{xk} , and
- (b) the force action required to balance the antagonistic force action of the quadriceps on the joint.

Since the electrical activity (EMG) of the muscle groups was recorded with surface electrodes, individual muscle activity within a muscle group could not be accurately defined. It is possible that the quadriceps activity recorded for this phase was due to contraction of the biarticular rectus femoris muscle, the only member of the quadriceps group that crosses the hip joint and that can therefore flex the hip as well as extend the knee (Basmajian, 1970). This deduction agrees with the analysis of Paul (1966) of the function of the hip in walking.

As the skater drives forward and the knee moves ahead of the support foot, Fig. 4.03, the joint is subject to a positive M_{xk} due to the vertical force, F_{zp} , and the posterior force, F_{yp} , on the foot, Fig. 3.20. Since a positive

M_{xk} tends to flex the knee, equilibrium is obtained by force action in the quadriceps femoris. Although electromyogram records, Fig. 4.02, indicate that both quadriceps and gastrocnemius muscle groups are active in the support phase, the force action of the gastrocnemius muscle is not considered to affect the knee. Being a biarticular muscle, the gastrocnemius can both flex the knee and produce plantar flexion of the ankle. However, the fibres of the gastrocnemius are so short that this muscle cannot flex the knee and plantar flex the ankle at the same time because of the slack in the muscle. (Basmajian, 1970). It is therefore assumed that in the support phase of the skating thrust, the gastrocnemius resists dorsi-flexion as the shank moves forward over the foot and does not contribute to force actions at the knee.

At push off, moment M_{xk} becomes negative due to the anterior force F_{yp} on the foot, Fig. 3.20, and the increased inertial forces of the shank and foot as the lower limb accelerates forward, Fig. 4.04. Since the hamstrings are inactive at push off and the force action in the quadriceps femoris is assumed to impart the forwards acceleration to the leg, the negative extension moment, M_{yk}, developed at push off must be equilibrated by force action in the gastrocnemius muscle. As the gastrocnemius cannot flex the knee and plantar flex the ankle at the same time plantar flexion of the ankle at push off must be due to force action of the soleus muscle, the great plantar flexor of the ankle and a

member of the triceps surae muscle group of the lower leg.

Ligament Forces

The forces calculated in the ligaments must be considered in conjunction with the limitations of the simplified muscle and ligament system of Fig. 3.12 and the equations used to obtain equilibrium conditions, Section 3.

The anterior-posterior forces acting on the joint were assumed to be balanced by forces developed in the cruciate ligaments. For the duration of the skating thrust, excepting push off, there is a negative posterior force, F_{yk} , imposed on the knee, Fig. 4.06. Equilibrium conditions at the joint are maintained by a tensile force developed in the posterior cruciate, Fig. 3.24. The horizontal component of the hamstrings muscle force also imposes a posterior force on the joint which must be balanced by an increased tensile force in the posterior cruciate. This explains the coincidence of peak posterior cruciate ligament force and maximum hamstrings muscle force as mentioned in the results section; illustrated in Fig. 4.08, and summarized in Table No. 3. As the skater thrusts forward to push off, the posterior force, F_{yk} , on the joint decreases while the horizontal component of the quadriceps force on the joint becomes anterior as the hip joint moves ahead of the knee, Fig. 4.03. The result is a small anterior force on the knee which is balanced by a small tensile force acting in the anterior cruciate. In all

tests, the posterior cruciate carried the greater force, a maximum force of 240 pounds compared to 62 pounds in the anterior cruciate. The force of friction acting at the articular surfaces of the joint was not considered when calculating the cruciate forces. Since the femoral condyles rotate backward on the tibia during the skating thrust, the force of friction on the joint is directed posteriorly and would therefore increase the tensile force in the posterior cruciate. Assuming a value of 0.02 for the coefficient of friction in the joint (Rydell, 1966), the maximum force of friction would be in the order of 18 pounds acting at the point in the skating thrust when the normal joint force is maximum.

Medial-lateral stability of the knee is maintained by tensile forces acting in the collateral ligaments of the joint. The valgus-varus moment, M_{yk} , is resisted by a force in either the medial collateral or lateral collateral whenever the centre of pressure of the normal joint force, R_z , falls outside the limiting value X_0 , as shown in Fig. 3.26. As the skater moves forward on to the support leg, Fig. 4.03, the knee joint is lateral with respect to the vertical force, F_{zp} , on the foot, Fig. 3.20, and this develops a positive moment, M_{yk} , on the joint. This positive moment tends to separate the lateral condyles of the joint and equilibrium is achieved through a tensile force in the lateral collateral. The magnitude of the lateral collateral force is directly

related to the relative angle of the shank to the vertical. This accounts for the wide range in tensile forces calculated in the lateral collateral as represented in Table No. 3. Minimum values correspond to upright angles of the shank while maximum values act when the knee is lateral a significant degree with respect to the foot. Approaching push off in the skating thrust, the knee moves medially and inside the vertical force, F_{zp} , on the foot, Fig. 3.20, and is subject to a negative moment, My_k . This negative My_k tends to separate the medial condyles of the joint and is resisted by a tensile force in the medial collateral. Again the magnitude of the force in the medial collateral is dependent on the angle of the shank with maximum values acting when the knee is medial a maximum amount with respect to the foot. Table No. 3 indicates that when a large medial collateral force is developed during a skating thrust, the force in the lateral collateral is minimal and vice versa.

Part of the valgus-varus moment, My_k , may be resisted by the cruciates. Brantigan and Voshell (1941) demonstrated that when the knee is in flexion some cruciate ligament tension is required to assist medial-lateral instability of the joint due to a slackening of the lateral collateral. However, Fig. 4.06 indicates that moment My_k is negative for the flexion portion of the skating thrust and no force acts in the collaterals during this phase, Fig. 4.08. On the other hand some of the force attributed to the lateral col-

lateral ligament is probably carried as tension in the ilio-tibial tract. Also, McCloy (1959) has stated that it is possible that a portion of the forces ascribed to the collateral ligaments may be taken by the quadriceps muscle group since the vastus medialis and vastus lateralis blend posteriorly with the collaterals through their insertion in the rectinaculum patellae and its' association with the capsular ligament of the joint. Morrison (1970) further suggests that the valgus-varus moment is partly equilibrated by differential force action of the lateral and medial hamstrings or the lateral and medial heads of the gastrocnemius. These statements are noteworthy if one accepts the theory of several authors such as Smillie (1951) that tension receptors in the articular ligaments, when activated, produce a reflex contraction in the associated muscle groups. This theory has not been proven and in fact is contradicted by Stener's (1959) experiments for the medial collateral ligament of the knee.

Articular Forces

The joint force, R_z , which acts normal to the articular surface of the knee joint attains a peak value at a point in the support phase of the skating thrust, Fig. 4.09, when the sum of the normal component of the quadriceps muscle force plus the external force, F_{zk} , is maximal, Equation 3.17. The maximum value of R_z developed in the

skating thrust was 888 pounds or 5.60 times the body weight of the test subject.

Test results indicate that during the support phase of the skating thrust the centre of pressure of joint force, R_z , is positioned initially over the medial condyles but then shifts to the lateral condyles at push off, Fig. 4.10. Since the medial condyle has a larger anatomical bearing area compared to the lateral condyle, Fig. 3.02, it follows that the compressive stress imposed at the medial articular surface of the joint is smaller than the stress of the lateral articular surface. Also, as Morrison (1970) has noted, the stresses acting in the shaft of the tibia would be lower on the medial side because the medial condyle overhangs the shaft of the tibia less than the lateral condyle.

The side or shear force, R_x , on the joint is relatively small, approximately 0.10 times the magnitude of the normal articular force, R_z , Fig. 4.09. The medial or lateral movement of the femur on the tibia is considered to be resisted by the tibial intercondylar eminence, by a friction force between the condyles and by tension in the ligament structures (Brantigan and Voshell, 1941). The femur tends to move laterally on the tibia during the support phase of the skating thrust and medially at push off.

The magnitude and direction of the anterior-posterior force, R_y , on the joint is reflected by the forces acting in the cruciate ligaments. For the greater portion of the

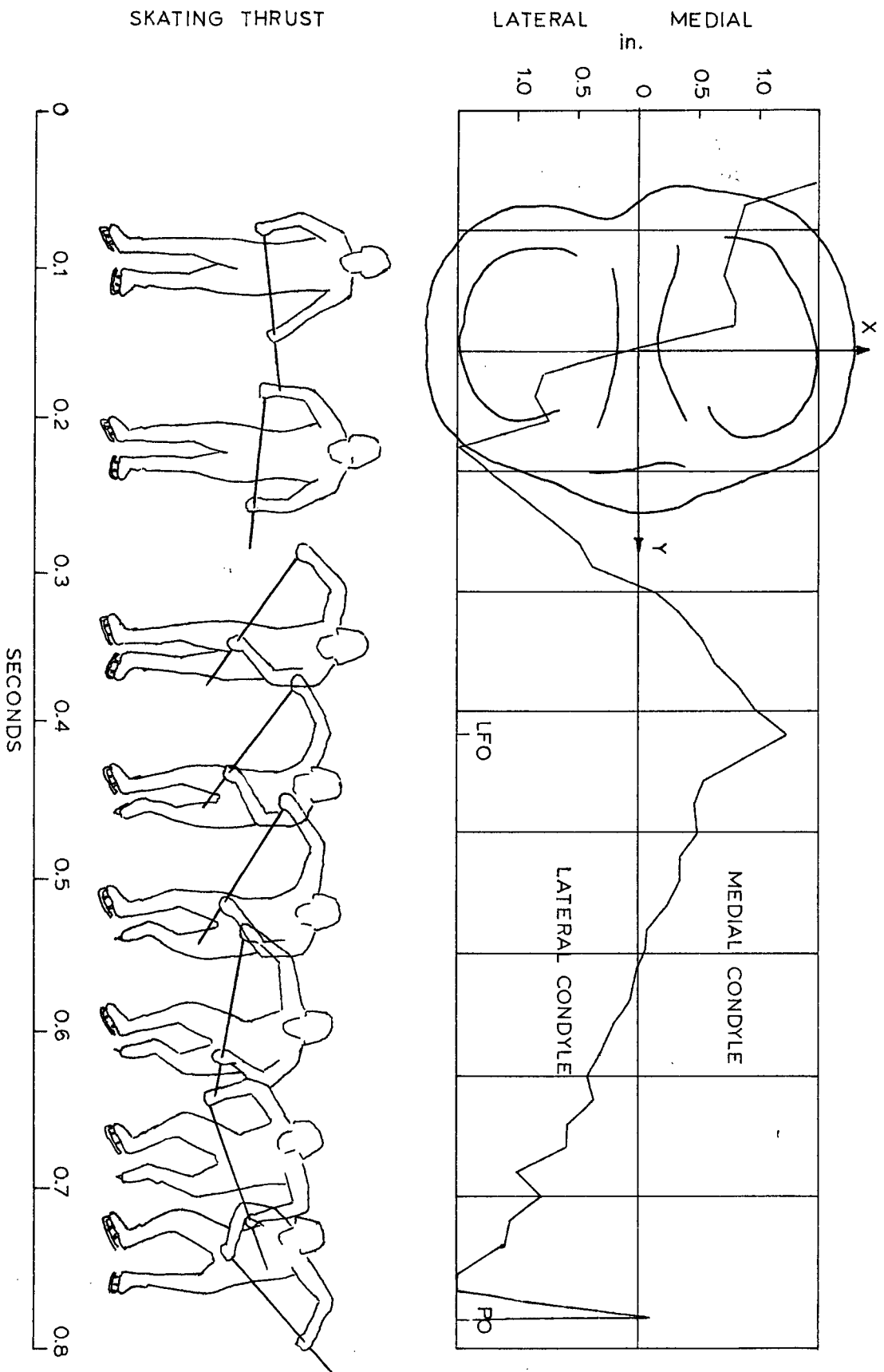


FIG.4.10 CENTRE OF PRESSURE ON CONDYLES OF KNEE

skating thrust the femur tends to glide forward on the tibia and is controlled by a tension developed in the posterior cruciate ligament, Fig. 4.08. At push off the femur is forced backward relative to the tibia and this motion is resisted by tension in the anterior cruciate. As stated previously, the effects of friction in the joint in the anterior-posterior direction were neglected.

Joint Torque

Fig. 4.09 indicates a positive inward torque, M_z , acting on the knee during the skating thrust. This torque produces medial rotation of the tibia on the femur which is resisted by the collateral ligaments. (Steindler, 1955) According to Morrison (1970) an inward torque on the joint is resisted by the oblique posterior fibres of the medial collateral ligament while Brantigan and Voshell (1941) demonstrated on intact knee joints that medial rotation is balanced by tension in a tightening lateral collateral ligament and the cruciates as they twist on themselves. It is therefore apparent that moment action, M_z , about the long axis of the tibia must be balanced by force actions in the articular ligaments and will alter the distribution of the ligament forces as calculated in the analysis. It is also suggested by certain authors (Steindler, 1965; Radin and Paul, 1970) that the menisci and tensor fascia latae aid in resisting the effects of a torque on the knee joint.

Forces at the Knee in Various Activities

The preceding results reveal little concerning the relative strain imposed on the ligaments and muscles of the knee since the actual tensile strength and stress-strain characteristic of human ligament and muscle tissue has not been experimentally determined to this date. Considerable research has been done by Tipton and associates (1967, 1975) and Zuckerman (1969, 1973) on the strength of ligaments from animals but it is difficult if not impossible to relate these results to the strength of human ligamentous tissue. Therefore we are forced to evaluate the significance of the present study by comparison with results of similar studies for other activities. (Morrison, 1969)

The mean maximum muscle and ligament forces calculated for the skating thrust and for various walking activities are listed in Table No. 4. The peak skating forces represent the mean of five trials on a single subject while the forces for walking represent the mean from three test subjects. Upon examination of the tabulated results, it is apparent that the maximum forces developed in the collateral ligaments, in particular the medial collateral, are significantly greater during a skating thrust as compared to level or inclined walking. The anterior cruciate force for the skating thrust is comparable to that developed in level walking but only 0.3 times the tensile force acting in the anterior cruciate when walking down an inclined ramp. The force acting in the posterior cruciate during the skating thrust is

TABLE NO. 4

THE MAXIMUM MUSCLE AND LIGAMENT
FORCES OF VARIOUS ACTIVITIES

Activity	Muscle Force, lbs			Ligament Force, lbs			
	H	Q	G	pc	ac	mc	lc
Level Walking	309	191	262	79	38	17	50
Walking Up Ramp	240	176	335	144	15	16	158
Walking Down Ramp	189	430	-	59	100	19	62
Walking Up Stairs	177	433	79	273	6	9	156
Walking Down Stairs	88	380	155	101	21	19	80
Skating Thrust	179	652	79	164	32	212	204

H.....hamstrings

pc.....posterior cruciate

Q.....quadriceps

ac.....anterior cruciate

G.....gastrocnemius

mc.....medial collateral

lc.....lateral collateral

twice as great as the force for level walking but less than the posterior cruciate force calculated when walking up stairs. The peak muscle force for the skating thrust, 652 pounds in the quadriceps, is double the maximum muscle force recorded in level walking, 309 pounds in the hamstrings.

A direct comparison of activities suggests that the skating thrust is comparable to walking upstairs in that the quadriceps muscle group exerts the maximum force in each case, while the forces acting in the gastrocnemius and hamstrings muscle groups are much smaller. However, the large forces developed in the quadriceps muscle group and the collateral ligaments during a skating thrust makes it unique when compared to either stair or ramp walking.

Peak articular forces including joint torque acting at the knee for the skating thrust and the various walking activities studied by Morrison (1969) are listed in Table No. 5. Again these results represent the maximum mean of five trials on a single subject for the skating thrust and the maximum mean from three test subjects for the walking activities. From Table No. 5 it is evident that the normal or vertical joint force, R_z , is significantly larger for skating, 5.48 times body weight compared to 4.25 times body weight for walking upstairs and 3.40 times body weight for level walking.

Probably the severest force imposed on the knee joint during the skating thrust is the joint torque. In the skating

TABLE NO. 5

MAXIMUM JOINT FORCES AND
TORQUES OF VARIOUS ACTIVITIES

Activity	Max. Joint Force		Mz lb-ins
	Rz/bw	Rx/bw	
Level Walking	3.40	0.26	239
Walking Up Ramp	3.97	-	-
Walking Down Ramp	3.95	-	-
Walking Up Stairs	4.25	0.89	-
Walking Down Stairs	3.83	-	-
Skating Thrust	5.48	0.51	696

Rz/bw.....Ratio normal joint force to body weight

Rx/bw.....Ratio shear force to body weight

Mz.....Joint torque

thrust a mean maximum torque of 696 pound-inches was developed compared to a maximum of 239 pound-inches for level walking. This large torque on the joint has serious implications when it is considered that the maximum values of torque and vertical joint force act at the same point in time during the skating thrust, Fig. 4.09.

CHAPTER V

SUMMARY AND CONCLUSIONS

The knee is probably subject to more stress and strain than any other joint of the body. The stability of the knee is maintained by the ligamentous structure of the joint, the articular cartilage and the bone architecture of the tibia and femur. During an athletic movement such as the skating thrust, contractile muscle forces plus external forces of reaction impose a considerable stress on the knee. These forces are necessarily balanced by the articular surfaces of the joint and by the tensile forces developed in the ligaments to prevent relative displacements of the joint.

The present study was designed to determine the magnitude and temporal sequence of muscle, ligament and articular forces acting at the knee joint during a simulated skating thrust. One male test subject, an accomplished hockey player, made 15 simulated skating thrusts. The reaction forces and point of application of these forces during the thrust were recorded with the Kistler force plate at the laboratory of the University of Washington. A synchronized cine film record of each trial was obtained from 16 mm film in both the frontal and lateral planes. Electromyographic data for the three main muscle groups (hamstrings, gastrocnemius and quadriceps)

active during the skating thrust was obtained from tests conducted on-ice and off-ice at the University of British Columbia. Anthropometric data after Dempster (1955), Braune and Fischer (1889) and Morrison (1968) allowed calculation of gravitational limb forces while acceleration data determined from the digitized film records was used to calculate limb inertial forces. Using D'Alembert's principle of equilibrium of bodies in motion, the joint forces and moments at the knee were determined from the force plate reaction forces, limb gravitational forces and limb inertial forces. The forces in each muscle group and ligament were determined from the calculated external force system acting at the knee and the required stability conditions of the joint.

Results showed that force action developed initially in the hamstrings to stabilize the joint as the skater shifted his weight to the support leg. As the support leg assumed the body weight, powerful force action developed in the quadriceps muscle to extend the knee and drive the skater forward past the support foot. The gastrocnemius exerted a small force to plantar flex or extend the ankle for the final push off that is characteristic of all accomplished skaters. The posterior cruciate ligament developed tension in order to resist the anterior displacement of the femur relative to the tibia during the thrust reaching a maximum force as the skater shifted his weight to the support foot. The forces developed in the anterior cruciate were relatively

small and unimportant in the skating thrust. Tensile force developed in the collateral ligaments was required to assure medio-lateral stability with the peak lateral collateral forces developed at the onset of the support phase and maximum medial collateral forces developed during the final extension of the leg through push off.

Although the current investigation cannot comment on the relative stability of the knee it can be stated that the joint is most susceptible to injury in skating when the external forces and torques of athletic competition are superimposed on the critical values of ligament and articular forces developed by the thrust itself. It therefore appears that the lateral collateral ligament would be most susceptible to a tensile strain at the onset of the support phase while the medial collateral is most vulnerable to injury as the skater drives forward at push off. Also, the coincidence of a maximum joint force, six times body weight, and a joint torque approaching 700 pound-inches during the support phase placed a considerable stress on the articular surfaces of the joint and the joint menisci. Damage to the menisci of the knee in the form of tearing is a common injury in the game of ice hockey.

The magnitude of the muscle, ligament and joint forces developed in the skating thrust were significantly greater than respective forces exerted during level walking while the cyclic pattern of the skating forces was comparable

to walking upstairs indicating a temporal similarity in these activities.

Conclusions

The following statements are made with respect to the biomechanics of the skating thrust.

- (1) The quadriceps are the most important muscle group in the skating thrust developing contractile forces of the order of 700 pounds when extending the knee joint.
- (2) The hamstrings and gastrocnemius muscle groups exert forces less than 200 pounds and 100 pounds respectively to stabilize the knee during the weight shift and push off phases of the skating thrust.
- (3) The collateral ligaments and the posterior cruciate are important in maintaining stability of the joint and tensile forces in excess of 250 pounds act in these structures.
- (4) The knee joint is subject to the combined effects of a joint force six times body weight and a joint torque approaching 700 pound-inches superimposed upon each other during the support phase of the skating thrust.
- (5) Medio-lateral joint displacement is not critical since shear forces less than 0.50 times body weight are imposed during the skating thrust.

REFERENCES

REFERENCES

- Adams, A. 1966. Effects of exercise upon ligament strength. Research Quarterly. 37:163.
- Andrews, J. G., Chao, F. Y., Johnston, R. C. and Stauffer, R. N. 1972. A general method for accurate kinematic analysis of biomechanical systems in motion. Procs. Orth. Res. Soc. 29.
- Basmajian, J. V. 1962. Muscles Alive; their functions revealed by electromyography. Williams and Wilkins, Baltimore.
- Beckett, R. and Chang, K. 1968. An evaluation of the kinematics of gait by minimum energy. J. Biomechanics. 1: 147-159.
- Bender, J. A. and Associates. 1964. Factors affecting the occurrence of knee injuries. J. Assoc. for Physical and Mental Rehabilitation. 18. No. 5:130.
- Brantigan, D. C. and Voshell, A. F. 1941. The mechanics of the ligaments and menisci of the knee joint. J. Bone and Joint Surgery. 23:44-46.
- Braune, W. and Fischer, O. 1889. The centre of gravity of the human body as related to the equipment of German infantryman (in German). Treat. of the Math-Phys. Class of the Royal Acad. of Sc. of Saxony. 26.
- Bresler, B. and Frankel, J. P. 1950. The focus and moments in the leg during level walking. ASME Transactions. 72:27.
- Chaffin, D. B. 1969. A computerized biomechanical model for development and use in studying gross body actions. J. Biomechanics. 2:429-441.
- Chao, E. Y. and Kwam, R. 1973. Application of optimization principles in determining applied moments in the human leg joint during gait. J. Biomechanics. 6:497-510.
- _____, Sim, F. H., Stauffer, R. N. and Johannson, K. J. 1973. Mechanics of ice hockey injuries. Mechanics and Sport, ASME Winter Meeting, Applied Mechanics Division. 4:143-154.

- Close, J. R. and Todd, F. N. 1959. The phasic activity of the muscles of the lower extremity. J. Bone and Joint Surgery. 41A. 2:189.
- Cunningham, D. and Brown, G. W. 1952. Two devices for measuring forces acting on the human body during walking. Procs. Soc. Exp. Stress Analysis. 9:75.
- Dempster, W. T. 1955. Space requirements of the seated operator. WADC Technical Report: 55-159. Report released to office of Technical Services, U.S. Dept. of Commerce, Wash.
- Denham, T. A. 1959. Hip mechanics. J. Bone and Joint Surgery. 41B:550-557.
- Dillman, C. J. 1970. A kinematic analysis of the recovery leg during sprint running. Selected Topics on Biomechanics. Procs. C.I.C. Symposium on Biomechanics. 137-165.
- Edwards, R. G., Lafferty, J. F. and Lange, K. D. 1970. Ligament strain in the human knee joint. ASME Transactions.
- Elftman, H. 1938. The measurement of the external force in walking. Science. 88:152-153.
- _____ 1939. Forces and energy changes in the leg during walking. Am. J. Physiology. 125:339-356.
- _____ The function of muscles in locomotion. Am. J. Physiology. 125:354-366.
- Engin, A. E. and Korde, M. S. 1974. Biomechanics of normal and abnormal knee joints. J. Biomechanics. 7:325-334.
- Fischer, O. 1906. Theoretical fundamentals of the mechanics of living bodies (in German). Berlin.
- Houtz, S. J. and Walsh, E. P. 1959. Electromyographic analysis of the function of the muscles acting on the ankle during weight bearing with special reference to the triceps surae. J. Bone and Joint Surgery. 41A:8.
- Hughston, J. C., Whatley, G. S. and Dodelin, R. A. 1961. The athlete and his knees. Southern Med. Journal. 54:1372-1378.
- Inman, V. T. 1947. Functional aspects of the abductor muscles of the hip. J. Bone and Joint Surgery. 39:607.

- Joseph, J. and Nightingale, A. 1952. Electromyography of muscles of posture; leg muscles in males. J. Physiology. 117:484.
- Karpovich, P. V., Singh, M. and Tipton, G. M. 1970. Effect of deep knee bends upon knee stability. Teor. Praxe Til Vyuch. 18:112-115.
- Kettelkamp, D. B. and Chao, E. V. 1972. A method for quantitative analysis of medial and lateral compressive forces at the knee during standing. Clinical Orthopedics and Related Research. 83:202.
- Klein, K. K. 1962. An instrument for testing the medial and lateral collateral ligament stability in man. Am. J. Surgery. 104:768, 11.
- _____. 1964. Specific progressive resistive exercise for increasing medial-lateral ligament stability and use of the knee ligament testing instrument for test-retest measurement. J. Assoc. for Physical and Mental Rehabilitation. 18. No. 5:135.
- _____. 1971. The deep squat exercise as utilized in weight training for athletes and its' effect on ligaments of the knee. J. Assoc. Phys. Ment. Rehab. 15:6-11, 23.
- _____ and Hall, W. L. 1963. The Knee in Athletics. American Association for Health, Physical Education and Recreation, Washington.
- Lanczos, C. 1957. Applied Analysis. Pitman, London.
- Linge, B. V. 1961. Behaviour of quadriceps muscle during walking. Procs. Netherland Orthopedic Society.
- Lippold, O. C. 1952. The relation between integrated action potentials in human muscle and its isometric tension. J. Physiology. 117:492.
- McLeish, R. D. and Charnley, J. 1970. Abduction forces in the one-legged stance. J. Biomechanics. 3:191-209.
- Morrison, J. B. 1968. Bio-engineering analysis of force actions transmitted by the knee joint. Biomedical Eng. 3:164-170.
- _____. 1969. Functions of the knee in various activities. Biomedical Eng. 4:573-580.

- _____. 1970. The mechanics of the knee joint in relation to normal walking. J. Biomechanics. 3:51.
- Murray, M. P., Drought, A. B. and Kory, R. C. 1964. Walking patterns of normal men. J. Bone and Joint Surgery. 46A: 335-360.
- O'Donoghue, D. H. 1950. Surgical treatment of fresh injuries to the major ligaments of the knee. J. Bone and Joint Surgery. 32A:721.
- Paul, J. P. 1964. Bio-engineering studies of forces transmitted by joints. Biomechanics and Related Bio-Engineering Topics. R. M. Kenedi (Ed.) :369.
- _____. 1966. The biomechanics of the hip joint and its clinical relevance. Procs. Royal Society of Medicine. 59:10.
- _____. Forces transmitted by joints in the human body. Institution of Mechanical Engineers Procs. 3J. 181:8-15.
- _____. 1967. Design aspects of endo-prostheses for the lower limb. Perspectives in Bio-medical Engineering. R. M. Kenedi (Ed.) :91.
- _____. 1971. Load actions on the human femur in walking and some resultant stresses. Exp. Mechanics. 3:121.
- Penrod, D., Davy, D. T. and Singh, D. P. 1974. An optimization approach to tendon force analysis. J. Biomechanics. 7:123-128.
- Radcliffe, C. W. 1962. The biomechanics of below knee prostheses in normal level walking. Artificial Limbs. 2:6.
- Radin, E. L. Response of joints to impact loading. J. Biomechanics. 6:51-57.
- _____. and Paul, I. L. 1970. Does cartilage compliance reduce skeletal impact loads? Arth. Rheum. 13:139.
- Rasch, D. J., Maniscolo, R., Pierson, W. R. and Logan, G. A. 1967. Effect of exercise, immobilization and intermittent stretching on the strength of knee ligaments of albino rats. J. Applied Physiology. 15:289.

- Rydell, N. 1965. Forces in the hip joint; intravital studies. Biomechanics and Related Bio-Eng. Topics. R. M. Kenedi (Ed.) :196.
-
- _____ 1966. Forces acting on the femoral head prosthesis. Acta. Orthop. Scand. Suppl. 88:37:1.
- Seireg, A. and Arvikar, R. J. 1973. A mathematical model for evaluation of forces in the lower extremities of the musculo-skeletal system. J. Biomechanics. 6:313-326.
-
- _____ 1975. The prediction of muscular load sharing and joint forces in the lower extremities during walking. J. Biomechanics. 8:89-102.
-
- _____ Gerath, M. 1975. An in-vivo investigation of wear in animal joints. J. Biomechanics. 8:169-172.
- Simon, S. R., Radin, E. L. and Paul, I. L. 1972. The response of joints to impact loading. J. Biomechanics. 5:267.
- Smillie, I. S. 1970. Injuries of the Knee Joint. Livingstone, London.
- Sorbie, C. and Zalter, R. 1964. Bio-engineering studies of the forces transmitted by joints. Biomechanics and Related Bio-Engineering Topics. R. M. Kenedi (Ed.) :369.
- Steindler, A. 1955. Kinesiology of the Human Body Under Normal and Pathological Conditions. Thomas, Springfield.
-
- _____ 1965. Kinesiology. Thomas, Springfield.
- Stern, J. T. 1974. Computer modelling of gross muscle dynamics. J. Biomechanics. 7:411.
- Thornton-Trump, A. B. and Daher, R. 1975. The prediction of reaction forces from gait data. J. Biomechanics. 8:173.
- Tipton, C. M., Schild, R. J. and Tomanek, R. J. 1967. Influence of physical activity on the strength of knee ligaments in rats. Am. J. Physiology. 212:783-787.
-
- _____ Flatt, A. E. 1967. The measurement of ligamentous strength in rats. J. Bone and Joint Surgery. 49A:63-72.

- _____, James, S. L., Mergner, W. and Cheng, T. K. T. 1970. Influence of exercise on the strength of the medial collateral knee ligament in dogs. Am. J. Physiology. 218:894-902.
- _____, Matthes, R. D. and Sandage, D. S. 1974. In situ measurement of junction strength and ligament elongation in rats. J. Appl. Physiology. 37:758-761.
- _____, Maynard, J. A. and Carey, R. A. 1975. The influence of physical activity on ligaments and tendons. Medicine and Science in Sports. 7:165-175.
- Viidik, A. 1966. Biomechanics and functional adaptation of tendons and joint ligaments. Studies on the Anatomy and Function of Bones and Joints. F. G. Evans (Ed.). Springer, Berlin.
- _____. 1967. Experimental evaluation of the tensile strength of isolated rabbit tendons. Bio-medical Eng. 2:64-67.
- _____. 1968. Elasticity and tensile strength of the anterior cruciate ligament in rabbits as influenced by training. Acta. Physiol. Scand. 74:372-380.
- Wang, C., Walker, P. S. and Wolf, B. 1973. The effects of flexion and rotation on the length patterns of ligaments of the knee. J. Biomechanics. 6:587-596.
- Williams, J. F. and Evenson, N. L. 1968. A force analysis of the hip joint. Bio-medical Eng. 3:365-370.
- Winter, D. A., Quanbury, A. D., Hobson, D. A., Sidwall, H. G., Reiner, G. D., Trenholm, B. G., Steinke, T. and Schlosser, H. 1974. Kinematics of normal locomotion from TV data. J. Biomechanics. 7:479.
- Zuckerman, J. and Stull, G. A. 1969. Effects of exercise on knee ligament separation force in rats. J. Applied Physiology. 26:716-719.
- _____. 1973. Ligamentous separation force in rats as influenced by training, detraining and cage restriction. Medicine and Science in Sports. 5:44-49.

APPENDICES

APPENDIX A

ANTHROPOMETRIC MEASUREMENTS

APPENDIX A

ANTHROPOMETRIC MEASUREMENTS

1. Body Segment Parameters

The following body segment parameters represent the average of five independent measurements.

Segment	Circumference, in	Radius, in	Length, in
shank	14.50	2.31	16.50
foot	13.30	2.07	10.50
ankle	12.80	2.02	-
knee	15.30	2.43	-

$$\text{radius of segment} = \frac{\text{circumference of limb}}{2\pi}$$

The length of a segment was measured from joint centre to joint centre and the circumference of a segment was measured at the joint centre and centre of gravity of the segment.

2. Calculation of Segment Weights

Dempster (1955) expressed the weight of each body segment as a percentage of the total body weight, based on measurements from living male subjects of various body types and age.

Test subject body weight = 165 lbs

Segment	Dempster %	Weight lbs
thigh	9.65	16.00
shank	4.50	7.43
foot	1.40	2.31

segment weight = Dempster % x body weight

3. Centre of Gravity of Body Segments

Dempster determined the distance of the mass centre of each body segment from the proximal end expressed as a percent of the length of the segment

Segment	Length, in	Dempster %	Centre Gravity, in
shank	16.5	0.433	7.15
foot	10.5	0.429	4.50

distance of c.g. from proximal end of segment = Dempster %
x segment length

In the case of the foot, the centre of gravity lies at the intersection of a vertical line 4.50 inches proximal to the heel and a line joining the ankle axis to the ball of the foot.

4. Moment of Inertia of Segment

The mass moment of inertia (I) of a body segment is equal to the product of the segment's mass and the radius of

gyration (r) of the segment. Braune and Fischer (1889) determined co-efficients to allow calculation of the radius of gyration of a segment.

Segment	Length, in	Diameter, in	C_3	C_4	rx	ry	rz
shank	16.5	4.62	0.25	0.35	4.13	4.13	1.62
foot	10.5	4.14	0.30	0.35	1.45	3.15	3.15

radius of gyration (r) is expressed in inches

C_3 is the Fischer coefficient for the radius of gyration for rotation about the axis through the mass centre and perpendicular to the longitudinal axis of the segment

radius of gyration = C_3 x length of segment

For rotation of the segment about the longitudinal axis, Fischer used the coefficient C_4 and the diameter of the segment to calculate the radius of gyration

radius of gyration = C_4 x diameter of segment

Segment	Weight, lbs	Ix	Iy	Iz
shank	7.43	3.92	3.92	0.60
foot	2.31	0.15	0.71	0.71

moment of inertia (I) = mass of segment x (radius of gyration)²
and is expressed in slug-in²

The coefficients of Fischer and Dempster are taken from a review of body segment parameters by Drillis, Contini and Bluestein (1964)

5. Anthropometric Scaling Factors

Scaling factors were required to obtain the test subject's co-ordinates of muscle and ligament attachment from the respective basic co-ordinates of Morrison as listed in Table No. 1 of the text. The dimensions used to obtain the scaling factors for the knee are,

X - the breadth of the femoral condyles measured from the lateral epicondyle to the medial condyle

Y - the depth of the femoral condyles measured from the anterior surface of the lateral condyle to the posterior surface of the medial condyle.

Z - the length of the tibia measured from the centre of the knee joint to the centre of the ankle joint.

For the pelvis a common scaling dimension was used for male subjects.

X - the distance between the anterior superior iliac spines of the pelvis

Therefore, a common scaling factor is calculated for the pelvis which is applied to the three co-ordinates of

muscle attachment at the pelvis.

Joint	Co-ordinate	Scaling Dimension		Scaling Factor
		Basic	Subject	
knee	X	3.50	3.78	1.07
knee	Y	3.55	3.64	1.03
knee Z	Z	16.00	16.16	1.01
pelvis	X	8.70	8.20	0.94

scaling dimensions expressed in inches

$$\text{scaling factor} = \frac{\text{dimension from test subject}}{\text{basic dimension from dissection}}$$

The co-ordinate of a muscle or ligament attachment to the skeleton of the test subject is then considered to be the basic dimension as measured from dissection multiplied by the appropriate scaling factor. For example the Xs co-ordinate of the patellar ligament attachment to the tibia, Xsq, is calculated as follows

$$\begin{aligned} \text{Xsq} = & (\text{Xs co-ordinate measured}) \\ & \times (\text{scaling factor in dissection}) \end{aligned}$$

APPENDIX B
INSTRUMENTATION

APPENDIX B

INSTRUMENTATION

1. Filming Equipment

Two cameras were required to obtain cinematographic data in the two planes of movement.

16 mm Locam: motor driven
adjustable film speed
internal pulse light

16 mm Bolex: spring loaded
set film speeds

Kodak 4X Reversal 320 ASA film with double edge perforations was used with both cameras. Filming speed was 64 frames/sec. A 35 mm Tektronix camera and a 35 mm Nikkormat camera were utilized to record the stored oscilloscope traces of the force plate output.

2. Data Reduction

The Vanguard Motion Analyzer of the Institute of Animal Resources (I.A.R.E.) capable of readings to the nearest 0.001 inch was used to reduce cinema and force plate data.

3. Electromyography

Bipolar electrodes placed on the belly of two muscle groups were connected to separate channels of a two-channel Sanborn Recorder. This allowed the electrical output of two muscle groups to be monitored simultaneously as a trace on paper.

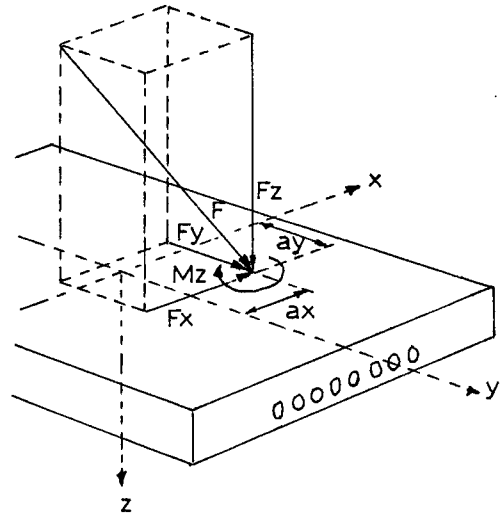
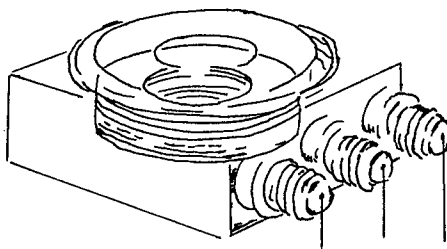
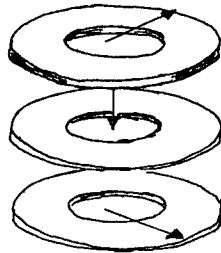
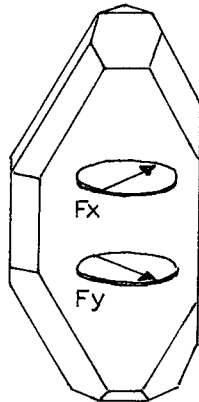
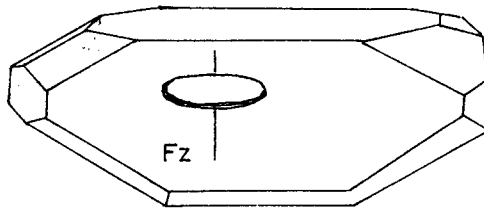
paper speed - 100 mm/sec

gain - same for both channels

4. Force Measuring Platform

The multi-component measuring platform Type 9261A designed by the Kistler Instruments is a piezoelectric transducer which measures any force applied to it in three orthogonal components. In addition the moment applied to the platform and the co-ordinates of the point of application of the force are recorded. Four quartz force-measuring-elements are fitted to the corners of the platform which has a high rigidity allowing operation with a minimum a measuring displacement as well as a wide frequency range.

The electrical charges yielded by the platform are strictly proportional to the measurands; by means of charge amplifiers they are converted into analog dc voltages, which then can be recorded, indicated or otherwise processed as required. In our case the force plate output was stored as six separate storage traces on three dual channel Tektronix oscilloscopes.



6 Variables Measured

Single 3-Component Force
Transducer Containing Shear
and Pressure Sensitive Quartz
Crystals

KISTLER FORCE PLATFORM BASED
ON PIEZOELECTRIC EFFECT OF
QUARTZ CRYSTALS

APPENDIX C

DATA REDUCTION

APPENDIX C

DATA REDUCTION

1. Cinema Scaling Factors

A surveyor's range pole was utilized as the reference image in determination of the X and Y scaling factors for reduction of cine film data.

Co-ordinate	Image, in	Actual, in	Scaling Factor
X	6.396	72.00	10.38
Y	5.592	72.00	12.88

The calculated scaling factors represent the average of ten measurements

$$\text{scaling factor} = \frac{\text{actual length of range pole}}{\text{image length of range pole}}$$

2. Force Plate Data Reduction

The synchronized force plate traces, recorded on 35 mm film, were digitized by horizontally incrementing the traces into 50 divisions corresponding to the 50 frames of the 16 mm film record that described the skating thrust. The actual values of the output components were determined by applying the force plate and oscilloscope calibration factors to each of the vertical co-ordinates defined by the

50 horizontal divisions. The calibration factors for the output variables in terms of measurand units per vertical division are,

Variable	Force Plate	Oscilloscope	M.U./div.
Fx	100 N/V	x 2 V/div.	= 200 N/div.
Fy	100 N/V	x 1 V/div.	= 100 N/div.
Fz	100 N/V	x 5 V/div.	= 500 N/div.
Mz	100 Nm/V	x 0.02V/div.	= 2 Nm/div.
Ax	5 Cm/V	x 0.5 V/div.	= 2.5 cm/div.
Ay	5 Cm/V	x 0.5 V/div.	= 2.5 cm/div.

$$1 \text{ N (Newton)} = 0.2248 \text{ lbs}$$

$$1 \text{ Nm (Newton-meter)} = (0.2248 \times 39.37) \text{ lb-ins}$$

$$1 \text{ cm (centimeter)} = 0.3937 \text{ in}$$

$$F_x = (200)(0.2248) = 44.96 \text{ lb/div.}$$

$$F_y = (100)(0.2248) = 22.48 \text{ lb/div.}$$

$$F_z = (500)(0.2248) = 112.40 \text{ lb/div.}$$

$$M_z = (2)(0.2248 \times 39.37) = 15.50 \text{ lb-in/div.}$$

$$A_x = (2.5)(0.3937) = 0.984 \text{ in/div.}$$

$$A_y = (2.5)(0.3937) = 0.984 \text{ in/div.}$$

APPENDIX D

LIMB AND JOINT CO-ORDINATES

APPENDIX D

LIMB AND JOINT CO-ORDINATES

1. Orthogonal Co-ordinates

The limb and joint co-ordinates were determined with respect to the centre axis of the force platform and for the following sign convention. (in inches)

X - positive medial to centre of platform

Y - positive forward of centre of platform

Z - positive above platform

The orthogonal co-ordinates of the limbs and joints are shown in Fig. D1 for the knee ahead of and medial to the centre axis of the force platform.

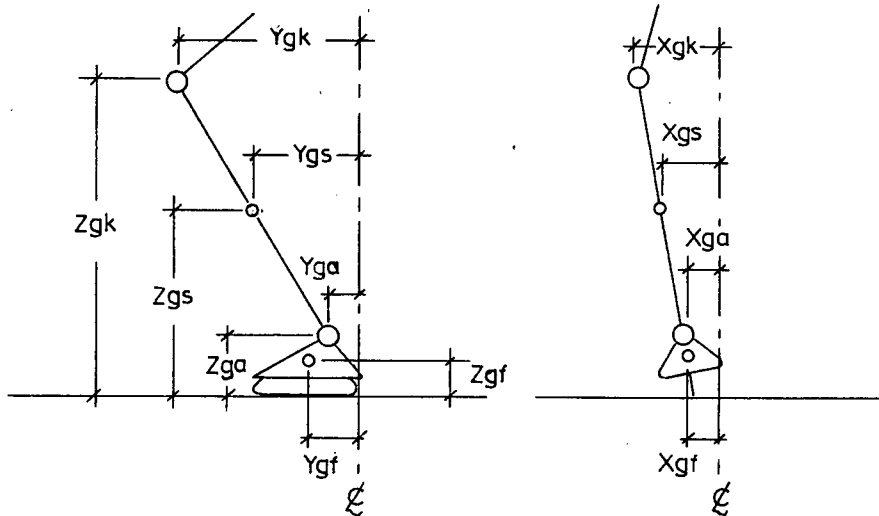


FIG. D1 LIMB AND JOINT CO-ORDINATES

The orthogonal co-ordinates of Fig. D1 represent the co-ordinates of the joint centre of the knee and ankle and the mass centre of the shank and foot. These co-ordinates were determined by correcting the co-ordinates of limb and joint surface markers for limb angle and limb radius.

2. Angular Limb Co-ordinates

The angular limb co-ordinates expressing limb angles were determined from the co-ordinates of the joint surface markers.

The angular co-ordinates for rotation of the shank and foot with respect to the X axis is shown in Fig. D2.

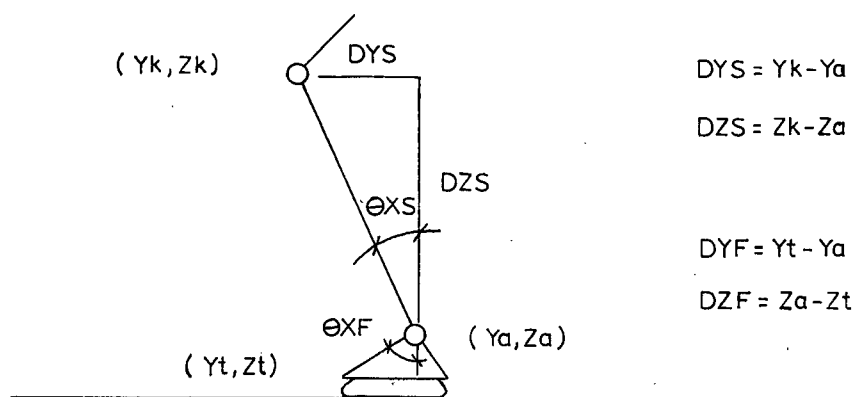


FIG. D2 ANGULAR LIMB CO-ORDINATES

$$\theta_{XS} = \arctan \frac{DYS}{DZS} \quad \theta_{XF} = \arctan \frac{DYF}{DZF}$$

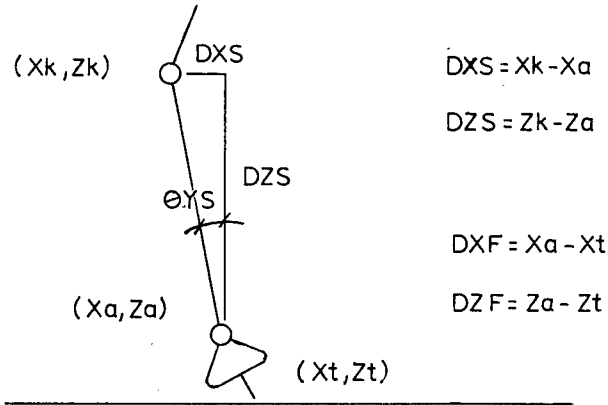


FIG. D3 ANGULAR LIMB CO-ORDINATES

$$\theta_{YS} = \arctan \frac{DXS}{DZS} \quad \theta_{YF} = \arctan \frac{DXF}{DZF}$$

The angular co-ordinate of the foot about its longitudinal axis, θ_{YF} , was directly determined as shown above in Fig. D3. The angular co-ordinate of the shank about its longitudinal axis, θ_{YS} , was calculated from a knowledge of the radius of the shank and the location of the mass centre marker of the shank as shown in Fig. D4.

Angular co-ordinate θ_{ZF} represents the rotation of the foot the vertical axis and is calculated as

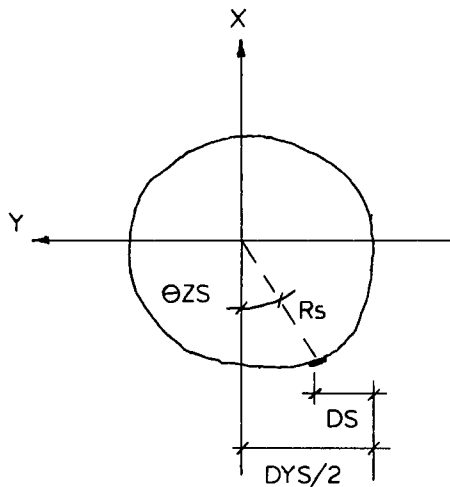
$$\theta_{ZF} = \arctan \frac{DXF}{DYF}$$

The angular rotation of the thigh about the X and Y

axes were calculated as follows

$$\theta_{XT} = \arctan \frac{D_{YT}}{D_{ZT}}$$

$$\theta_{YT} = \arctan \frac{D_{XT}}{D_{ZT}}$$



R_s - radius of shank

Y_{SA} - anterior co-ordinate of shank

Y_{SP} - posterior co-ordinate of shank

Y_S - co-ordinate of shank marker

$$DYS = Y_{SA} - Y_{SP}$$

$$DS = Y_S - Y_{SP}$$

FIG. D4 ROTATION OF SHANK ABOUT LONG AXIS

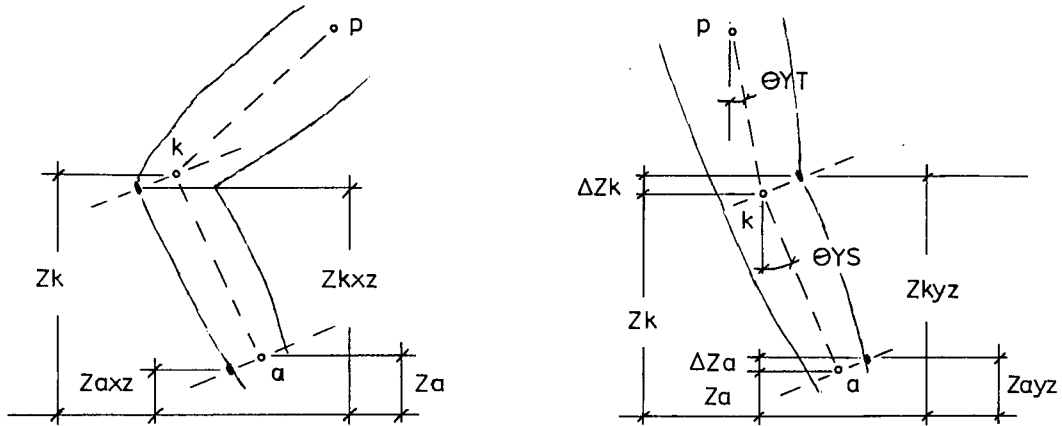
where the angular rotation of the shank θ_{ZS} is calculated as follows

$$\theta_{ZS} = \arcsin \frac{DYS/2 - DS}{R_s}$$

3. Limb and Joint Centre Co-ordinates

The YZ plane was chosen as the reference measuring plane in calculation of the co-ordinates of joint centres and mass centres.

'Z' Co-ordinate



Side View, YZ Plane

Front View, XZ Plane

FIG. D5 'Z' CO-ORDINATE OF KNEE AND ANKLE

$$\Delta Z_k = R_{xk} \cdot \sin \theta_{YT}$$

$$Z_k = Z_{kyz} - R_{xk} \cdot \sin \theta_{YT}$$

WHERE Z_k represents the actual co-ordinate and height of the knee joint centre and R_{xk} is the radius of the knee joint in X direction.

$$\Delta Z_a = R_a \cdot \sin \theta_{YS}$$

$$Z_a = Z_{ayz} - R_a \cdot \sin \theta_{YS}$$

where Z_a represents the actual co-ordinate and height of the

ankle joint centre and R_a is the radius of the ankle joint. The vertical co-ordinate of the shank mass centre is calculated similarly.

$$\Delta Z_s = R_s \cdot \sin \theta_{YS}$$

$$Z_s = Z_{syZ} - R_s \cdot \sin \theta_{YS}$$

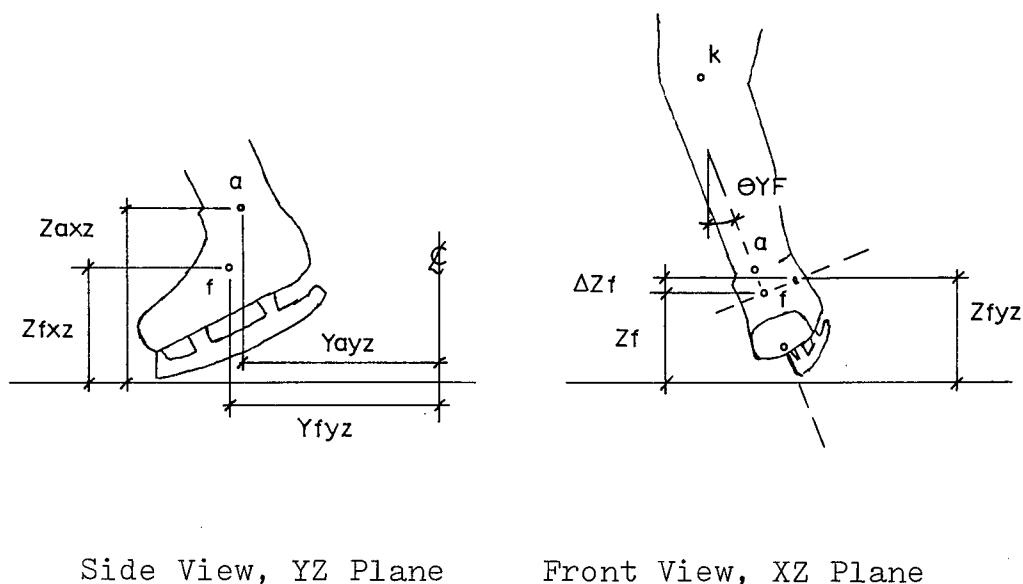


FIG. D6 'Z' CO-ORDINATE OF FOOT

$$\Delta Z_f = R_f \cdot \sin \theta_{YF}$$

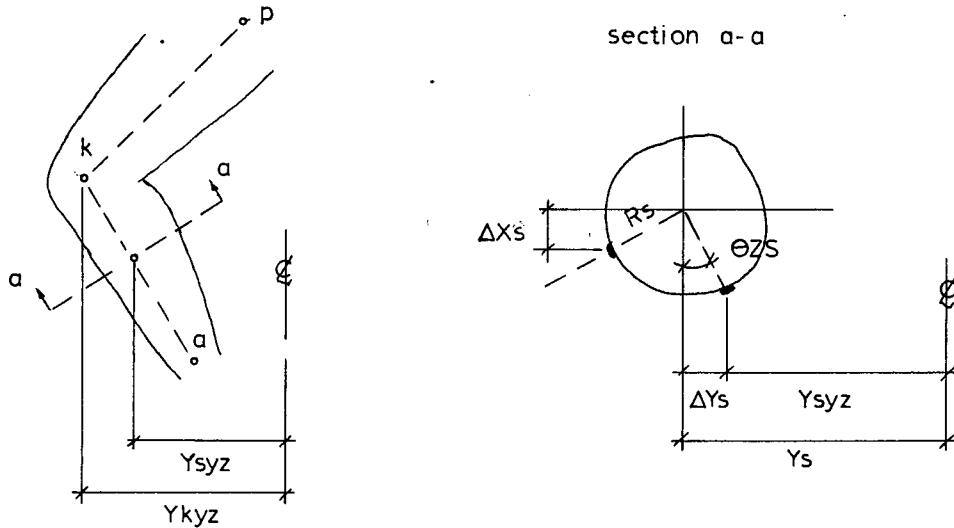
$$Z_f = Z_{fyz} - R_f \cdot \sin \theta_{YF}$$

where R_f is the width of the foot at the mass centre of the foot.

'Y' Co-ordinate

The Y co-ordinate of the joint centres and limb mass

centres is determined by correcting the Y co-ordinate of the surface marker measured in the YZ plane for rotation of the limb about its long axis, Fig. D7.



Side View, YZ Plane

Vertical View, XY Plane

FIG. D7 'Y' CO-ORDINATE OF KNEE AND SHANK

$$\Delta Y_s = R_s \cdot \sin \theta_{ZS}$$

$$Y_s = Y_{syz} + R_s \cdot \sin \theta_{ZS}$$

where Y_s is the actual co-ordinate of the mass centre of the shank and R_s is the radius of the shank at the mass centre.

The Y_f co-ordinate of the knee is determined similarly from shank rotation as

$$\Delta Y_k = R_{xk} \cdot \sin \theta_{ZS}$$

$$Y_k = Y_{kyz} + R_{xk} \cdot \sin \theta_{ZS}$$

where R_{xk} represents the calculated radius of the knee at the joint marker in X direction.

The Y co-ordinate of the ankle joint centre and the foot mass centre was calculated from the θ_{ZF} foot rotation applied to the YZ co-ordinate of the respective surface markers shown in Fig. D6 so that

$$Y_a = Y_{ayz} + R_a \cdot \sin \theta_{ZF}$$

$$Y_f = Y_{fyz} + R_f \cdot \sin \theta_{ZF}$$

'X' Co-ordinate

The X co-ordinate of the knee joint centre and shank mass centre were determined from the X co-ordinate of the surface markers measured in the XZ plane and the shank rotation.

$$X_k = X_{kxz} + R_{yk} \cdot \sin \theta_{ZS}$$

$$X_s = X_{sxz} + R_s \cdot \sin \theta_{ZS}$$

while the X co-ordinate of the ankle joint centre and the foot mass centre was calculated from the rotation of the foot about its vertical axis, θ_{ZF}

$$X_a = X_{axz} + R_a \cdot \sin \theta_{ZF}$$

$$X_f = Y_{fxz} + R_f \cdot \sin \theta_{ZF}$$

APPENDIX E

MUSCLE AND LIGAMENT CO-ORDINATES

APPENDIX E

MUSCLE AND LIGAMENT CO-ORDINATES

The co-ordinates of all muscle and ligament attachments were determined in terms of the same axes -- the grid axes with origin at the centre of the force platform.

1. Medial Collateral Ligament

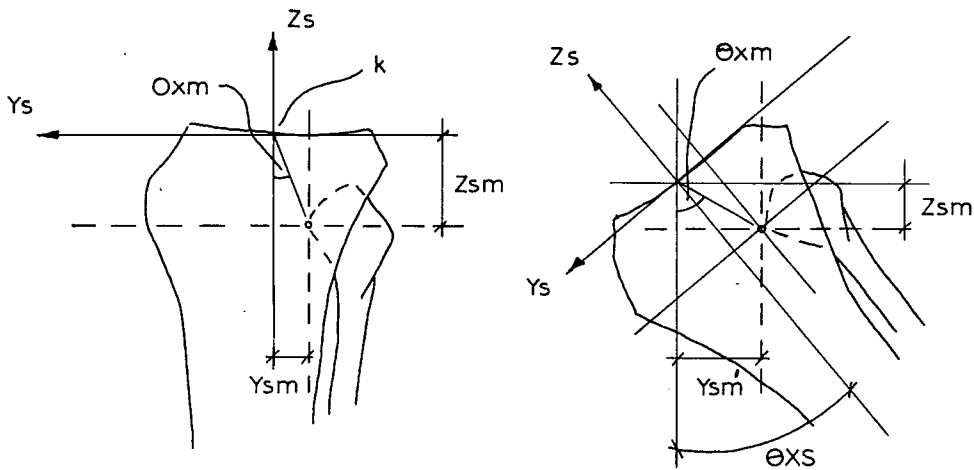


FIG. E1 MEDIAL COLLATERAL ATTACHMENT TO TIBIA
IN YZ PLANE FOR ROTATION θ_{xs}

$$\tan \theta_{xm} = \frac{Y_{sm}}{Z_{sm}}$$

$$R_{myz}^2 = Y_{sm}^2 + Z_{sm}^2$$

$$\theta_{xm}' = \theta_{xm} + \theta_{xs}$$

$$Z_{sm}' = R_{myz} \cdot \cos \theta_{xm}'$$

$$Y_{sm}' = R_{myz} \cdot \sin \theta_{xm}'$$

for rotation in the XZ plane (θ_{YS}) and rotation in the XY plane (θ_{ZS}) the co-ordinates of attachment reduce to

$$Z_{sm} = Z_{sm}' - \cos \theta_{YS}$$

$$Y_{sm} = Y_{sm}' - \cos \theta_{ZS}$$

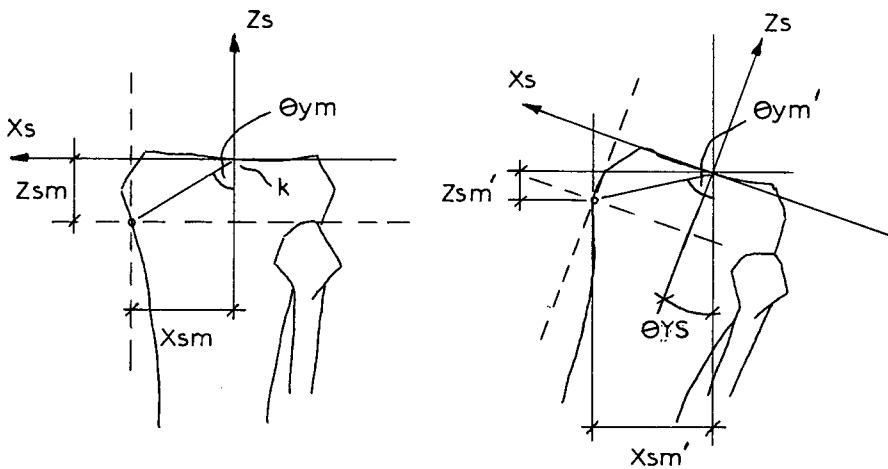


FIG. E2 MEDIAL COLLATERAL ATTACHMENT TO TIBIA
IN XZ PLANE FOR ROTATION θ_{YS}

$$\tan \theta_{ym} = \frac{X_{sm}}{Z_{sm}}$$

$$R_{mxz} = X_{sm}^2 + Z_{sm}^2$$

$$\theta_{ym}' = \theta_{ym} + \theta_{YS}$$

$$X_{sm}' = R_{mxz} \cdot \sin \theta_{ym}'$$

for rotation of tibia in XY plane (θ_{ZS}) the co-ordinate of

attachment reduces to

$$X_{sm} = X_{sm}' - \cos \theta_{ZS}$$

The co-ordinates of medial ligament attachment to the tibia with respect to the grid axes are therefore

$$X_{gm} = X_{gk} + R_{mxz} \cdot \sin \theta_{ym}' \cdot \cos \theta_{ZS}$$

$$Y_{gm} = Y_{gk} - R_{myz} \cdot \sin \theta_{xm}' \cdot \cos \theta_{ZS}$$

$$Z_{gm} = Z_{gk} - R_{myz} \cdot \cos \theta_{xm}' \cdot \cos \theta_{YS}$$

where X_{gk} , Y_{gk} , Z_{gk} are the grid co-ordinates of the tibial axes of the knee

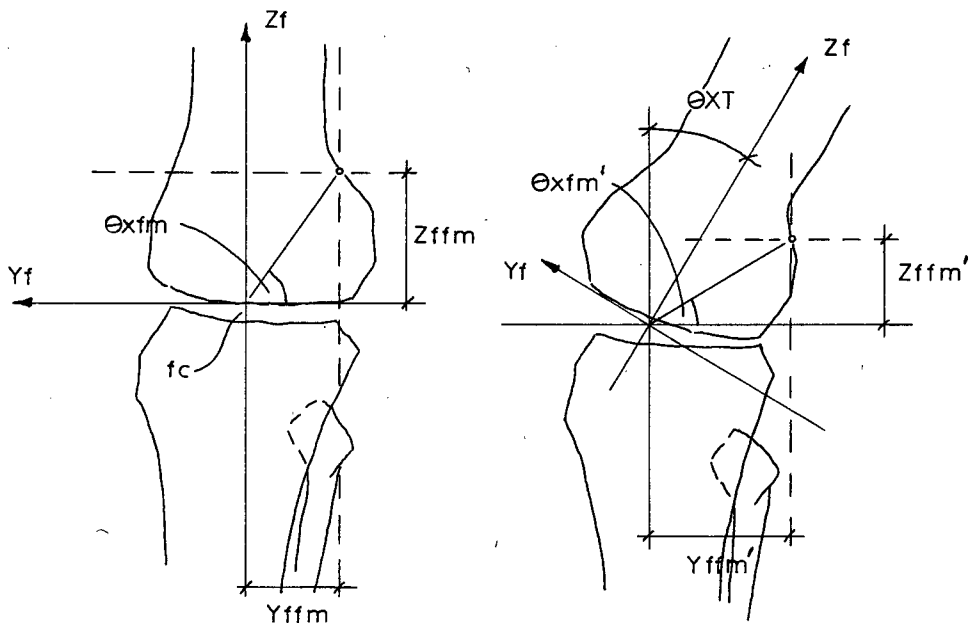


FIG. E3 MEDIAL COLLATERAL ATTACHMENT TO FEMUR
IN YZ PLANE FOR ROTATION θ_{XT}

$$\tan \theta_{x\text{fm}} = \frac{Z_{\text{ffm}}}{Y_{\text{ffm}}}$$

$$R_{\text{fmyz}}^2 = Y_{\text{ffm}}^2 + Z_{\text{ffm}}^2$$

$$\theta_{x\text{fm}}' = \theta_{x\text{fm}} - \theta_{\text{YT}}$$

$$Z_{\text{ffm}}' = R_{\text{fmyz}} \cdot \sin \theta_{x\text{fm}}'$$

$$Y_{\text{ffm}}' = R_{\text{fmyz}} \cdot \cos \theta_{x\text{fm}}'$$

for rotation of femur in XZ plane (θ_{YT}) and rotation in XY plane (θ_{ZT}) the co-ordinates of attachment reduce to

$$Z_{\text{ffm}} = Z_{\text{ffm}}' \cdot \cos \theta_{\text{YT}}$$

$$Y_{\text{ffm}} = Y_{\text{ffm}}' \cdot \cos \theta_{\text{ZT}}$$

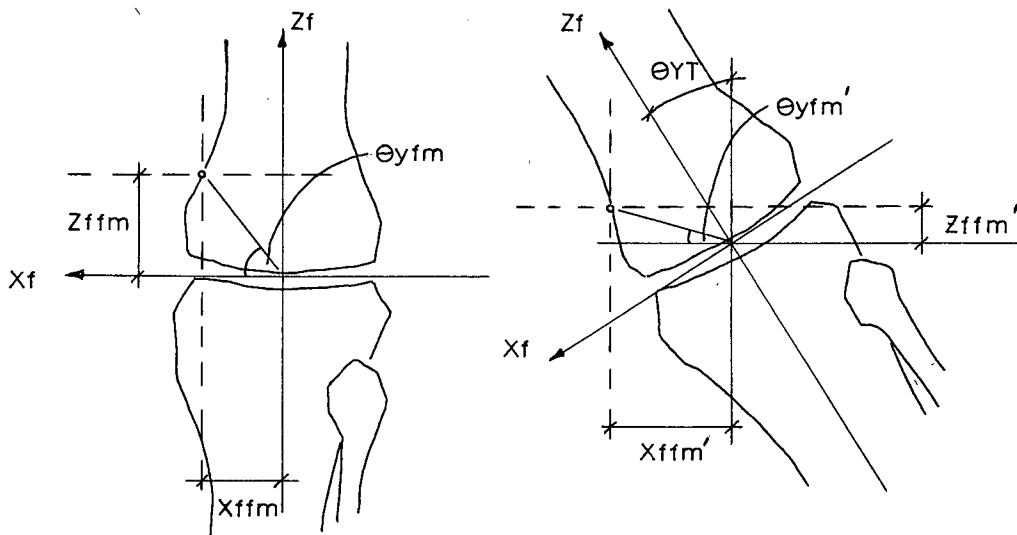


FIG. E4 MEDIAL COLLATERAL ATTACHMENT TO FEMUR
IN XZ PLANE FOR ROTATION θ_{YT}

$$\tan \theta_{y\text{fm}} = \frac{Z_{\text{ffm}}}{X_{\text{ffm}}}$$

$$R_{\text{fmxz}}^2 = X_{\text{ffm}}^2 + Z_{\text{ffm}}^2$$

$$\theta_{y\text{fm}}' = \theta_{y\text{fm}} - \theta_{\text{YT}}$$

$$X_{\text{ffm}}' = R_{\text{fmxz}} \cdot \cos \theta_{y\text{fm}}'$$

corrected for rotation of the femur in the XY plane (θ_{ZT})

$$X_{ffm} = X_{ffm}' \cdot \cos \theta_{ZT}$$

The co-ordinates of medial ligament attachment to the femur with respect to the grid axes are therefore

$$X_{gfm} = X_{gf} + R_{fmxz} \cdot \cos \theta_{yfm}' \cdot \cos \theta_{ZT}$$

$$Y_{gfm} = Y_{gf} - R_{fmyz} \cdot \cos \theta_{xgm}' \cdot \cos \theta_{ZT}$$

$$Z_{gfm} = Z_{gf} + R_{fmyz} \cdot \sin \theta_{xgm}' \cdot \cos \theta_{YT}$$

where X_{gf} , Y_{gf} , Z_{gf} are the grid co-ordinates of the femoral axes of the knee

The co-ordinates of lateral ligament attachment to the fibula and femur are calculated similarly.

2. Lateral Collateral Ligament

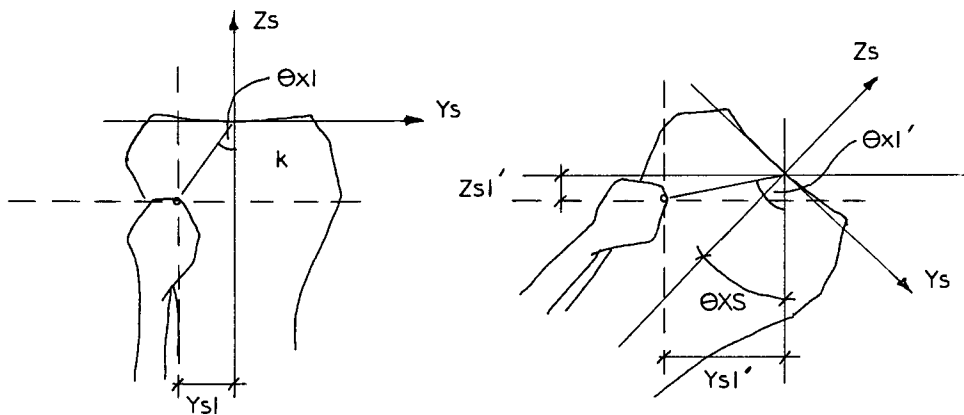


FIG. E5 LATERAL COLLATERAL ATTACHMENT TO FIBULA IN YZ PLANE FOR ROTATION θ_{XS}

$$\tan \theta_{xl} = \frac{Y_{sl}}{Z_{sl}}$$

$$R_{lyz}^2 = Y_{sl}^2 + Z_{sl}^2$$

$$\theta_{xl}' = \theta_{xl} + \theta_{XS}$$

$$Z_{sl}' = R_{lyz} \cdot \cos \theta_{xl}'$$

$$Y_{sl}' = R_{lyz} \cdot \sin \theta_{xl}'$$

corrected for rotation of the tibia in the XZ plane (θ_{YS})
and the XY plane (θ_{ZS}) the co-ordinates reduce to

$$Z_{sl} = Z_{sl}' \cdot \cos \theta_{YS}$$

$$Y_{sl} = Y_{sl}' \cdot \cos \theta_{ZS}$$

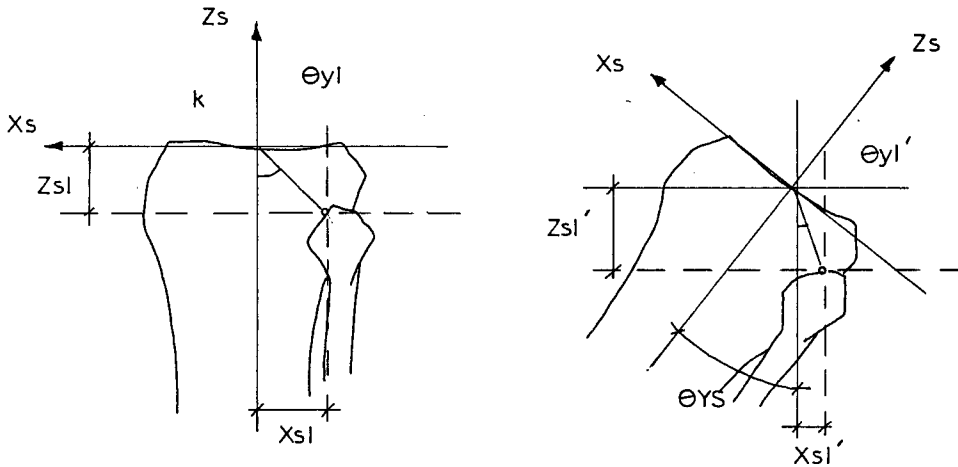


FIG. E6 LATERAL COLLATERAL ATTACHMENT TO FIBULA IN XZ PLANE FOR ROTATION θ_{YS}

$$\tan \theta_{yl} = \frac{X_{sl}}{Z_{sl}}$$

$$R_{lxz}^2 = X_{sl}^2 + Z_{sl}^2$$

$$\theta_{yl}' = \theta_{yl} - \theta_{YS}$$

$$Xsl' = Rl_{xz} \cdot \sin \theta_{yl'}$$

corrected for rotation of the tibia in the XY plane (θ_{ZS})

$$Xsl = Xsl' \cdot \cos \theta_{ZS}$$

The co-ordinates of the lateral ligament attachment to the fibula with respect to the axes are therefore

$$Xgl = Xgk - Rl_{xz} \cdot \sin \theta_{yl'} \cdot \cos \theta_{ZS}$$

$$Ygl = Ygk - Rl_{yz} \cdot \sin \theta_{xl'} \cdot \cos \theta_{ZS}$$

$$Zgl = Zgk - Rl_{yz} \cdot \cos \theta_{xl'} \cdot \cos \theta_{YS}$$

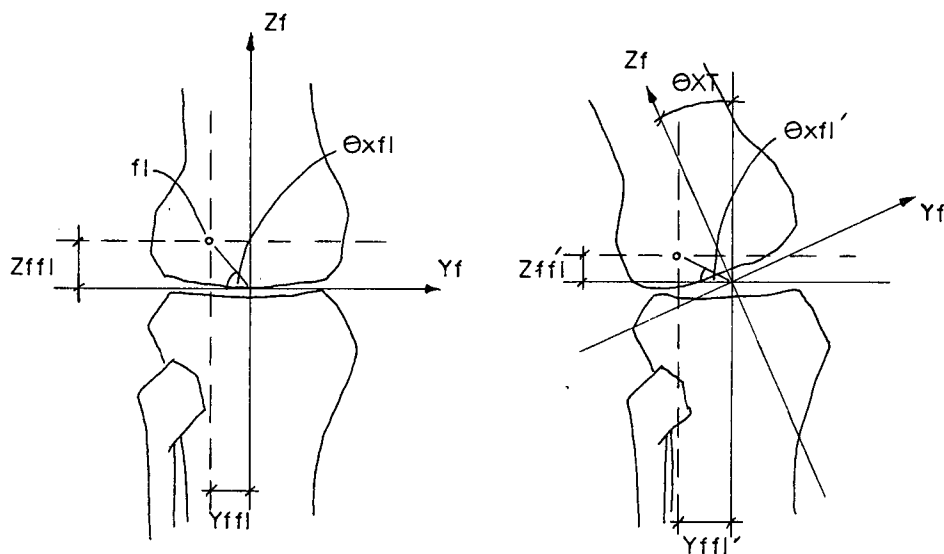


FIG. E7 LATERAL COLLATERAL ATTACHMENT TO FEMUR IN YZ PLANE FOR ROTATION θ_{XT}

$$\tan \theta_{xfl} = \frac{Z_{ffl}}{Y_{ffl}}$$

$$R_{flyz}^2 = Y_{ffl}^2 + Z_{ffl}^2$$

$$\theta_{xfl}' = \theta_{xfl} - \theta_{XT}$$

$$Y_{ffl}' = R_{flyz} \cdot \cos \theta_{xfl}'$$

$$Z_{ffl}' = R_{flyz} \cdot \sin \theta_{xfl}'$$

corrected for rotation of the femur in the XZ plane (θ_{YT})
and rotation in the XY plane (θ_{ZT}) the co-ordinates reduce to

$$Z_{ffl} = Z_{ffl}' \cdot \cos \theta_{YT}$$

$$Y_{ffl} = Y_{ffl}' \cdot \cos \theta_{ZT}$$

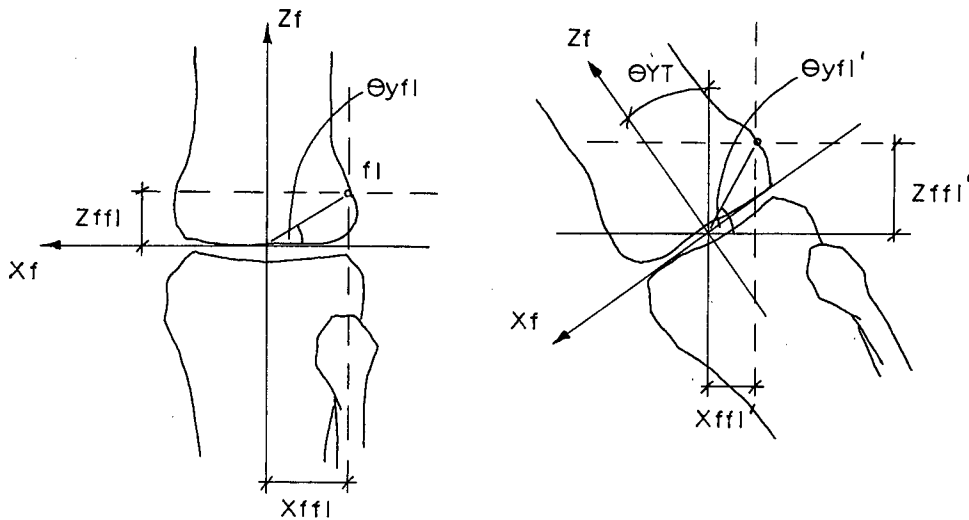


FIG. E8 LATERAL COLLATERAL ATTACHMENT TO
FEMUR IN XZ PLANE FOR ROTATION θ_{YT}

$$\tan \theta_{yfl} = \frac{Z_{ffl}}{X_{ffl}}$$

$$R_{flxz}^2 = X_{ffl}^2 + Z_{ffl}^2$$

$$\theta_{yfl}' = \theta_{yfl} + \theta_{YT}$$

$$X_{ffl} = R_{flxz} \cdot \cos \theta_{yfl}'$$

corrected for rotation of femur in XY plane (θ_{ZT}) the co-ordinate reduces to

$$X_{ffl} = X_{ffl}' \cdot \cos \theta_{ZT}$$

The co-ordinates of lateral ligament attachment to the femur with respect to the grid axes are

$$X_{gfl} = X_{gf} - R_{flxz} \cdot \cos \theta_{yfl}' \cdot \cos \theta_{ZT}$$

$$Y_{gfl} = Y_{gf} - R_{flyz} \cdot \cos \theta_{xfl}' \cdot \cos \theta_{ZT}$$

$$Z_{gfl} = Z_{gf} + R_{flyz} \cdot \sin \theta_{xfl}' \cdot \cos \theta_{YT}$$

3. Anterior Cruciate Ligament

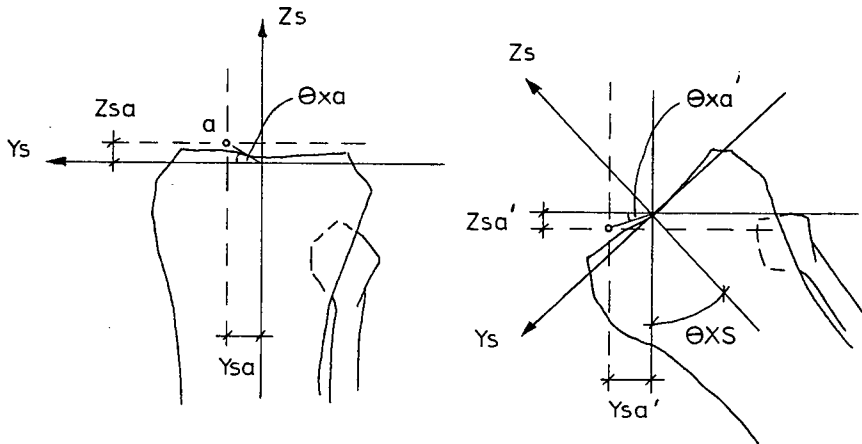


FIG. E9 ANTERIOR CRUCIATE ATTACHMENT TO TIBIA
IN YZ PLANE FOR ROTATION θ_{XS}

$$\tan \theta_{xa} = \frac{Z_{sa}}{Y_{sa}}$$

$$Rayz^2 = Y_{sa}^2 + Z_{sa}^2$$

$$\theta_{xa'} = \theta_{xa} - \theta_{XS}$$

$$Z_{sa'} = Rayz \cdot \sin \theta_{xa'}$$

$$Y_{sa'} = Rayz \cdot \cos \theta_{xa'}$$

corrected for rotation of tibia in XZ plane (θ_{YS}) and the XY plane (θ_{ZS})

$$Z_{sa} = Z_{sa'} \cdot \cos \theta_{YS}$$

$$Y_{sa} = Y_{sa'} \cdot \cos \theta_{ZS}$$

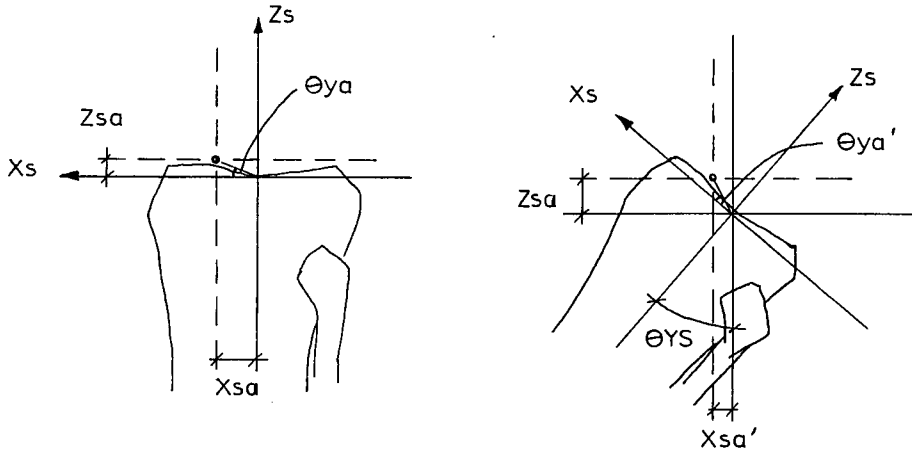


FIG. E10 ANTERIOR CRUCIATE ATTACHMENT TO TIBIA IN XZ PLANE FOR ROTATION θ_{YS}

$$\tan \theta_{ya} = \frac{Z_{sa}}{X_{sa}}$$

$$Raxz^2 = X_{sa}^2 + Z_{sa}^2$$

$$\theta_{ya'} = \theta_{ya} + \theta_{YS}$$

$$X_{sa'} = Raxz \cdot \cos \theta_{ya'}$$

corrected for rotation of the tibia in the XY plane (θ_{ZS})

$$Xsa = Xsa' \cdot \cos \theta ZS$$

The co-ordinates of anterior cruciate ligament attachment to the tibia with respect to the grid axes are therefore

$$Xga = Xgk + Raxz \cdot \cos \theta ya' \cdot \cos \theta ZS$$

$$Yga = Ygk + Rayz \cdot \cos \theta xa' \cdot \cos \theta ZS$$

$$Zga = Zgk + Rayz \cdot \sin \theta xa' \cdot \cos \theta YS$$

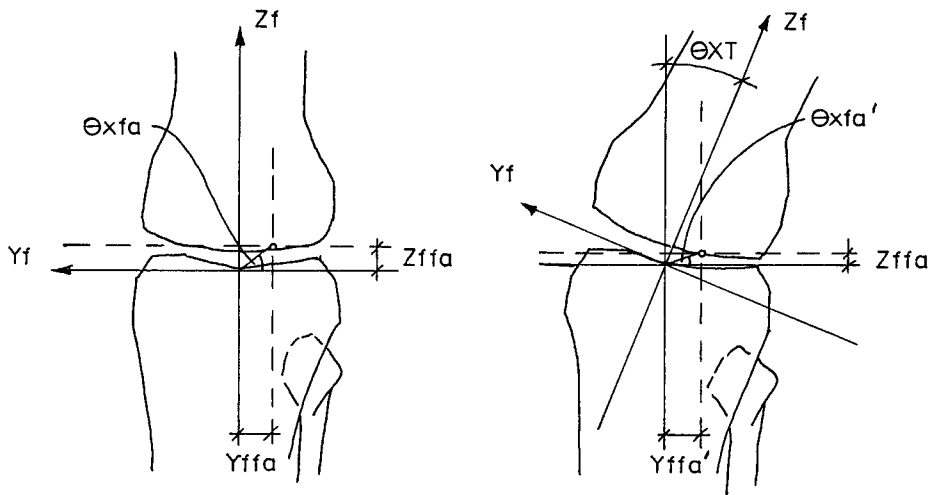


FIG. E11 ANTERIOR CRUCIATE ATTACHMENT TO FEMUR
IN YZ PLANE FOR ROTATION θ_{XT}

$$\tan \theta_{sfa} = \frac{Zffa}{Yffa}$$

$$R_{fayz}^2 = Yffa^2 + Zffa^2$$

$$\theta_{xfa'} = \theta_{xfa} - \theta_{XT}$$

$$Zffa' = R_{fayz} \cdot \sin \theta_{xfa'}$$

$$Yffa' = R_{fayz} \cdot \cos \theta_{xfa'}$$

corrected for rotation of the femur in the XZ plane (θ_{YT})
and rotation in the XY plane (θ_{ZT})

$$Y_{ffa} = Y_{ffa'} \cdot \cos \theta_{ZT}$$

$$Z_{ffa} = Z_{ffa'} \cdot \cos \theta_{YT}$$

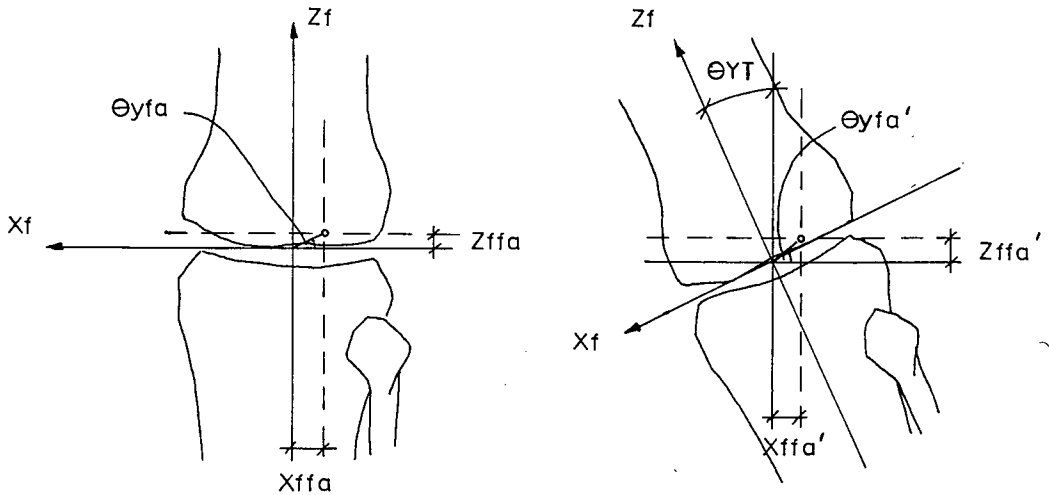


FIG. E12 ANTERIOR CRUCIATE ATTACHMENT TO FEMUR
IN XZ PLANE FOR ROTATION θ_{YT}

$$\tan \theta_{yfa} = \frac{Z_{ffa}}{X_{ffa}}$$

$$R_{faxz}^2 = X_{ffa}^2 + Z_{ffa}^2$$

$$\theta_{yfa'} = \theta_{yfa} + \theta_{YT}$$

$$X_{ffa'} = R_{faxz} \cdot \cos \theta_{yfa'}$$

corrected for rotation of the femur in the XY plane (θ_{ZT})

$$X_{ffa} = X_{ffa'} \cdot \cos \theta_{ZT}$$

The co-ordinates of anterior cruciate ligament

attachment to the femur with respect to the grid axes

$$X_{gfa} = X_{gf} - R_{faxz} \cdot \cos \theta_{yfa'} \cdot \cos \theta_{ZT}$$

$$Y_{gfa} = Y_{gf} - R_{fayz} \cdot \cos \theta_{xfa'} \cdot \cos \theta_{ZT}$$

$$Z_{gfa} = Z_{gf} + R_{fayz} \cdot \sin \theta_{xfa'} \cdot \cos \theta_{YT}$$

4. Posterior Cruciate Ligament

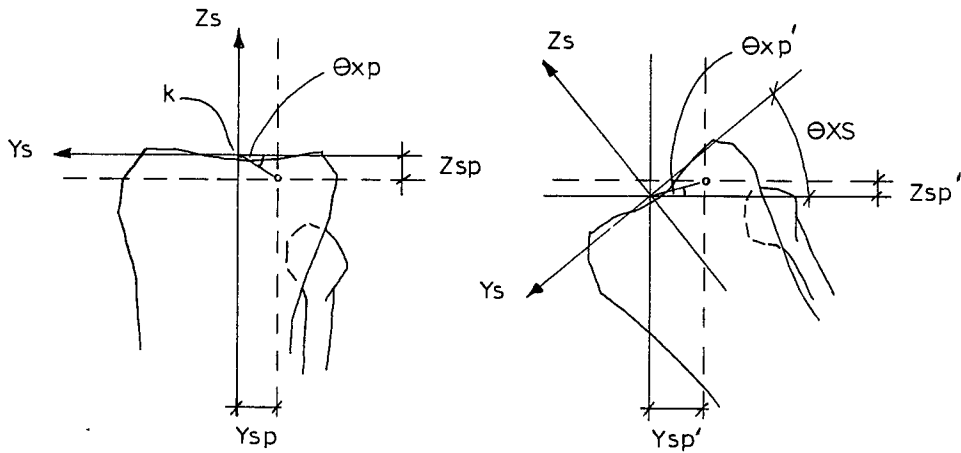


FIG. E13 POSTERIOR CRUCIATE ATTACHMENT TO TIBIA
IN YZ PLANE FOR ROTATION θ_{XS}

$$\tan \theta_{xp} = \frac{Z_{sp}}{Y_{sp}}$$

$$R_{pyz}^2 = Y_{sp}^2 + Z_{sp}^2$$

$$\theta_{xp'} = \theta_{xp} - \theta_{XS}$$

$$Z_{sp'} = R_{pyz} \cdot \sin \theta_{xp'}$$

$$Y_{sp'} = R_{pyz} \cdot \cos \theta_{xp'}$$

corrected for rotation of the tibia in the XZ plane (θ_{YS})
and rotation in the XY plane (θ_{ZS})

$$Y_{sp} = Y_{sp'} \cdot \cos \theta_{ZS}$$

$$Z_{sp} = Z_{sp'} \cdot \sin \theta_{YS}$$

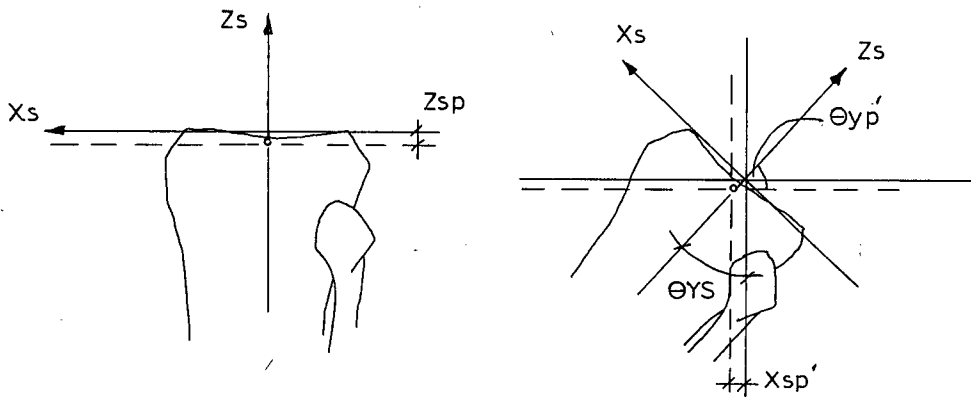


FIG. E14 POSTERIOR CRUCIATE ATTACHMENT TO TIBIA
IN XZ PLANE FOR ROTATION θ_{YS}

$$R_{pxz} = Z_{sp}$$

$$\theta_{yp'} = \theta_{YS}$$

$$X_{sp'} = Z_{sp} \cdot \sin \theta_{YS}$$

corrected for rotation of the tibia in the XY plane (θ_{ZS})

$$X_{sp} = X_{sp'} \cdot \cos \theta_{ZS}$$

The co-ordinates of posterior cruciate ligament

attachment to the tibia with respect the grid axes

$$X_{gp} = X_{gk} + Z_{sp} \cdot \theta_{YS} \cdot \cos \theta_{ZS}$$

$$Y_{gp} = Y_{gk} - R_{pyz} \cdot \cos \theta_{xp'} \cdot \cos \theta_{ZS}$$

$$Z_{gp} = Z_{gk} - R_{pyz} \cdot \sin \theta_{xp'} \cdot \cos \theta_{YS}$$

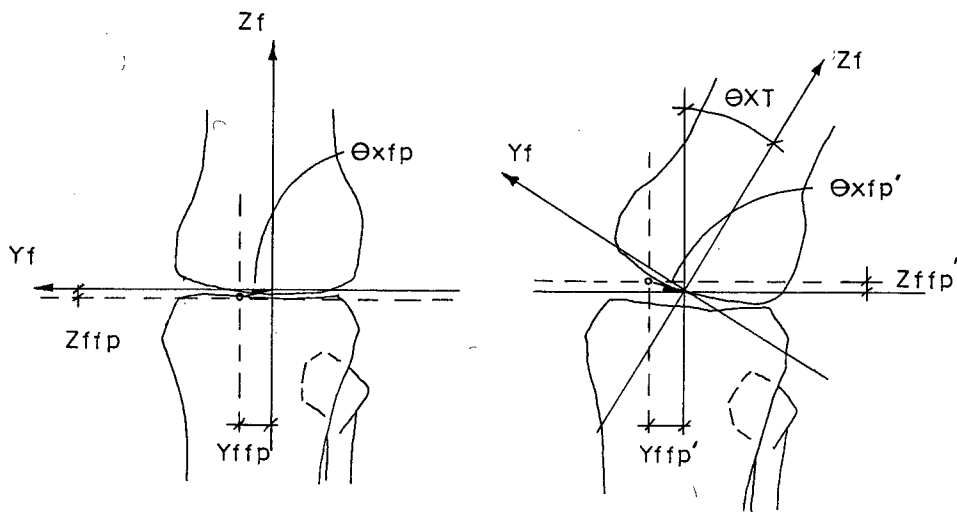


FIG. E15 POSTERIOR CRUCIATE ATTACHMENT TO FEMUR
IN YZ PLANE FOR ROTATION θ_{XT}

$$\tan \theta_{xfp} = \frac{Z_{ffp}}{Y_{ffp}}$$

$$R_{pyz}^2 = Y_{ffp}^2 + Z_{ffp}^2$$

$$\theta_{xfp'} = \theta_{xfp} - \theta_{XT}$$

$$Z_{ffp'} = R_{pyz} \cdot \sin \theta_{xfp'}$$

$$Y_{ffp'} = R_{pyz} \cdot \cos \theta_{xfp'}$$

corrected for rotation of the femur in the XZ plane (θ_{YT})
and the XY plane (θ_{ZT})

$$Y_{ffp} = Y_{ffp'} \cdot \cos \theta_{ZT}$$

$$Z_{ffp} = Z_{ffp'} \cdot \cos \theta_{YT}$$

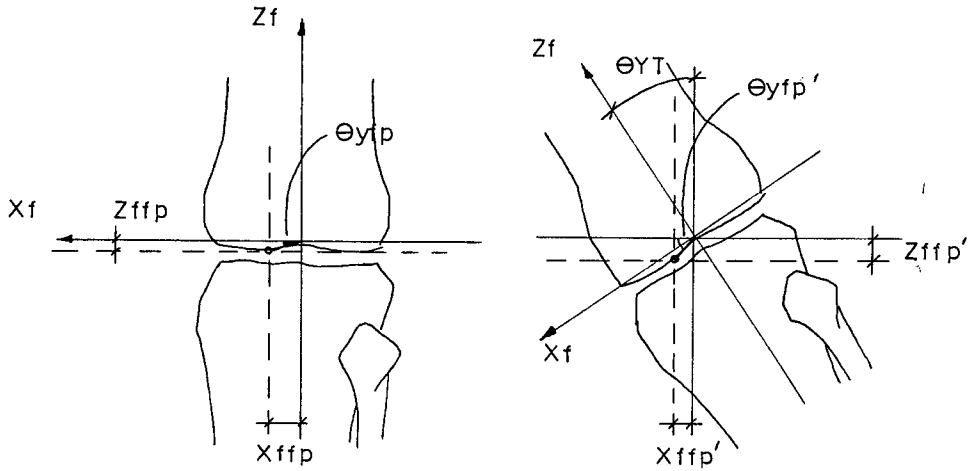


FIG. E16 POSTERIOR CRUCIATE ATTACHMENT TO FEMUR
IN XZ PLANE FOR ROTATION θ_{YT}

$$\tan \theta_{yfp} = \frac{Z_{ffp}}{X_{ffp}}$$

$$R_{fpzx}^2 = X_{ffp}^2 + Z_{ffp}^2$$

$$\theta_{xfp'} = \theta_{yfp} + \theta_{YT}$$

$$X_{ffp'} = R_{fpzx} \cdot \cos \theta_{yfp'}$$

corrected for rotation of the femur in the XY plane (θ_{ZT})

$$X_{ffp} = X_{ffp'} \cdot \cos \theta_{ZT}$$

The co-ordinates of posterior cruciate ligament attachment to the femur with respect to the grid axes are

$$X_{gfp} = X_{gf} + R_{fpxz} \cdot \cos \theta_{yfp}' \cdot \cos \theta_{ZT}$$

$$Y_{gfp} = Y_{gf} + R_{fpyz} \cdot \cos \theta_{xfp}' \cdot \cos \theta_{ZT}$$

$$Z_{gfp} = Z_{gf} - R_{fpyz} \cdot \sin \theta_{xfp}' \cdot \cos \theta_{YT}$$

MUSCLE CO-ORDINATES

The co-ordinates of the hamstring and gastrocnemius muscle attachments were calculated to allow determination of respective lines of force action for these muscle groups. The line of force action for the quadriceps group was determined from equation 3.01 of section No. 3.

1. Hamstrings Muscle Group

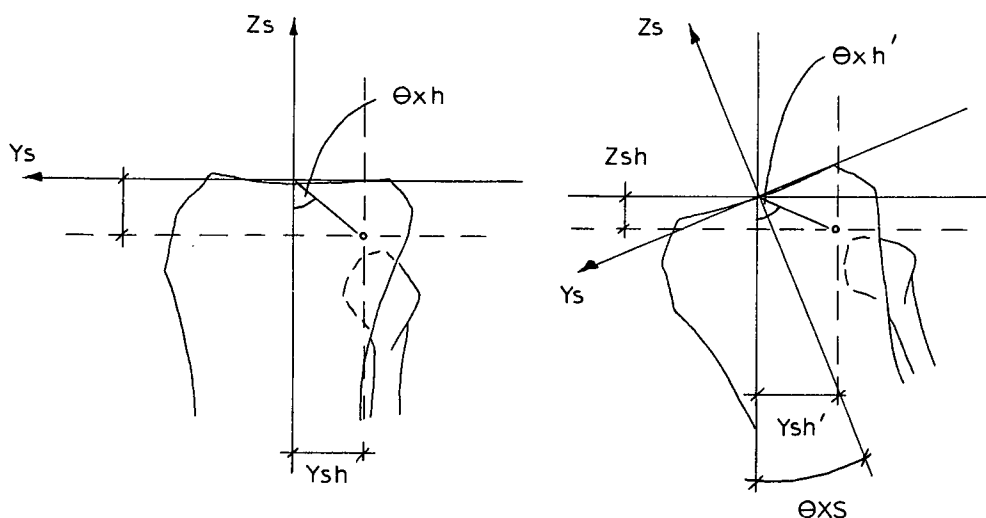


FIG. E17 HAMSTRINGS ATTACHMENT TO TIBIA
IN YZ PLANE FOR ROTATION θ_{XS}

$$\tan \theta_{xh} = \frac{Y_{sh}}{Z_{sh}}$$

$$R_{hyz}^2 = Y_{sh}^2 + Z_{sh}^2$$

$$\theta_{xh'} = \theta_{xh} + \theta_{XS}$$

$$Y_{sh}' = R_{hyz} \cdot \sin \theta_{xh}'$$

$$Z_{sh}' = R_{hyz} \cdot \cos \theta_{xh}$$

corrected for rotation in the XZ plane (θ_{YS}) and for rotation in the XY plane (θ_{ZS})

$$Y_{sh} = Y_{sh}' \cdot \cos \theta_{YS}$$

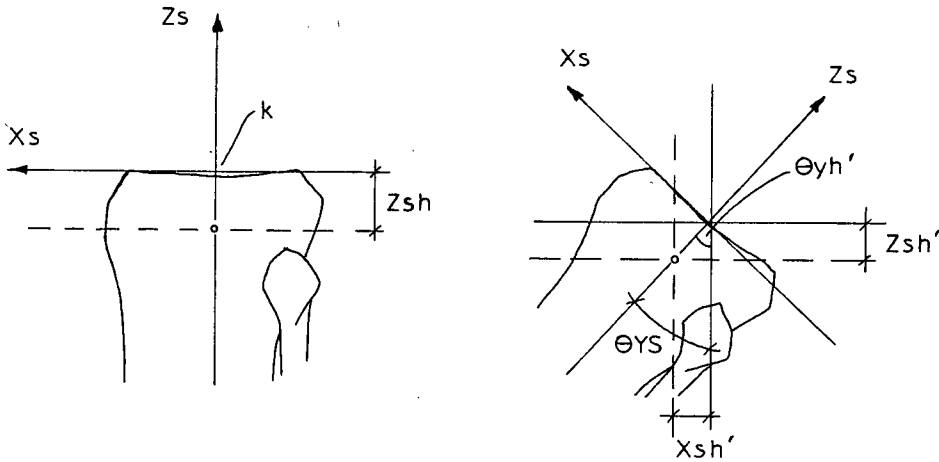


FIG. E18 HAMSTRINGS ATTACHMENT TO TIBIA
IN XZ PLANE FOR ROTATION θ_{YS}

$$R_{hxz} = Z_{sh}$$

$$\theta_{yh}' = \theta_{YS}$$

$$X_{sh}' = Z_{sh} \cdot \sin \theta_{YS}$$

corrected for rotation of the tibia in the XY plane (θ_{ZS}) the co-ordinate reduces to

$$X_{sh} = X_{sh}' \cdot \cos \theta_{ZS}$$

The co-ordinates of hamstring attachment to the tibia

with respect to the grid axes are

$$X_{gh} = X_{gk} + Z_{sh} \cdot \sin \theta_{YS} \cdot \cos \theta_{ZS}$$

$$Y_{gh} = Y_{gk} - R_{hyz} \cdot \sin \theta_{xh'} \cdot \cos \theta_{ZS}$$

$$Z_{gh} = Z_{gk} - R_{hyz} \cdot \cos \theta_{xh'} \cdot \cos \theta_{YS}$$

The hamstrings being a biarticular muscle group cross the knee joint and hip joint to insertion in the pelvis.

To determine the co-ordinates of attachment to the pelvis with respect to the grid axes, the basic co-ordinates with respect to Morrison's pelvic origin at the anterior ilia^c spine (p) are transposed to the femoral head origin (fh).

The co-ordinates of hamstring muscle group attachment to pelvis with respect to the grid axes are

$$X_{gph} = X_{gfh} + (X_{ph} - X_{pfh})$$

$$Y_{gph} = Y_{gfh} - (Y_{ph} - Y_{pfh})$$

$$Z_{gph} = Z_{gfh} - (Z_{ph} - Z_{pfh})$$

The co-ordinates of hamstrings attachment to the pelvis represent a common origin of insertion for the muscles which make up the hamstrings muscle group.

The calculations for hamstrings attachment to the

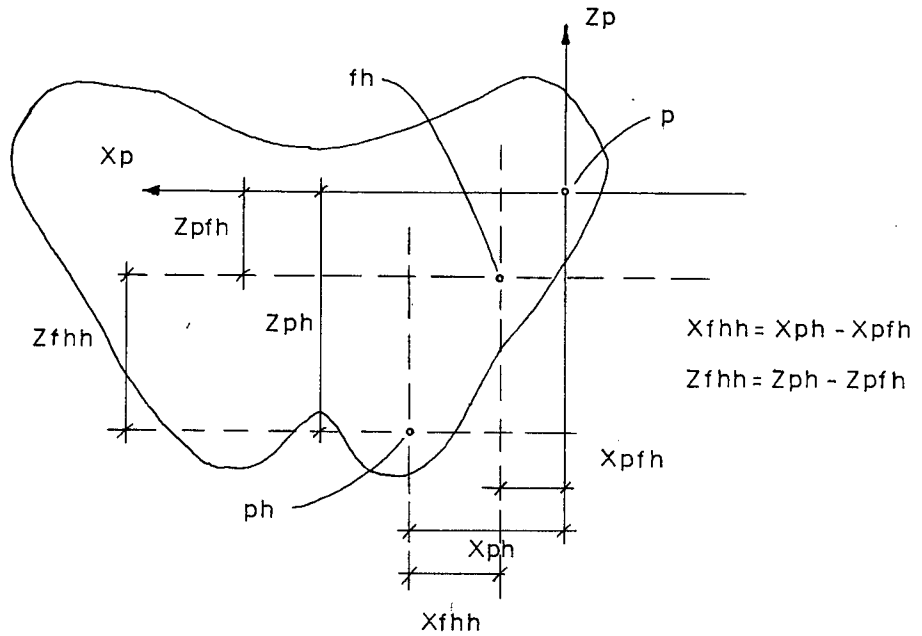


FIG. E19 HAMSTRINGS ATTACHMENT TO PELVIS IN XZ PLANE WITH RESPECT TO FEMORAL HEAD

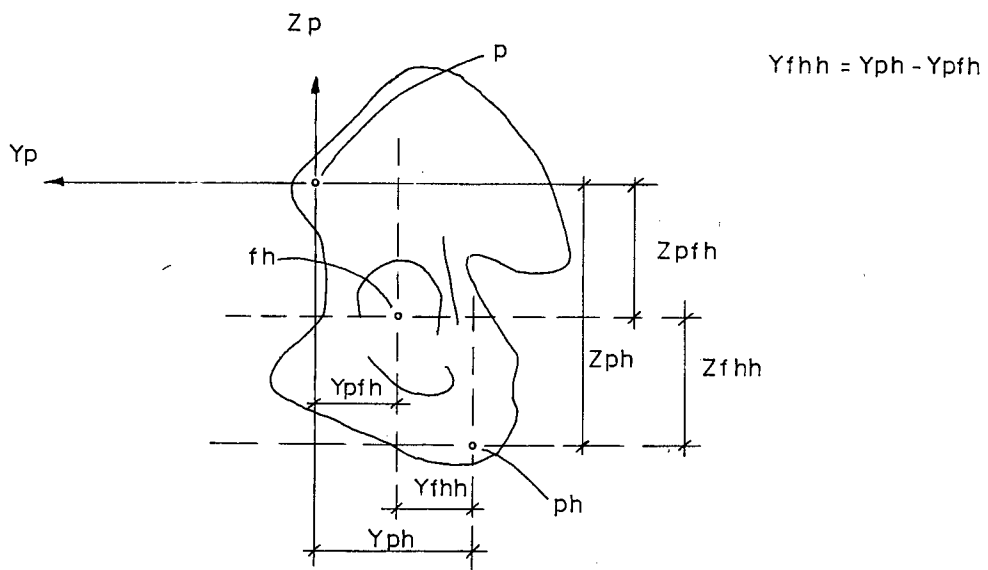


FIG. E20 HAMSTRINGS ATTACHMENT TO PELVIS IN YZ PLANE WITH RESPECT TO FEMORAL HEAD

pelvis have not been corrected for rotations of the pelvis, θ_{XP} , θ_{YP} and θ_{ZP} , as these rotations could not be determined from the surface markers used. However these rotations are assumed small.

2. Gastrocnemius Muscle Group

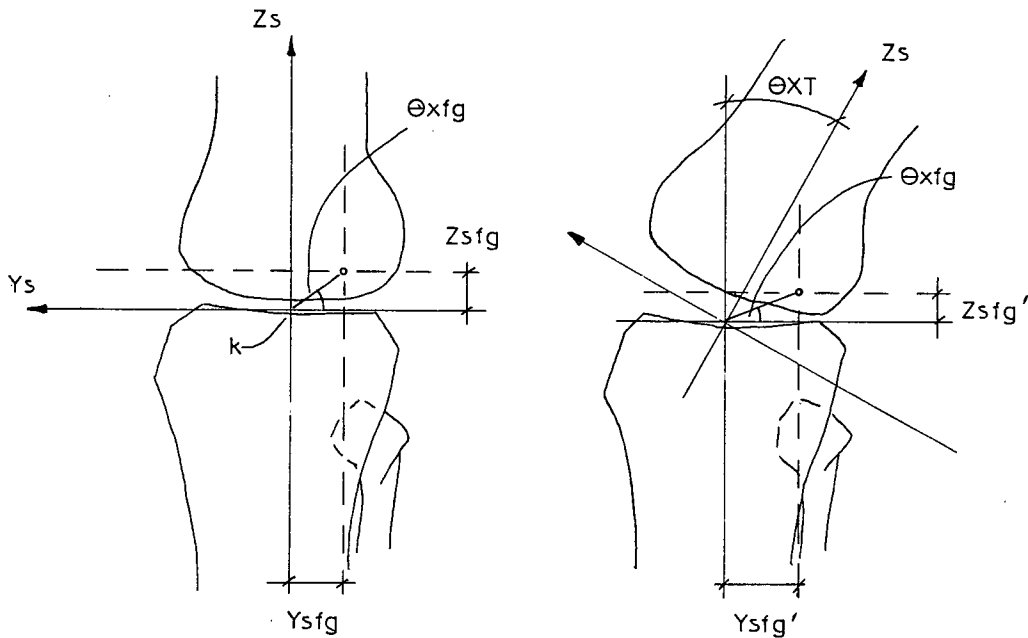


FIG. E21 GASTROCNEMIUS ATTACHMENT TO FEMUR
IN YZ PLANE FOR ROTATION θ_{XT}

$$\tan \theta_{xfg} = \frac{Z_{sfg}}{Y_{sfg}}$$

$$R_{fgyz}^2 = Y_{sfg}^2 + Z_{sfg}^2$$

$$\theta_{xfg'} = \theta_{xfg} - \theta_{XT}$$

$$Y_{sfg'} = R_{fgyz} \cdot \cos \theta_{xfg}$$

$$Z_{sfg'} = R_{fgyz} \cdot \sin \theta_{xfg'}$$

corrected for rotation in the XZ plane (θ_{YT}) and rotation in

the XY plane (θ_{ZT})

$$Y_{sfg} = Y_{sfg'} \cdot \cos \theta_{ZT}$$

$$A_{sfg} = Z_{sfg'} \cdot \cos \theta_{YT}$$

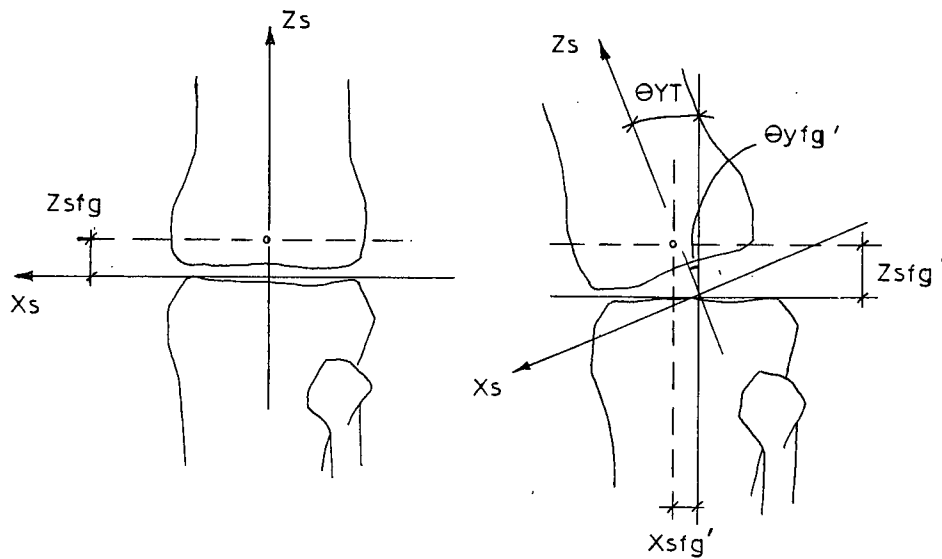


FIG. E22 GASTROCNEMIUS ATTACHMENT TO FEMUR
IN XZ PLANE FOR ROTATION θ_{YT}

$$R_{fgxz} = Z_{sfg}$$

$$\theta_{yfg'} = \theta_{YT}$$

$$X_{sfg'} = Z_{sfg} \cdot \sin \theta_{YT}$$

corrected for rotation of the femur in the XY plane (θ_{ZT})

$$X_{sfg} = X_{sfg'} \cdot \cos \theta_{ZT}$$

The co-ordinates of gastrocnemius muscle group attachment to the femur with respect to the grid axes

$$X_{gfg} = X_{gk} + Z_{sgf} \cdot \sin \theta_{YT} \cdot \cos \theta_{ZT}$$

$$Y_{gfg} = Y_{gk} - R_{fgyz} \cdot \cos \theta_{xfg'} \cdot \cos \theta_{ZT}$$

$$Z_{gfg} = Z_{gk} + R_{gxz} \cdot \sin \theta_{xfg'} \cdot \cos \theta_{YT}$$

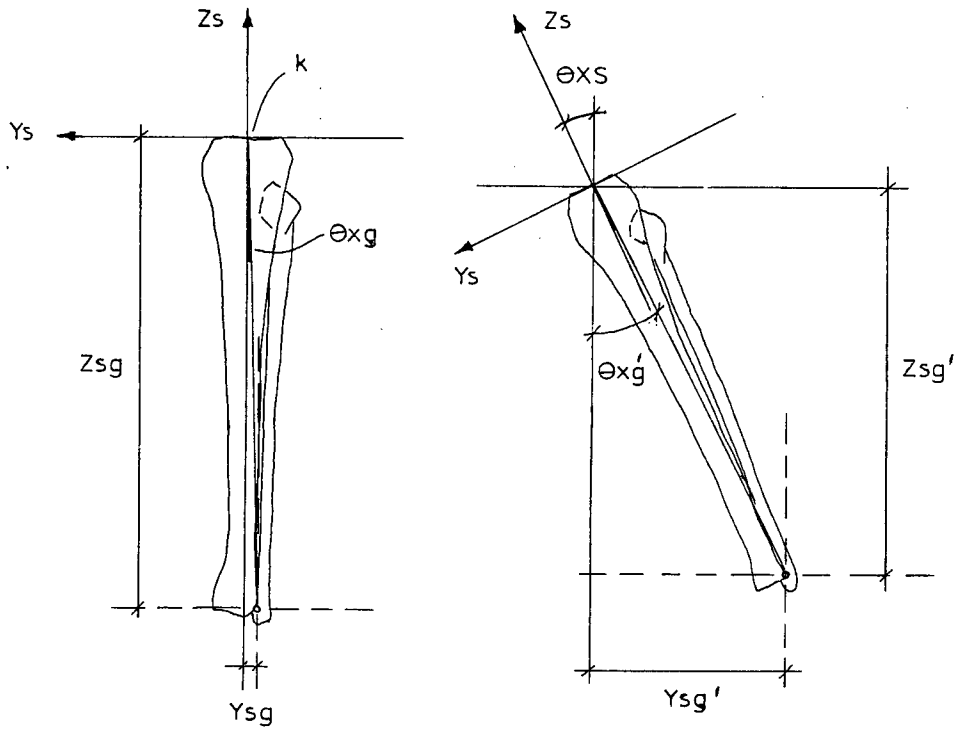


FIG. E23 GASTROCNEMIUS ATTACHMENT TO TIBIA
IN YZ PLANE FOR ROTATION θ_{XS}

$$\tan \theta_{xg} = \frac{Y_{sg}}{Z_{sg}}$$

$$R_{gyz}^2 = Y_{sg}^2 + Z_{sg}^2$$

$$\theta_{xg'} = \theta_{xg} + \theta_{XS}$$

$$Y_{sg'} = R_{gyz} \cdot \sin \theta_{xg'}$$

$$Z_{sg'} = R_{gyz} \cdot \cos \theta_{xg'}$$

corrected for rotation of the tibia in the XY plane (θ_{ZS})

and the plane (θ_{YS})

$$Y_{sg} = Y_{sg'} \cdot \cos \theta_{ZS}$$

$$Z_{sg} = Z_{sg'} \cdot \cos \theta_{YS}$$

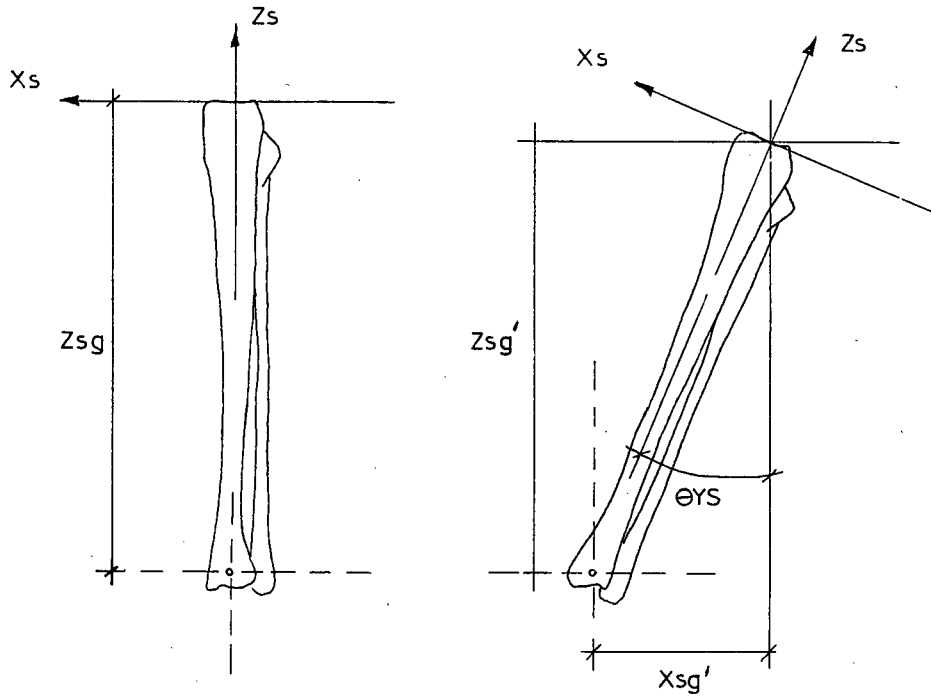


FIG. E24 GASTROCNEMIUS ATTACHMENT TO TIBIA
IN XZ PLANE FOR ROTATION θ_{YS}

$$R_{gxz} = Z_{sg}$$

$$\theta_{xg'} = \theta_{YS}$$

$$X_{sg'} = Z_{sg} \cdot \sin \theta_{YS}$$

corrected for rotation of the tibia in the XY plane (θ_{ZS})

$$X_{sg} = X_{sg'} \cdot \cos \theta_{ZS}$$

The co-ordinates of gastrocnemius attachment to the

tibia with respect to the grid axes are

$$X_{gg} = X_{gk} + Z_{sg} \cdot \sin \theta_{YS} \cdot \cos \theta_{ZS}$$

$$Y_{gg} = Y_{gk} - R_{gyz} \cdot \sin \theta_{xg'} \cdot \cos \theta_{ZS}$$

$$Z_{gg} = Z_{gk} - R_{gyz} \cdot \cos \theta_{xg'} \cdot \cos \theta_{YS}$$

APPENDIX F

MUSCLE AND LIGAMENT FORCES

APPENDIX F

MUSCLE AND LIGAMENT FORCES

1. Quadriceps Muscle Group

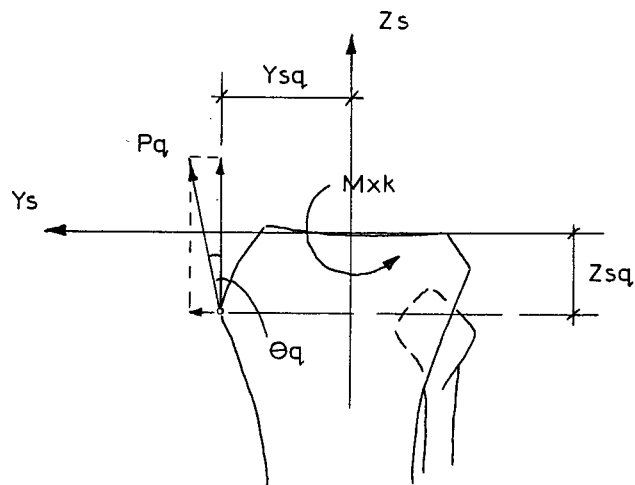


FIG. F1 FORCE ACTION OF QUADRICEPS MUSCLE GROUP IN THE YZ PLANE

$$M_{xk} = P_q \cdot \cos \theta_q \cdot Y_{sq} + P_q \cdot \sin \theta_q \cdot Z_{sq}$$

$$P_q = M_{xk} / (\cos \theta_q \cdot Y_{sq} + \sin \theta_q \cdot Z_{sq})$$

where θ_q is the angle of the quadriceps to the Z_s axis in the Y_sZ_s plane and M_{xk} is the moment on the knee in the Y_sZ_s plane

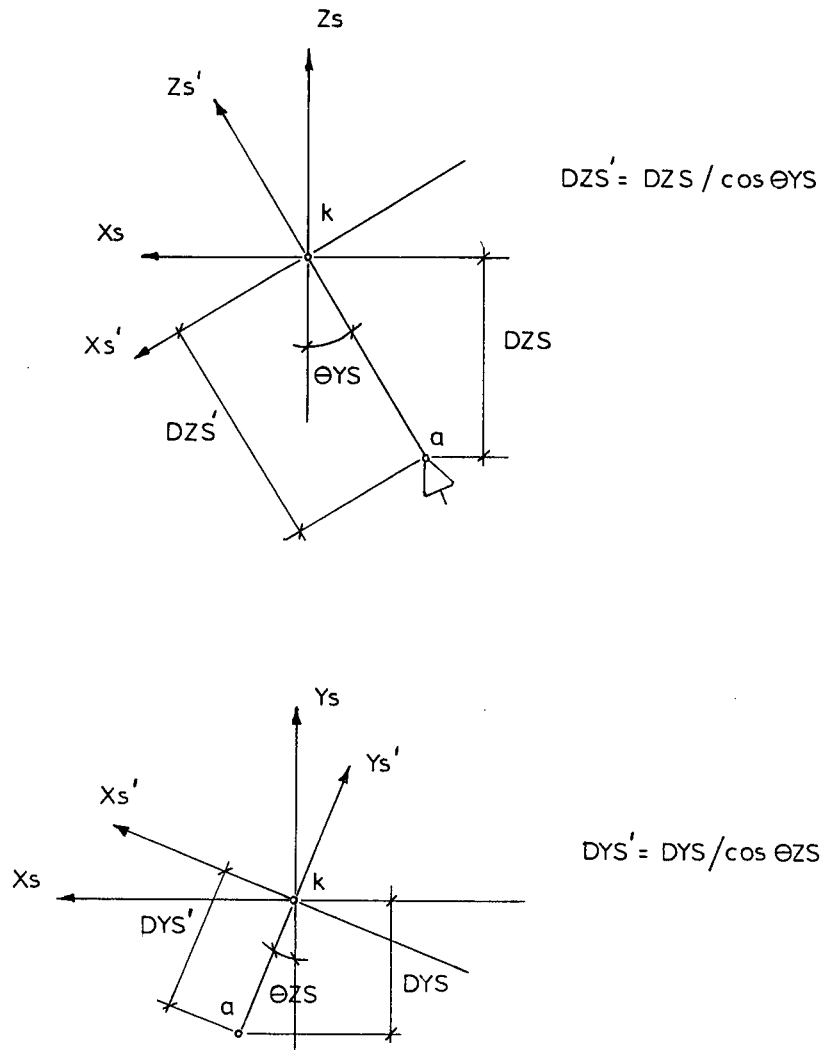


FIG. F2 ANGLE OF SHANK IN $Y_s Z_s$ PLANE
 $\theta_{XS} (+) \text{ ARCTAN } (DYS' / DZS')$

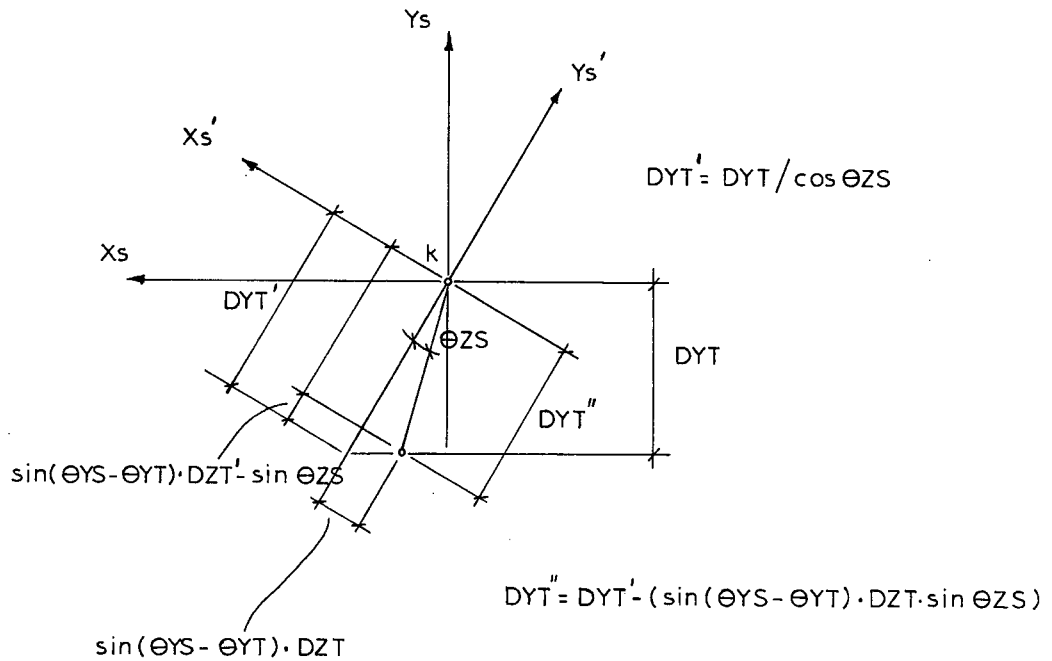
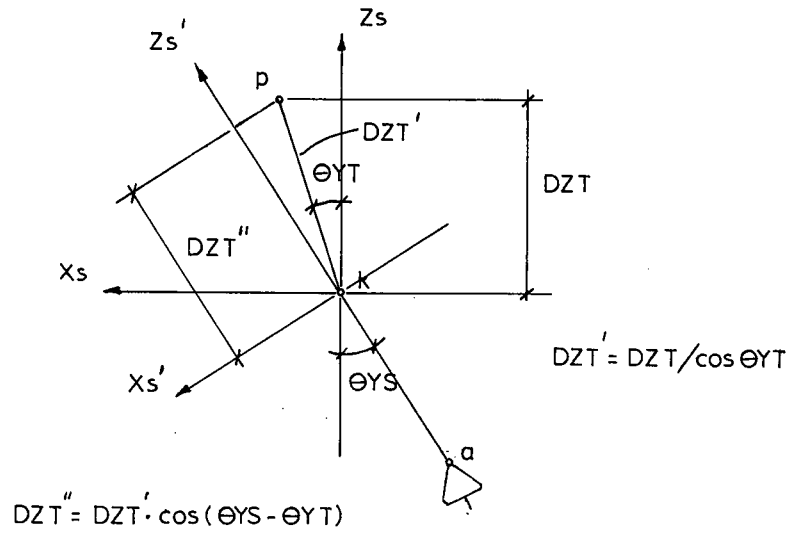


FIG. F3 ANGLE OF THIGH IN $Y_s Z_s$ PLANE
 $\theta_{XT} = \text{ARCTAN} (DYT''/DZT'')$

$$\theta_q = 0.31 \times 10^{-4} (\phi) - 8.4 \times 10^{-3} (\phi)^2 + 0.37 \times 10^{-2} (\phi) + 15$$

$\Phi = \theta_{XS} + \theta_{XT}$ where θ_{XS} and θ_{XT} are calculated in the $YsZs$ plane as in Fig. F2 and F3

2. Hamstrings Muscle Group

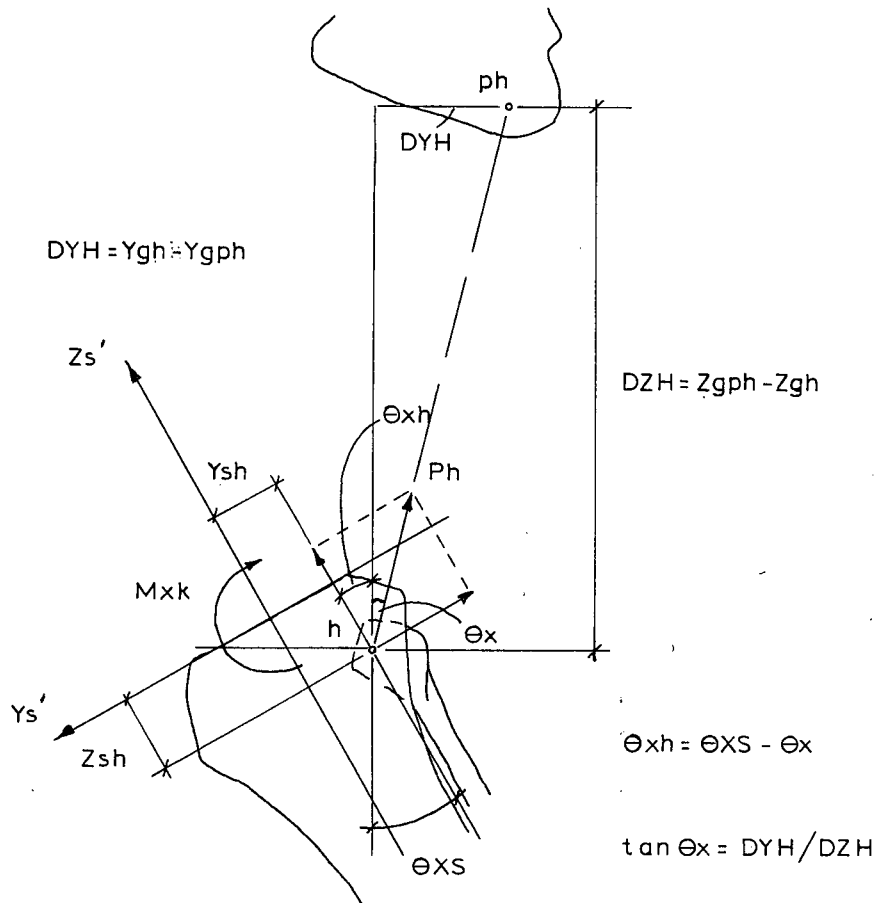


FIG. F4 FORCE ACTION OF HAMSTRINGS MUSCLE GROUP IN THE YZ PLANE

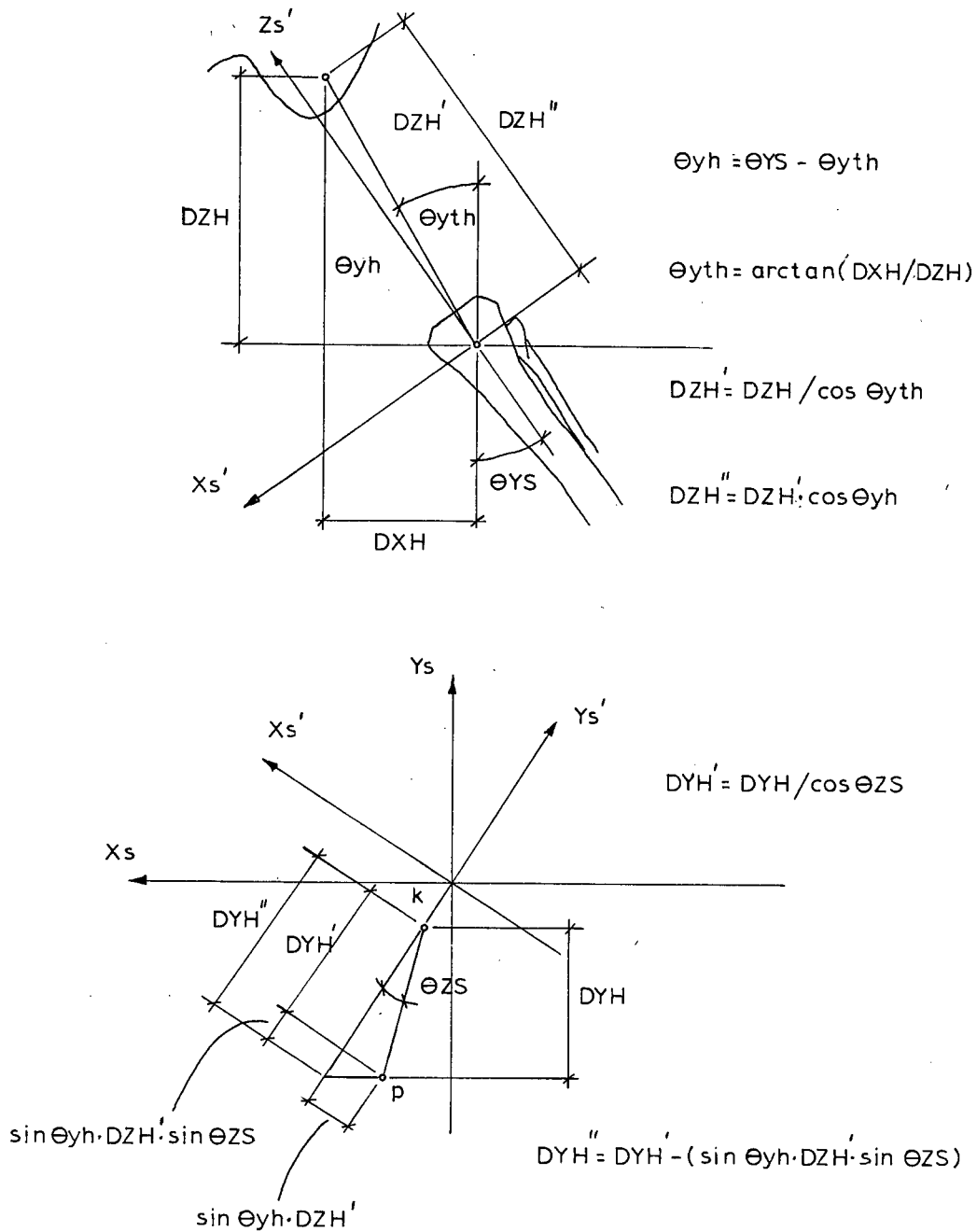


FIG. F5 ANGLE OF HAMSTRINGS IN $YsZs$ PLANE
 $\Theta_X = \arctan (DYH''/DZH'')$

$$M_{xk} = P_h \cdot \cos \theta_{xh} \cdot Y_{sh} + P_h \cdot \sin \theta_{xh} \cdot Z_{sh}$$

$$P_h = M_{xk} / (\cos \theta_{xh} \cdot Y_{sh} + \sin \theta_{xh} \cdot Z_{sh})$$

$\theta_{xh} = \theta_x + \theta_{XS}$ is the angle of the hamstrings to the Z_s axis in the Y_sZ_s plane with θ_x calculated as in Fig. F5 and θ_{XS} as in Fig. F2

3. Gastrocnemius Muscle Group

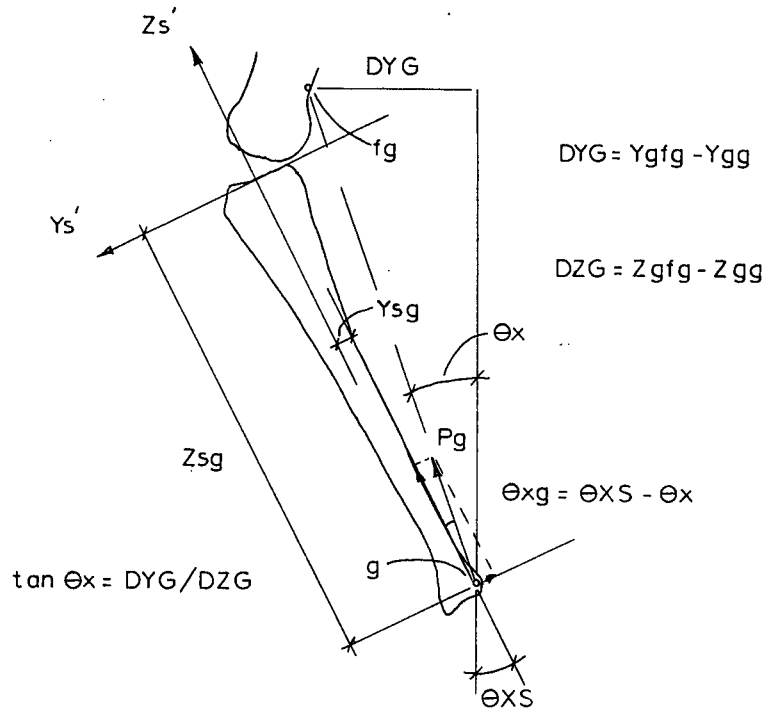


FIG. F6 FORCE ACTION OF GASTROCNEMIUS MUSCLE GROUP IN THE YZ PLANE

$$M_{xk} = P_q \cdot \sin \theta_{xg} \cdot Z_{sg} + P_q \cdot \cos \theta_{xg} \cdot Y_{sg}$$

$$P_g = M_{xk} / (\sin \theta_{xg} \cdot Z_{sg} + F_g \cdot \cos \theta_{xg} \cdot Y_{sg})$$

$\theta_{xg} = \theta_{XS} - \theta_X$ is the angle of the gastrocnemius to the Z_s axis in the Y_sZ_s plane with θ_X calculated as in Fig. F7 and θ_{XS} from Fig. F2

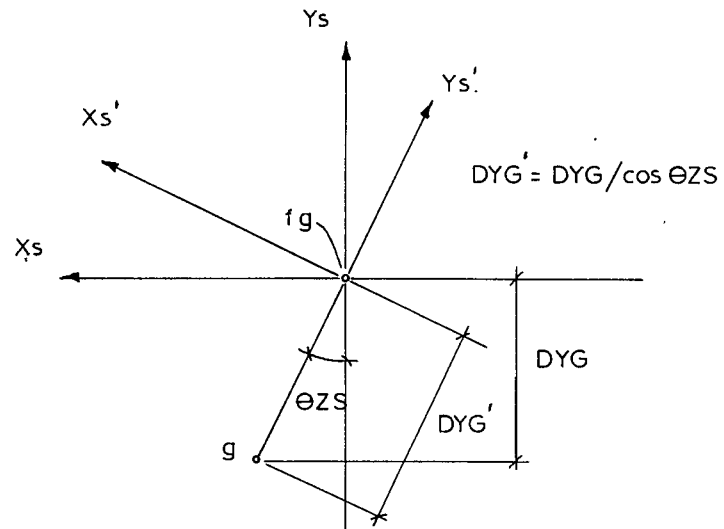
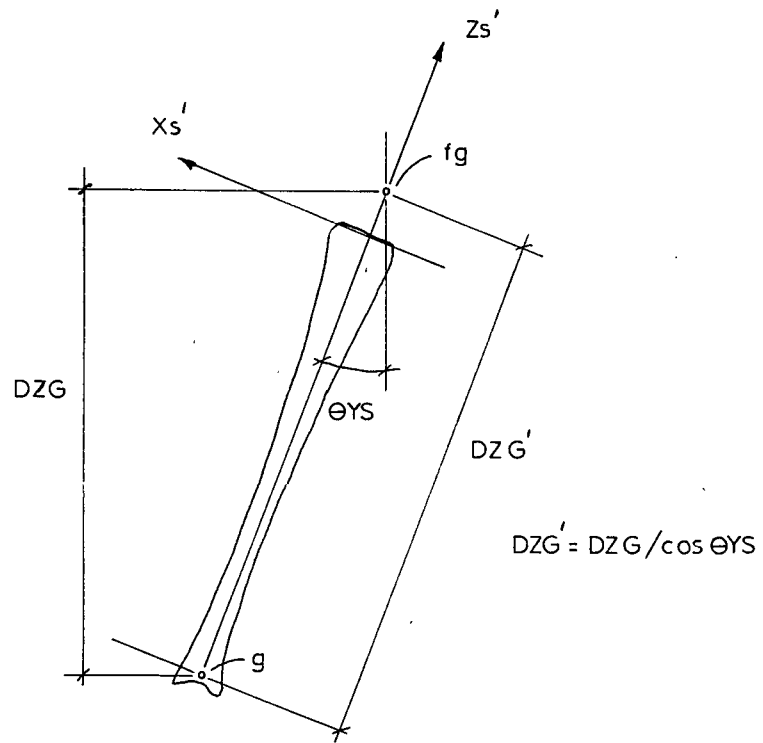


FIG. F7 ANGLE OF GASTROCNEMIUS IN Y_sZ_s PLANE
 $\theta_X = \text{ARCTAN} (DYG' / DZG')$

LIGAMENT FORCES

1. Anterior Cruciate Ligament

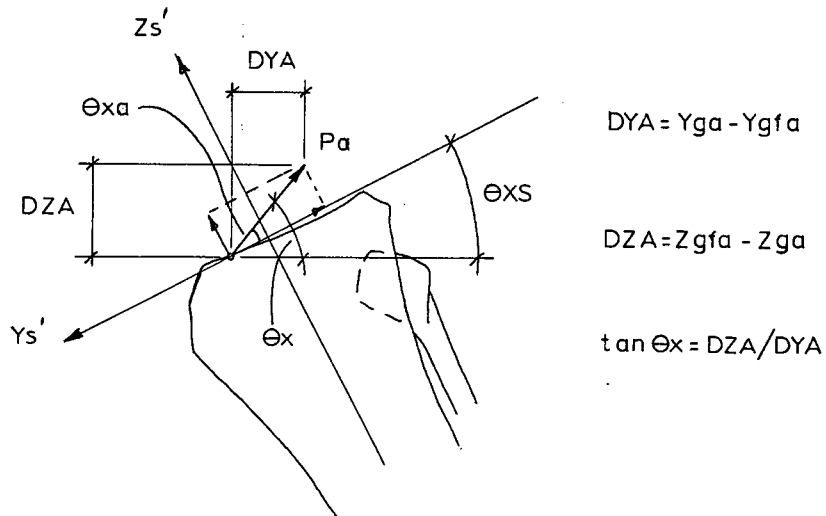


FIG. F8 FORCE ACTION OF ANTERIOR CRUCIATE LIGAMENT IN YZ PLANE

$$F_{ym} + F_{yk} = P_a \cdot \cos \theta_{xa}$$

$$P_a = (F_{ym} + F_{yk}) / \cos \theta_{xa}$$

$\theta_{xa} - \theta_x - \theta_{xs}$ is the angle of the anterior cruciate to the Y_s axis in the Y_sZ_s plane with θ_x calculated as in Fig. F9 and θ_{xs} from Fig. F2

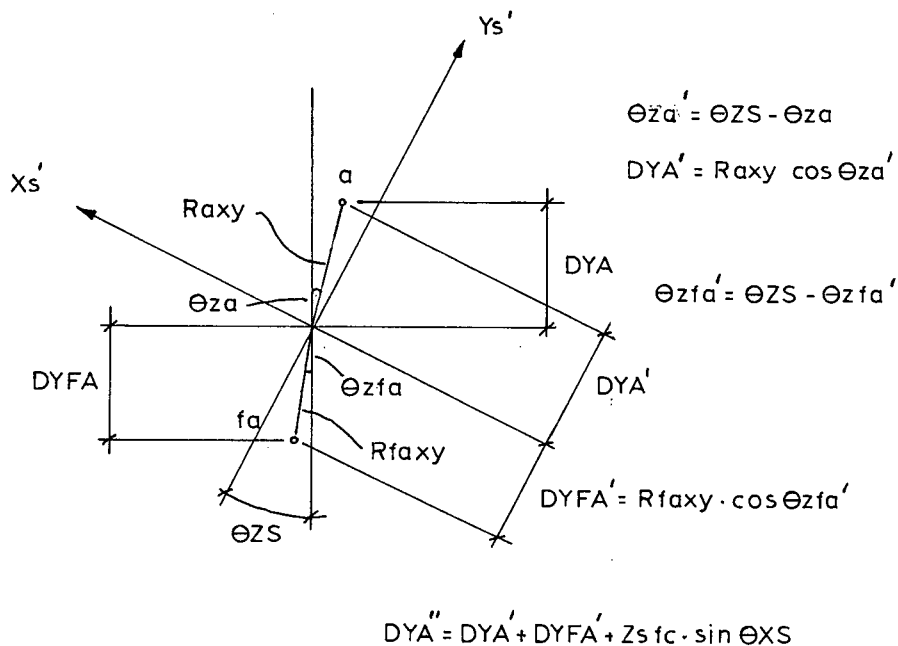
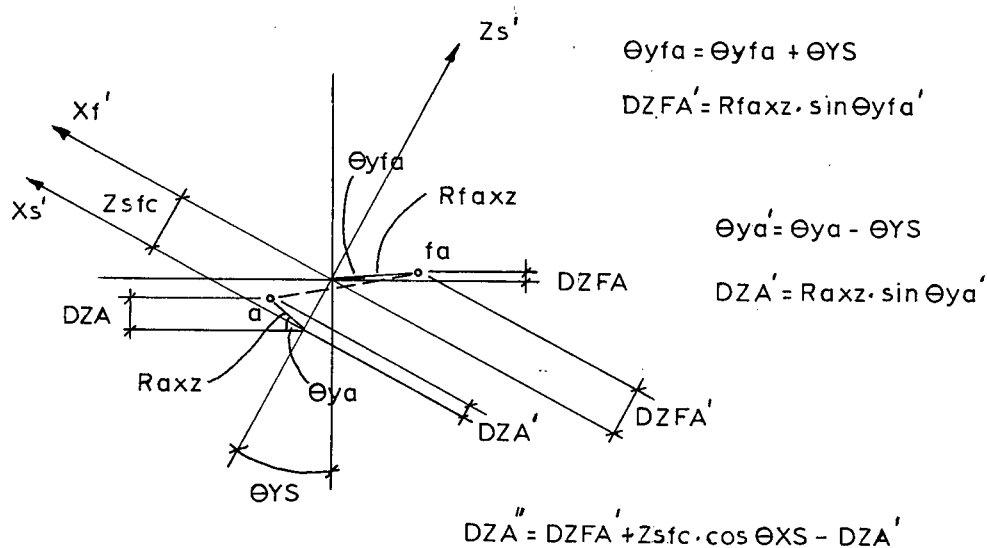


FIG. F9 ANGLE OF ANTERIOR CRUCIATE IN YsZs PLANE
 $\theta_X = \text{ARCTAN} (DZA''/DYA'')$

2. Posterior Cruciate Ligament

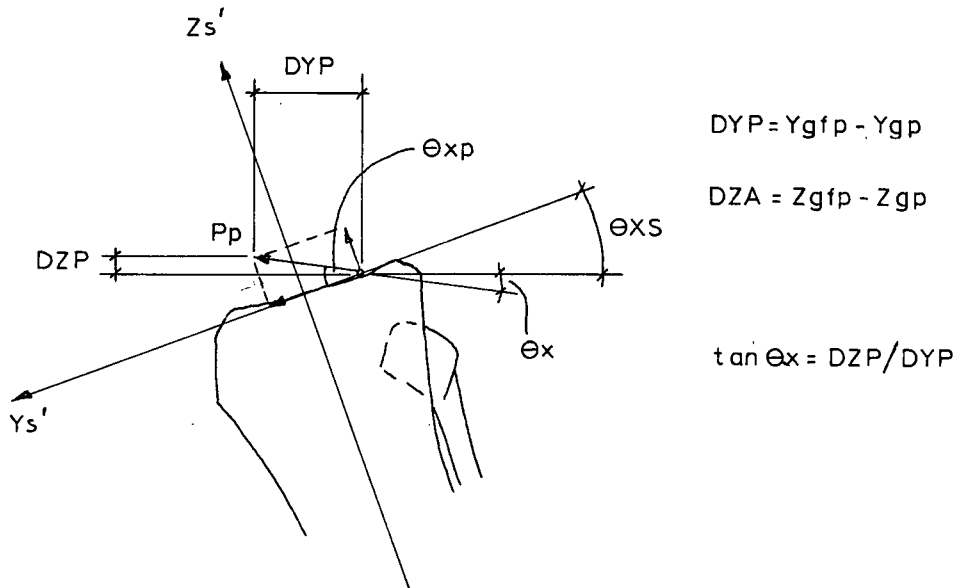
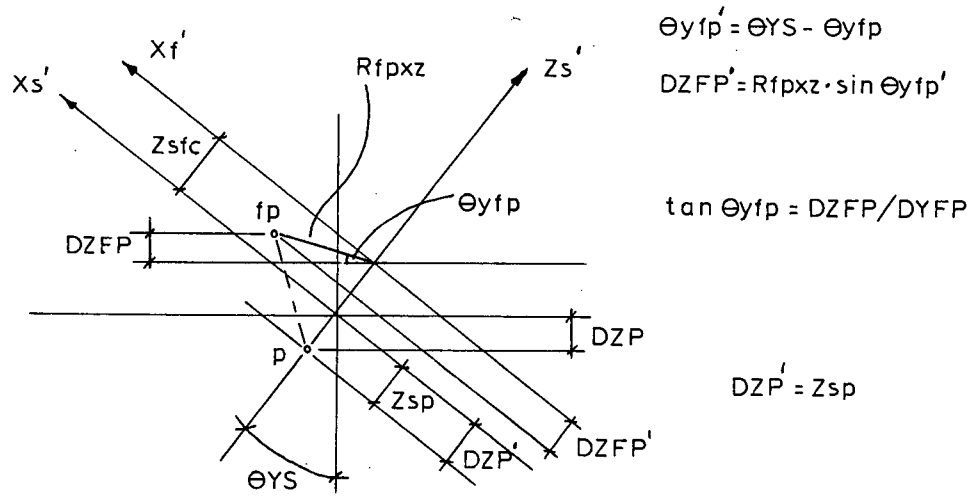


FIG. F10 FORCE ACTION OF POSTERIOR CRUCIATE LIGAMENT IN YZ PLANE

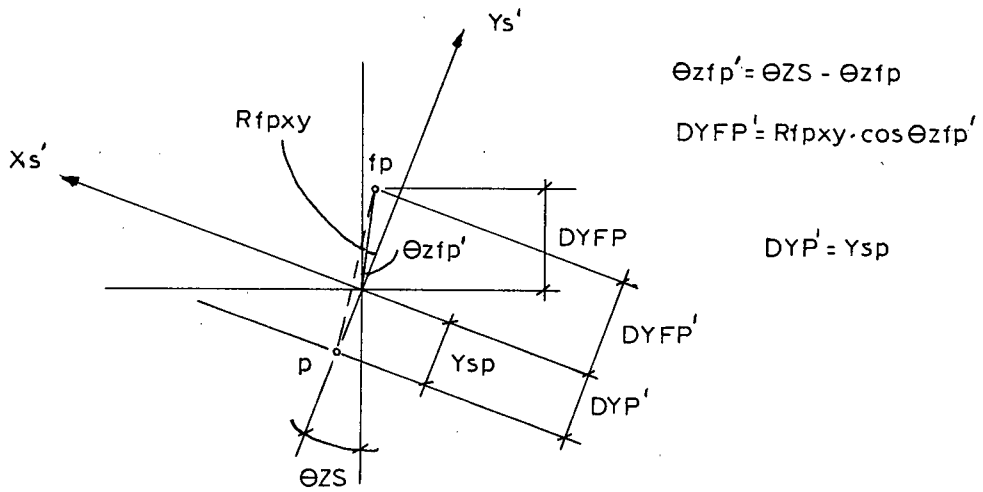
$$F_{ym} + F_{yk} = P_p \cdot \cos \theta_{xp}$$

$$P_p = (F_{ym} + F_{yk}) / \cos \theta_{xp}$$

$\theta_{xp} = \theta_x + \theta_{XS}$ is the angle of the posterior cruciate to the Y_s axis in the $Y_s Z_s$ plane with θ_x calculated as in Fig. F11 and θ_{XS} from Fig. F2



$$DZP'' = DZP' + Zsfc \cdot \cos \Theta_{XS} - DZFP'$$



$$DYP'' = DYP' + DYFP' + Zsfc \cdot \sin \Theta_{XS}$$

FIG. F11 ANGLE OF POSTERIOR CRUCIATE IN Y_sZ_s PLANE; $\Theta_X = \text{ARCTAN} (DZP'' / DYP'')$

3. Lateral Collateral Ligament

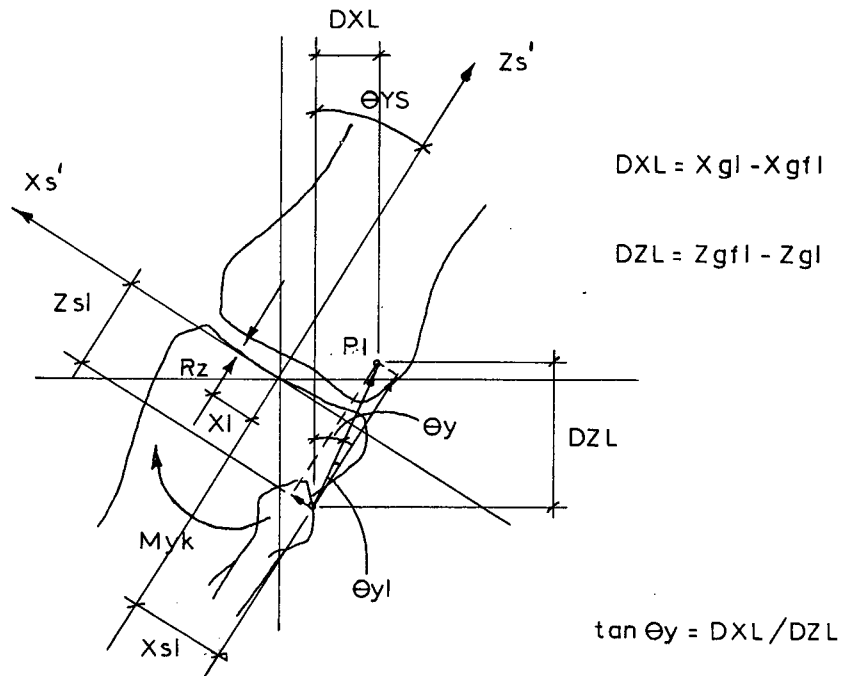
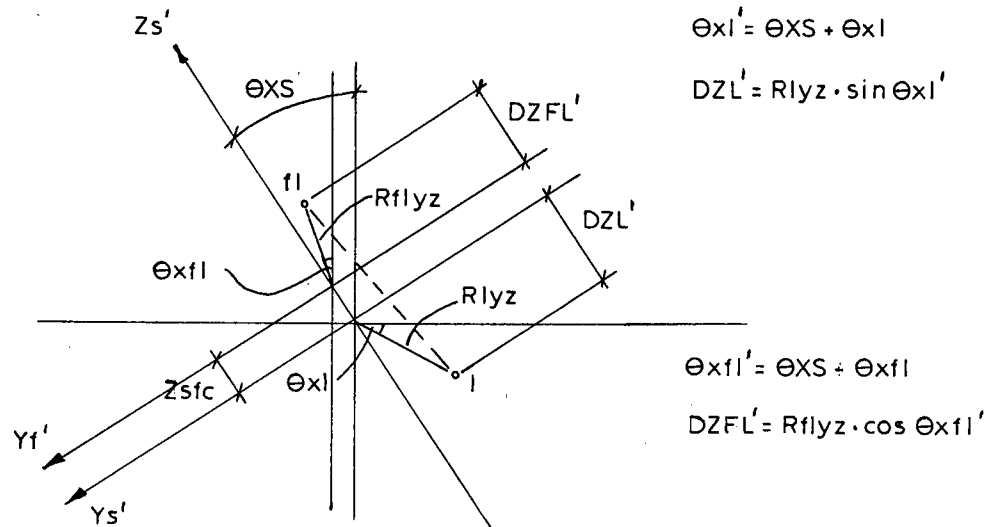


FIG. F12 FORCE ACTION OF LATERAL COLLATERAL
LIGAMENT IN XZ PLANE

$$R_z = F_{zk} + F_{zm} + F_{zcr}$$

$$P1 = (Myk + Rz \cdot X1) / (\cos \theta_{y1} \cdot Xs1 - \sin \theta_{y1} \cdot Zs1 - \cos \theta_{y1} \cdot Y1)$$

$\theta_{yl} = \theta_{YS} - \theta_Y$ is the angle of the lateral collateral to the Z_S axis in the $Y_S Z_S$ plane with θ_Y calculated as in Fig. F13 and θ_{YS} from Fig. F2



$$DZL'' = DZL' + DZFL' + Zsfc \cdot \cos \theta_{YS}$$

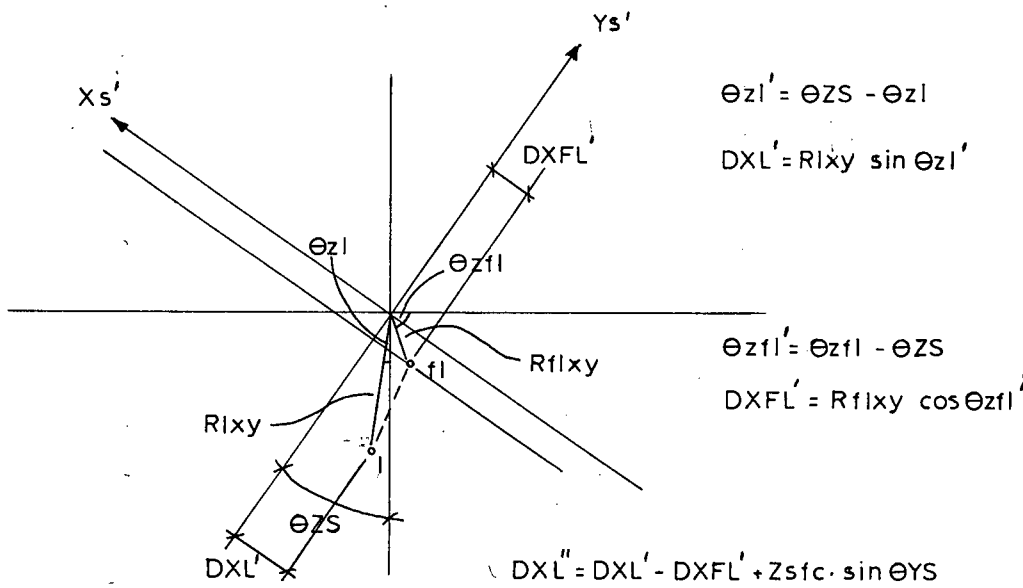


FIG. F13 ANGLE OF LATERAL COLLATERAL IN X_sZ_s PLANE, $\theta_y = \text{ARCTAN} (DXL''/DZL'')$

4. Medial Collateral Ligament

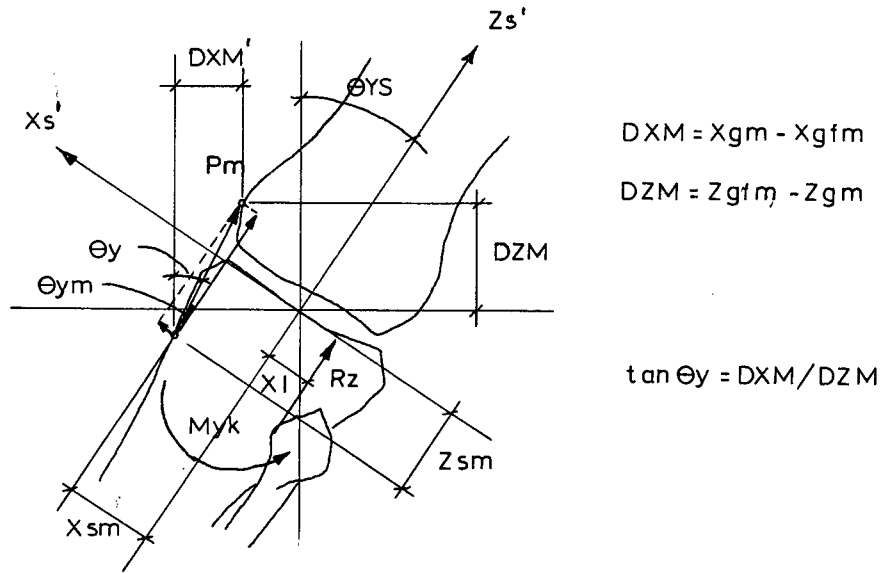
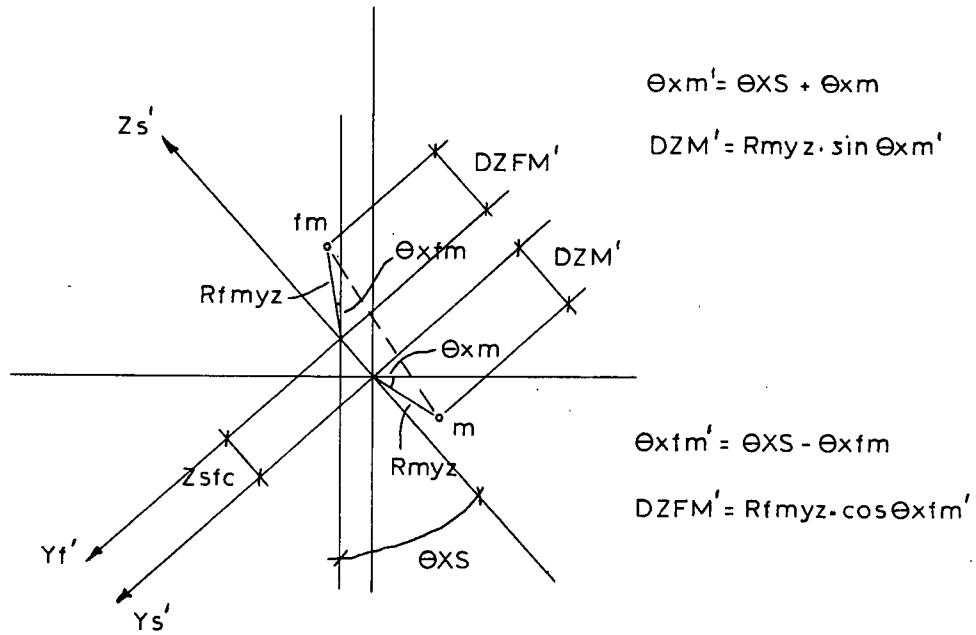


FIG. F14 FORCE ACTION OF MEDIAL COLLATERAL LIGAMENT IN XZ PLANE

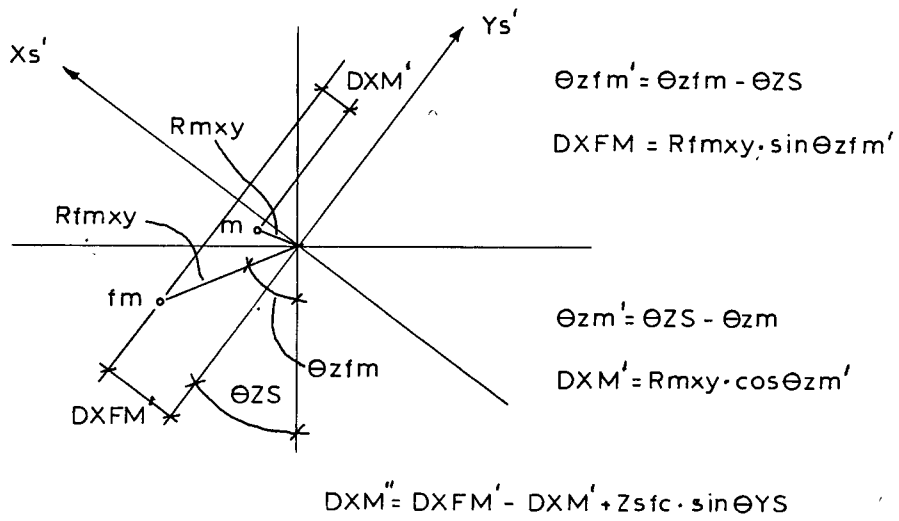
$$R_z = F_{ZK} + F_{ZM} + F_{ZCR}$$

$$P_m = (My_k + R_z \cdot X_l) / (\cos \theta_{ym} \cdot X_{sm} + \sin \theta_{ym} \cdot Z_{sm} - \cos \theta_{ym} \cdot X_l)$$

$\theta_{ym} = \theta_{YS} - \theta_Y$ is the angle of the medial collateral to the Z_s axis in the $X_s Z_s$ plane with θ_Y calculated as in Fig. F15 and θ_{YS} from Fig. F2



$$DZM'' = DZM' + DZFM' + Zsfc \cdot \cos \theta_{YS}$$



$$DXM'' = DXFM' - DXM' + Zsfc \cdot \sin \theta_{YS}$$

FIG. F15 ANGLE OF MEDIAL COLLATERAL IN X_sZ_s PLANE, $\theta_Y = \text{ARCTAN} (DXM''/DZM'')$

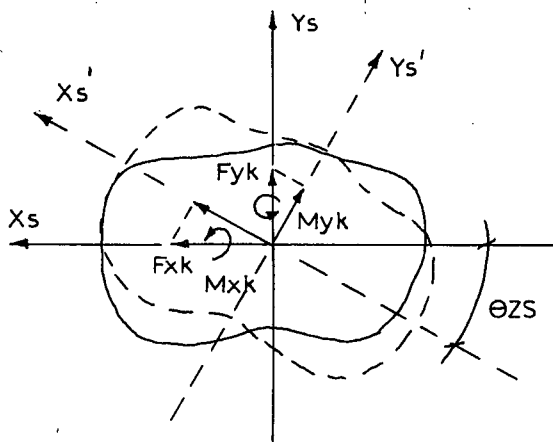
APPENDIX G

RESOLUTION OF EXTERNAL FORCE SYSTEM

APPENDIX G

RESOLUTION OF EXTERNAL FORCE SYSTEM

XY Plane



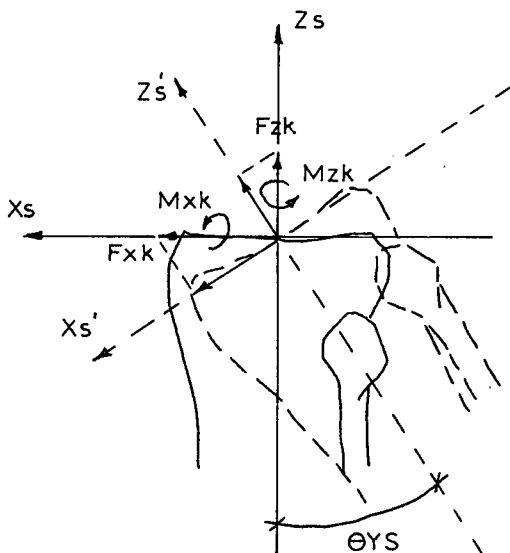
$$F_{xk}' = F_{xk} \cdot \cos \theta_{zs} + F_{yk} \cdot \sin \theta_{zs}$$

$$F_{yk}' = F_{yk} \cdot \cos \theta_{zs} - F_{xk} \cdot \sin \theta_{zs}$$

$$M_{xk}' = M_{xk} \cdot \cos \theta_{zs} + M_{yk} \cdot \sin \theta_{zs}$$

$$M_{yk}' = M_{yk} \cdot \cos \theta_{zs} - M_{xk} \cdot \sin \theta_{zs}$$

XZ Plane



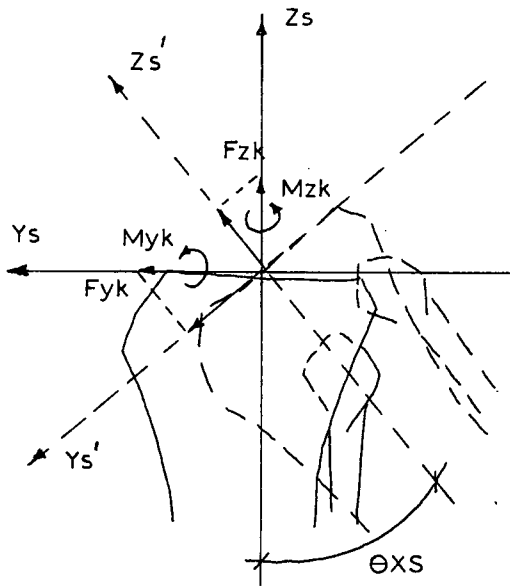
$$F_{xk}' = F_{xk} \cdot \cos \theta_{ys} - F_{zk} \cdot \sin \theta_{ys}$$

$$F_{zk}' = F_{zk} \cdot \cos \theta_{ys} + F_{xk} \cdot \sin \theta_{ys}$$

$$M_{xk}' = M_{xk} \cdot \cos \theta_{ys} - M_{zk} \cdot \sin \theta_{ys}$$

$$M_{zk}' = M_{zk} \cdot \cos \theta_{ys} + M_{xk} \cdot \sin \theta_{ys}$$

YZ Plane



$$F_{yk}' = F_{yk} \cdot \cos \theta_{XS} - F_{zk} \cdot \sin \theta_{XS}$$

$$F_{zk}' = F_{zk} \cdot \cos \theta_{XS} + F_{yk} \cdot \sin \theta_{XS}$$

$$M_{yk}' = M_{yk} \cdot \cos \theta_{XS} - M_{zk} \cdot \sin \theta_{XS}$$

$$M_{zk}' = M_{zk} \cdot \cos \theta_{XS} + M_{yk} \cdot \sin \theta_{XS}$$

Equations of Resolved External Force System

$$F_{xk}' = F_{xk} \cdot \cos \theta_{ZS} \cdot \cos \theta_{YS} + F_{yk} \cdot \sin \theta_{ZS} - F_{zk} \cdot \sin \theta_{YS}$$

$$F_{yk}' = F_{yk} \cdot \cos \theta_{ZS} \cdot \cos \theta_{XS} - F_{xk} \cdot \sin \theta_{ZS} - F_{zk} \cdot \sin \theta_{XS}$$

$$F_{zk}' = F_{zk} \cdot \cos \theta_{YS} \cdot \cos \theta_{XS} + F_{yk} \cdot \sin \theta_{XS} + F_{xk} \cdot \sin \theta_{YS}$$

$$M_{xk}' = M_{xk} \cdot \cos \theta_{ZS} \cdot \cos \theta_{YS} + M_{yk} \cdot \sin \theta_{ZS} - M_{zk} \cdot \sin \theta_{YS}$$

$$M_{yk}' = M_{yk} \cdot \cos \theta_{ZS} \cdot \cos \theta_{XS} - M_{xk} \cdot \sin \theta_{ZS} - M_{zk} \cdot \sin \theta_{XS}$$

$$M_{zk}' = M_{zk} \cdot \cos \theta_{XS} \cdot \cos \theta_{YS} + M_{xk} \cdot \sin \theta_{YS} + M_{yk} \cdot \sin \theta_{XS}$$

APPENDIX H

LIMB ACCELERATIONS

APPENDIX H

LIMB ACCELERATIONS

1. Linear Limb Acceleration

A numerical differentiation technique based on finite differences (Lanczos, 1957) was used to determine the linear limb accelerations of the foot and shank. The linear accelerations of the foot and shank in the X, Y and Z directions were calculated from the respective displacements of the centre of mass of the foot and shank. Therefore the linear accelerations are calculated as follows:

$$\ddot{X}_n = \frac{4X_n - 4 + 4X_{n-3} + X_{n-2} - 4X_{n-1} - 10X_{n-4} - 4X_{n-5} + X_{n-6} + 4X_{n-7} + 4X_{n-8}}{100t^2}$$

X_n - displacement of centre of mass of segment in X direction at time, n

\ddot{X}_n - acceleration of centre of mass in X direction at time, n

n - point in time

t - time interval of displacement from n to n + 1

Similar equations give the acceleration of centre of mass of a segment in the Y and Z directions

$$Y_n = 4Y_{n-4} + 4Y_{n-3} + Y_{n-2} - 4Y_{n-1} - 10Y_n \\ - 4Y_{n+1} + Y_{n+2} + 4Y_{n+3} + 4Y_{n+4} / 100t^2$$

$$Z_n = 4Z_{n-4} + 4Z_{n-3} + Z_{n-2} - 4Z_{n-1} - 10Z_n \\ - 4Z_{n+1} + Z_{n+2} + 4Z_{n+3} + 4Z_{n+4} / 100t^2$$

3. Angular Limb Acceleration

The angular accelerations of the foot and shank were determined from the respective angular displacements of the foot and shank. The angular accelerations are calculated about the X, Y and Z axes passing through the centre of mass of the segment as follows:

$$\ddot{\theta}_x = 4\theta_{x,n-4} + 4\theta_{x,n-3} + \theta_{x,n-2} - 4\theta_{x,n-1} - 10\theta_{x,n} \\ - 4\theta_{x,n+1} + \theta_{x,n+2} + 4\theta_{x,n+3} + 4\theta_{x,n+4} / 100t^2$$

$\theta_{x,n}$ - angular displacement of segment about the X axis at time, n

$\ddot{\theta}_x$ - angular acceleration of segment about the X axis at time, n

n - point in time

t - time interval of displacement from n to n + 1

Similar equations give the angular acceleration of the segment about the Y and Z axes

$$\ddot{\theta}_Y = 4\theta_{Y,n-4} + 4\theta_{Y,n-3} + \theta_{Y,n-2} - 4\theta_{Y,n-1} - 10\theta_{Y,n} \\ - 4\theta_{Y,n+1} + \theta_{Y,n+2} + 4\theta_{Y,n+3} + 4\theta_{Y,n+4} / 100t^2$$

- 190 -

$$\begin{aligned} \theta Z_n = & 4\theta Z_n - 4 + 4\theta Z_n - 3 + \theta Z_n - 2 - 4\theta Z_n - 1 - 10\theta Z_n \\ & - 4\theta Z_n + 1 + \theta Z_n + 2 + 4\theta Z_n + 3 + 4\theta Z_n + 4 / 100t^2 \end{aligned}$$